Order Number 1342292

Flexural creep in pure and filled acrylic resin systems

Nandi, Ranjan Kaushik, M.S.

Rice University, 1990

U·M·I
300 N. Zeeb Rd.
Ann Arbor, MI 48106

RICE UNIVERSITY

FLEXURAL CREEP IN PURE AND FILLED ACRYLIC RESIN SYSTEMS

by

Ranjan K. Nandi

A THESIS SUBMITTED
IN PARTIAL FULFILLMENT OF THE
REQUIREMENTS FOR THE DEGREE

MASTER OF SCIENCE

APPROVED, THESIS COMMITTEE:

Dr. C.D. Armeniades, Professor, Director

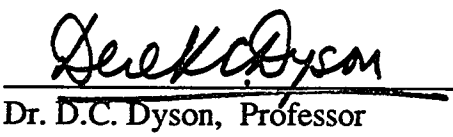

Dr. D.C. Dyson, Professor

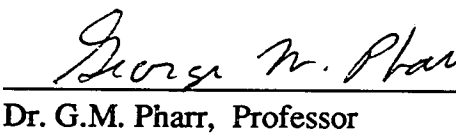

Dr. G.M. Pharr, Professor

Houston, Texas
March, 1990

ABSTRACT

Flexural creep in pure and filled acrylic resin systems

by

Ranjan K. Nandi

The creep behavior of poly (methyl methacrylate) and acrylic polymer concrete (PC) systems based on methyl methacrylate was studied in flexure. Creep in both pure and filled systems followed a power law time dependence. A differential form of the power law equation was used to eliminate the irregularities associated with time-independent and transient strains in the experimental data.

$$de_{tot}/dt = \ln nk + (n-1) \ln t$$

where e_{tot} is the total strain and n and k are constants in the power law equation. Plots of creep rates versus time yielded good linear fits to the data, the slopes providing values for 'n', the power exponent. Vertical superposition was then used to reduce data at different stresses and resin contents, for the PCs onto a single master curve using different shift-factors. This data reduction was expressed in the form of an empirical expression :

$$e(t, S, v) = e_0(ref) \cdot EXP(K_S \cdot [S - S_{ref}]) \cdot EXP(K_v \cdot [v - v_{ref}]) \cdot t^n$$

which expresses the total creep strain as a product of separable functions of time (t), stress (S) and the resin volume fraction (v).

ACKNOWLEDGEMENTS

I would like to express my sincere gratitude to my thesis advisor and thesis committee chairman Dr. C.D. Armeniades for his valuable advice, guidance and support. His constant encouragement is deeply appreciated.

I would like to thank my other committee members, Dr. D.C. Dyson and Dr. G.M. Pharr for their time serving on the advisory committee.

I would like to thank Dick Chronister, the department technician, for his valuable suggestions and help in modifying the experimental set-up and preparing the specimens; to Lindy and Diana, the department secretaries, for patiently helping me out with all the minor details that go towards preparing a thesis.

The generous financial support of the Rice University Chemical Engineering Department is gratefully acknowledged.

To My Parents

TABLE OF CONTENTS

LIST OF FIGURES

CHAPTER 1

INTRODUCTION

1.1 DESCRIPTION OF POLYMER CONCRETE

Concrete in general can be defined as an artificial conglomerate consisting of aggregate (or filler) and a fluid binder, which solidifies as the system "sets" or cures. Unlike portland cement concrete, which uses a paste of cement and water as binder, in polymer concretes (PCs) a synthetic polymer such as a polyester, epoxy or acrylic is utilized as a binder. In other words, polymer concrete (PC) is a composite material in which a mineral aggregate such as sand and gravel is combined with a liquid organic resin and hardened through polymerization reactions.

Polymer concretes have various advantages over conventional, portland cement concretes. They have higher tensile, compressive and flexural strengths, and rapid cure rates. Many PCs achieve full strengths in several hours or less, whereas portland cement systems require 2-4 weeks. Also, they have excellent resistance to impact, abrasion, weathering, freeze-thaw, chemicals, water and salt sprays. Disadvantages include high cost and the failure to bond to wet surfaces. However, their biggest drawback lies in

their viscoelastic behavior. Due to their viscoelastic properties PCs can creep significantly and be highly sensitive to temperature changes. Table 1 shows a comparison of the properties of PC with Portland Cement Concrete (PCC).

1.2 ELASTIC AND TIME - DEPENDENT RESPONSE TO STRESS

When a polymeric material is subjected to a constant load, the resulting deformation tends to increase with time as entangled chain segments undergo conformational changes in response to external stress. The process is called creep. Accordingly, creep tests measure the time - dependent strain on specimens subjected to constant stress. Residual deformation is found immediately upon removal of the load. This gradually reduces with the passage of time and in some cases a tested specimen may regain its original dimensions. The process is called creep recovery.

The same type of conformational changes in the macromolecular matrix that generate creep also give rise to a time dependent decay in stress when viscoelastic materials are subject to constant deformation. The process is called stress relaxation. Consequently, stress relaxation tests measure the time dependent stress on specimens under constant strain.

TABLE 1. Comparison of the properties of Polymer Concrete with those of Portland Cement Concrete.

Property	Polymer Concrete	Portland Cement
Compressive Strength, psi	5,700 - 21,300	4,000 - 5,000
Tensile Strength, psi	1,000 - 2,000	300 - 360
Flexural Strength, psi	3000	700
Modulus Of Rupture, psi	1,200 - 3,000	470 - 530
Modulus Of Elasticity, $*10^6$ psi	1.0 - 2.0	2.8 - 3.6
Hardness, Impact Hammer, psi	55	32

Data from creep and stress relaxation tests are interconvertible though the methods involved are quite complex[1]. The following equation, however, provides to a first approximation a relation between creep and stress relaxation.

$$[\, e_t/e_0 \,]_{creep} = [\, S_0/S_t \,]_{\text{stress relaxation}} \qquad (1.1.1)$$

where : e_t = creep strain at time t

e_0 = creep strain at time 0

S_t = stress at time t, and

S_0 = stress at time 0

1.2.1 MODELS

The simplest models for representing creep and stress relaxation utilize Hookean springs and Newtonian dashpots, connected in series (Maxwell model, Fig. 1.2.1) or in parallel (Voigt model, Fig. 1.2.2). The modulus of the spring is E and the viscosity of the dashpot is η. In the Maxwell model[1] a constant strain is imposed and the stress is measured as a function of time. The stress due to the spring is eE and that due to the dashpot is $\eta(de/dt)$. In this

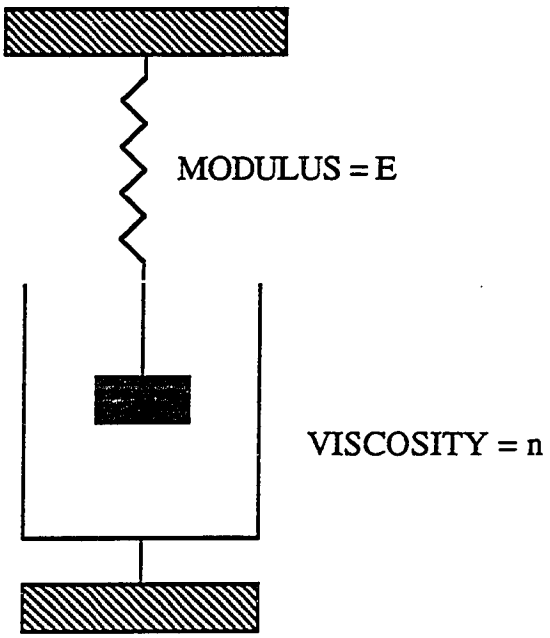

Figure 1.2.1 Representation of a Maxwell unit.

model the net rate of change is zero as a change in the elongation of the spring is compensated by an equivalent change in the dashpot. We therefore have :

$$de/dt = (1/E)\ ds/dt + S/\eta = 0 \qquad (1.2.1)$$

The solution of equation (1.2.1) gives :

$$S/S_0 = EXP\ (-Et/\eta) = EXP\ (-t/\tau) \qquad (1.2.2)$$

where τ = relaxation time = η/E.

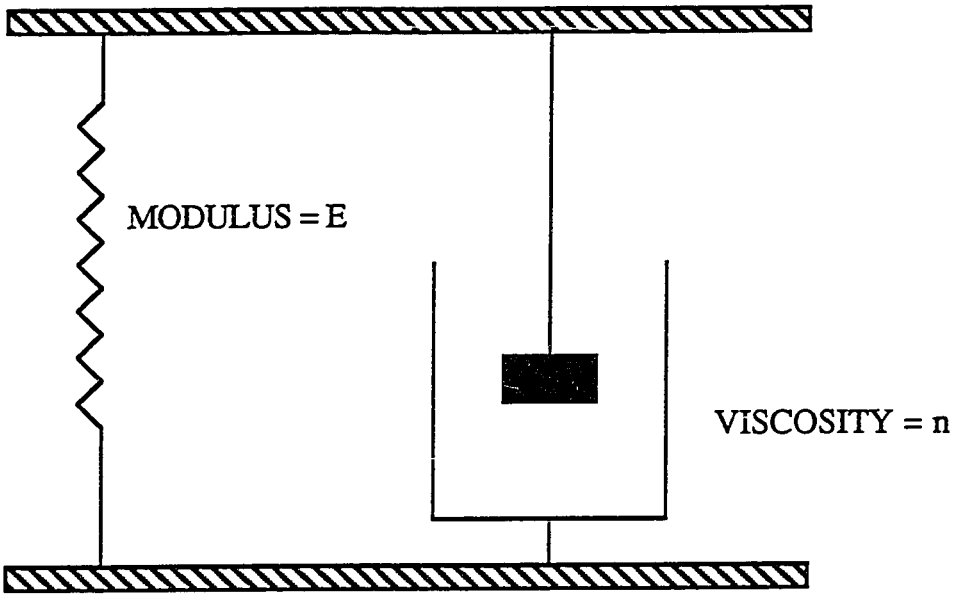

FIGURE 1.2.2 Representation of a Voigt unit.

In the Kelvin or Voigt model[2] (Figure 1.2.2) a constant stress is imposed and the strain response is measured as a function of time. The spring and dashpot are in parallel and the total stress is given by :

$$S = E.e + \eta .de/dt \qquad (1.2.3)$$

Assuming constant stress and, $e_0 = 0$ at $t = 0$, integration of equation (1.2.3) gives :

$$e = S/e.\ EXP\ (-t/\tau) \qquad (1.2.4)$$

where $\tau = \eta/E$, is the retardation time.

A better approximation of creep is given by the four element model as shown in Figure (1.2.3). Here we have a spring of modulus E_1, followed by a spring E_2 and dashpot η_2 in parallel, and finally a dashpot η_3 in series. At constant loading, the total elongation is a sum of the elongations of the three component parts. Therefore we have :

$$e = S_0/E_1 + S_0/E_2\ (1 - EXP\ (-t/\tau)) + S_0 t/\eta_3 \qquad (1.2.3)$$

where $\tau = \eta_2/E_2$ is called the retardation time.

Upon immediate removal of the load there is an instant reduction owing to the elastic part S_0/E_1. The recovery for the residual deformation is given by :

$$e = e_2.\ EXP\ [-(t-t_1)/\tau] + S_0 t_1/\eta_3 \qquad (1.2.4)$$

where $e_2 = S_0/E_2\ \{1 - EXP\ [-t_1/\tau]\}$.

Except for the viscous part due to the dashpot all the creep is recoverable. Figure (1.2.4) shows the creep and creep recovery of a four element model.

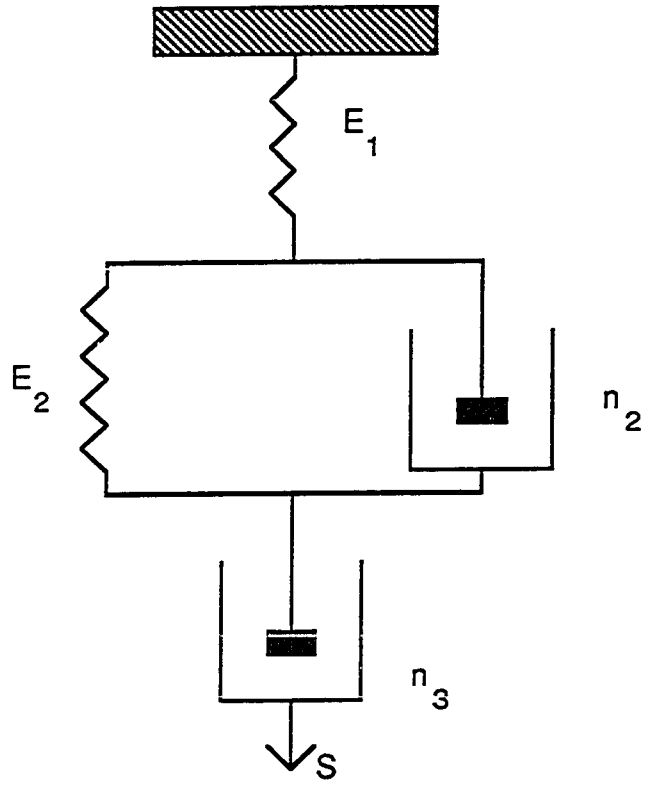

FIGURE 1.2.3 Representation of a four element model.

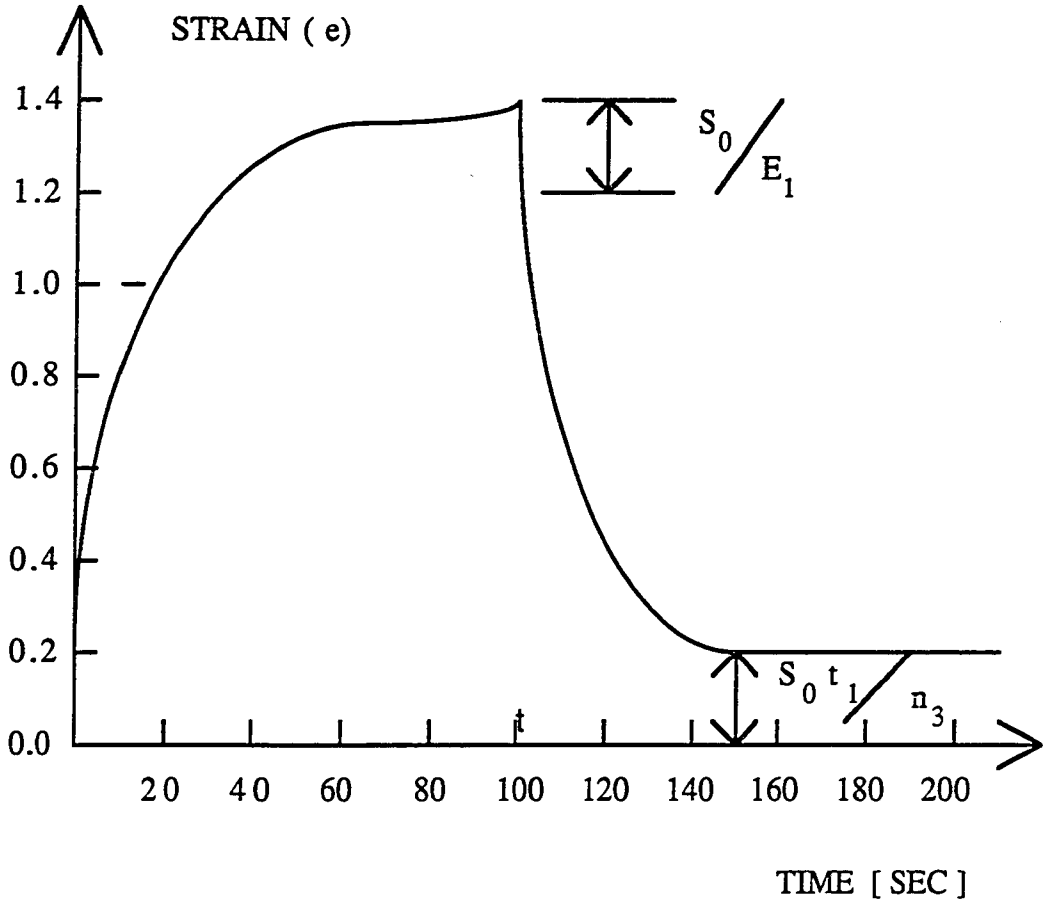

FIGURE 1.2.4 Creep and creep recovery of a four element model.

1.3 PREVIOUS WORK ON POLYMER CREEP

Early studies on creep were carried out by Weber[3] in 1835. He found that upon application of a load to a raw silk filament, the

initial elastic extension was followed by a further time dependent deformation. He noticed that removal of the load caused an elastic contraction equal to the initial elastic extension. With further passage of time further contraction took place and in some cases the specimen recovered to its original dimensions. He called this creep phenomenon an elastic after effect. Based on simple hypotheses he made an attempt to fit creep and recovery curves. He proposed the following relationship between the creep rate and deformation :

$$de/dt = f(e) \qquad (1.3.1)$$

$$\& \quad e = K\,(t+c)^n \qquad (1.3.2)$$

Where K, C, n are constants.

One of the earliest and most popular creep laws was that of Norton[4] who worked on different alloys. According to this model,

$$de/dt = K\,(S/S_0)^n \qquad (1.3.3)$$

where, S = applied stress, and K, n are material constants.

A model developed by Eyring[5] for the effect of the applied shear component in creep still remains to be one of the most

accepted models to describe such creep behavior. He considered the transition of a particle from an initial position to a final position by overcoming an energy barrier. The principle can be suitably applied to the creep process in plastics, as creep probably involves only localized segmental rearrangments (as indicated by decreasing flow rates with time and a large recovery of flow). Assuming that the barrier to rearrangement has the free energy height ΔF^* relative to the initial state, the probability of a segment having this energy ΔF^* at any time is proportional to $\exp(-\Delta F^*/kT)$ where k is the Boltzmann constant. With the application of a shear stress the rearranging segments that move in phase with the stress absorb mechanical energy which contributes to the energy required for crossing the barrier. If the flow element absorbs mechanical energy τb on moving from the initial position to the top of the barrier then the energy associated with T, the absolute temperature, is reduced to $(\Delta F^* - \tau b)$. The flux now becomes proportional to $\exp\{-(\Delta F^* - \tau b)/kT\}$, with a probality of one half of continuing to the final position. Again, the probality of a backward transition is proportional to $\exp\{-(\Delta F^* + \tau b)/kT\}$. The net forward flux of rearrangements is then given by :

$$(\text{net flux}) = 2 \exp\{-\Delta F^*/kT\} \cdot \sinh\{\tau b/kT\}. \qquad (1.3.4)$$

Findley[6] proposed a model which seemed to describe most creep

curves quite accurately. His equation was of the form :

$$e\,(tot) = e_0 + Kt^n \qquad (1.3.5)$$

The value of e_0 is not necessarily that of the elastic strain but a value of strain used to fit different test data. Taking logarithms,

$$Ln\,(\,e(tot) - e_0\,) = Ln\,K + n\,Ln\,t \qquad (1.3.6)$$

A plot of (e(tot) - e_0) versus time on logarithmic scales gives us a straight line with the value of n being predicted from the slope. A method of successive approximations may be used to find the value of e_0. Three different times are chosen such that one is the geometric mean of the other two. If t_1, t_2, t_3 are the three times chosen then t_3 = Sq. rt ($t_1 . t_2$). Using some some simple mathematics and substitutions we get :

$$e_0 = (\,e_1 e_2 - e_3^2) \,/\, (\,e_1 + e_2 - 2e_3\,) \qquad (1.3.7)$$

where e_1, e_2 and e_3 are the strains corresponding to the times t_1, t_2, t_3. He later[7] found that e_0 and K could be represented by hyperbolic functions such that :

$$e_0 = e_0' \text{ Sinh } S/S_e \qquad (1.3.8)$$

$$\& \qquad K = K' \text{ Sinh } S/S_k \qquad (1.3.9)$$

where S_e, S_k, e_0', and K' are constants.

Equation (1.3.5) reduces to :

$$e_t = e_0' \text{ Sinh } S/S_e + K' \text{ Sinh } S/S_k \qquad (1.3.10)$$

An extension of Norton's model by Marin and Pao[8], who used Plexiglass and Lucite (different forms of PMMA) for their experiments, provided the following relation :

$$e = DS^m + BtS^n \qquad (1.3.11)$$

where D, m, B, n are material constants which depend upon the loading mode.

McLoughlin's[9] equation was,

$$\text{Log } (Z_0 - \text{Log}_{10} E) = A + B \text{ Log}_{10} t \qquad (1.3.12)$$

where, $Z_0 = \text{Log}_{10} E_0 + C/K \, . \, [10^{(Kx_0/C_0)}]$

$$A = \text{Log}_{10}\ C/K$$

$$B = K/C_0$$

His equation predicted the creep of PMMA quite well to temperatures of 60^0C.

McVetty[10] used the following equation for creep in chrome steel :

$$de/dt = K + K_0\ \text{EXP}\ (-pt) \qquad (1.3.13)$$

where K, K_0, p are constants of the material, temperature and stress level. On integration.

$$e = e_0 + Kt - (K_0/p).\ \text{Exp}\ (-pt) \qquad (1.3.14)$$

where e_0 is the integration constant.

A similar law using logarithmic functions instead of exponentials was suggested by Weaver[2] where the strain was given by :

$$e = -b + Kt + a\ \text{Log}\ t \qquad (1.3.15)$$

where b, K, a are material and temperature constants for a given stress level.

Previous creep studies on polymer concretes are rather limited. Howdyshell[11] measured the creep characteristics of polyester PC. He used three different stress-strength ratios of 0.23, 0.44 and 0.66 for a testing period of 1000 hours. He found that the only specimens which withstood the full length of time were those at the 0.23 level. The others failed prematurely. On comparison of the creep strains of polymer concretes with those in portland cement concretes it was seen that strain decreased with increasing times in PCC whereas they reached an asymptotic value in PCs.

Prin and Cubaud[12] studied the application of PCs in the construction industry. They chose polyester as the parent resin and then investigated the mechanical properties of the polyester concrete. In flexural tests they noticed that the slenderness ratio affects the behavior of the PC. The material had a tendency to exhibit less linearity at higher values of slenderness. Also, creep strains at compressive stress-strength ratios of 0.5 are less than the coresponding elastic strains and stabilize in about 1-3 months.

Knab[13] studied the short term and long term flexural behavior of reinforced polyester concrete beams. He developed a mathematical model to predict long term deflection. Significant deformations were observed under both long and short term loadings thus limiting to a great extent its use in structural applications.

Ohama[14] performed compressive creep tests on polyester concretes and developed the following equation for creep strain :

$$e_c = t / A + B.t \qquad (1.3.17)$$

where e_c is the creep strain and A and B are arbitrary constants. He used low stress to strength ratios for his experiments, the highest being 0.18.

Okada et al.[15] studied the influence of temperature on polyester concrete behavior. Using low stress to strength ratios it was found that creep increased increased with an increase in the resin content and the temperature.

Broniewski et al.[16] performed compressive creep experiments on epoxy based PC's. The creep strain according to their model is given by,

$$e_t = e_0 (t / b)^m \qquad (1.3.18)$$

where b, m are arbitrary constants, e_t the time dependent strain and e_0 the initial strain. The equation can be used in PC systems without fibre reinforcement as well as systems containing steel fibers at different volume fractions.

Helal[17] found that at high stresses there is a large deviation of creep behavior of PC from traditional viscoelastic theories. Reinforced concrete beams were not successful in enhancing mechanical properties owing to severe internal stresses caused by high shrinkage deformations during polymerization. As a result inadmissible deflections, severe cracking, and eventually premature failure was observed in diagonal tension. He found that specimens that did not fail could be represented by the hyperbolic creep law of Ross.

Hsu[18] performed some flexural studies on MMA based PCs. He used stress to strength ratios of 0.3, 0.4, 0.5. He found that a higher stress to strength ratio resulted in a larger strain. Also the creep was not linearly proportional to the applied stress, an observation made previously by Helal during his polyester concrete studies. The specimens were loaded for one year and it was seen that 20% of the final creep took place within the first day and about 50% in the next 5 days. Creep in PC was one to two times higher than that in conventional concrete.

Dharmarajan[19] attempted to describe the creep behavior in polyester and epoxy based polymer concretes. He used a "triple superposition scheme" to develop a constitutive equation for prediction of long term creep in PCs. He investigated the influence of stress, temperature and resin content on the creep responses of

the PC, and reduced the data onto a chosen reference state. This successful data reduction made it possible to describe the creep compliance of PC systems as a product of separable functions of time(t), stress(S), temperature(T) and resin volume fraction(v), such that :

$$J(t, T, S, v) = J_r . [\exp (-H/RT) . \exp (K_S . S) . \exp (K_v . v) . t]^m \quad \text{------} \quad (1.3.19)$$

Some recent work was done by Kumar[20] on poly methyl methacrylate in flexure. He developed a constitutive equation which expressed creep strains as separable functions of time, temperature and stress. The model he used for curve fitting was :

$$e_{tot} (t, S) = M (S) + N (S \text{ or } T \text{ or both}) . f (t) \quad (1.3.16)$$

where S is the applied stress, T the temperature and t the time.

Accordingly plots of $\{e_{tot} - M(S)\}$ versus time on a logarithmic scale yielded straight lines but only for times greater than six hours. He considered this time to be the duration of transient strains and neglected the data for the first six hours, based on this assumption. The other observation he made was that the creep response curves are highly sensitive to changes in the value of

M(S). Consequently he used different curve fitting packages to obtain values for M(S) which gave the best linear fit to the experimental data. The values he got for M(S), the time independent strain, were close to the elastic strain values for that material. His constitutive equation, an extension of Findley's work, had a power law dependence with an exponent 0.24.

The previous studies on polymer concrete have certain limitations. A major portion of the work has been restricted to polyesters and epoxies. Not much emphasis has been put on acrylic based PCs. The commonly used mode of testing is of the compressive type even though the systems fail more readily in tension and flexure than in compression. Previous experimental work show that a power law dependence of creep is probably one the most accurate models for describing creep responses in polymers and composites. Doubts remain,however, concerning the nature and the value of the power law coefficient 'n' of equation (1.3.5). These questions leave us room for further study.

An important detriment to the accurate representation of creep strains developed in polymer concretes is the inability to extract with conviction the creep strain from the total strain of the specimen, which contains its elastic deformation, as well as, any transient strains, due to misalignment or other experimental factors. Models developed by Turner[21] and Kumar[20] where :

e_{tot} (t, S) = M (S) + N (S or T or both) . f (t), showed a strong dependence of the [etot - M (S)] versus time plots (logarithmic coordinates), on the value of M (S) (Figure 1.3.1). Kumar assigned a time period of six hours to the duration of the transients as it was after this time that he obtained straight line correlations (Figure 1.3.2). However, this was typical to his case where he worked solely on unfilled PMMA. From his observations though, one thing becomes increasingly clear: the importance of separating the time independent and transient strains from the creep strains.

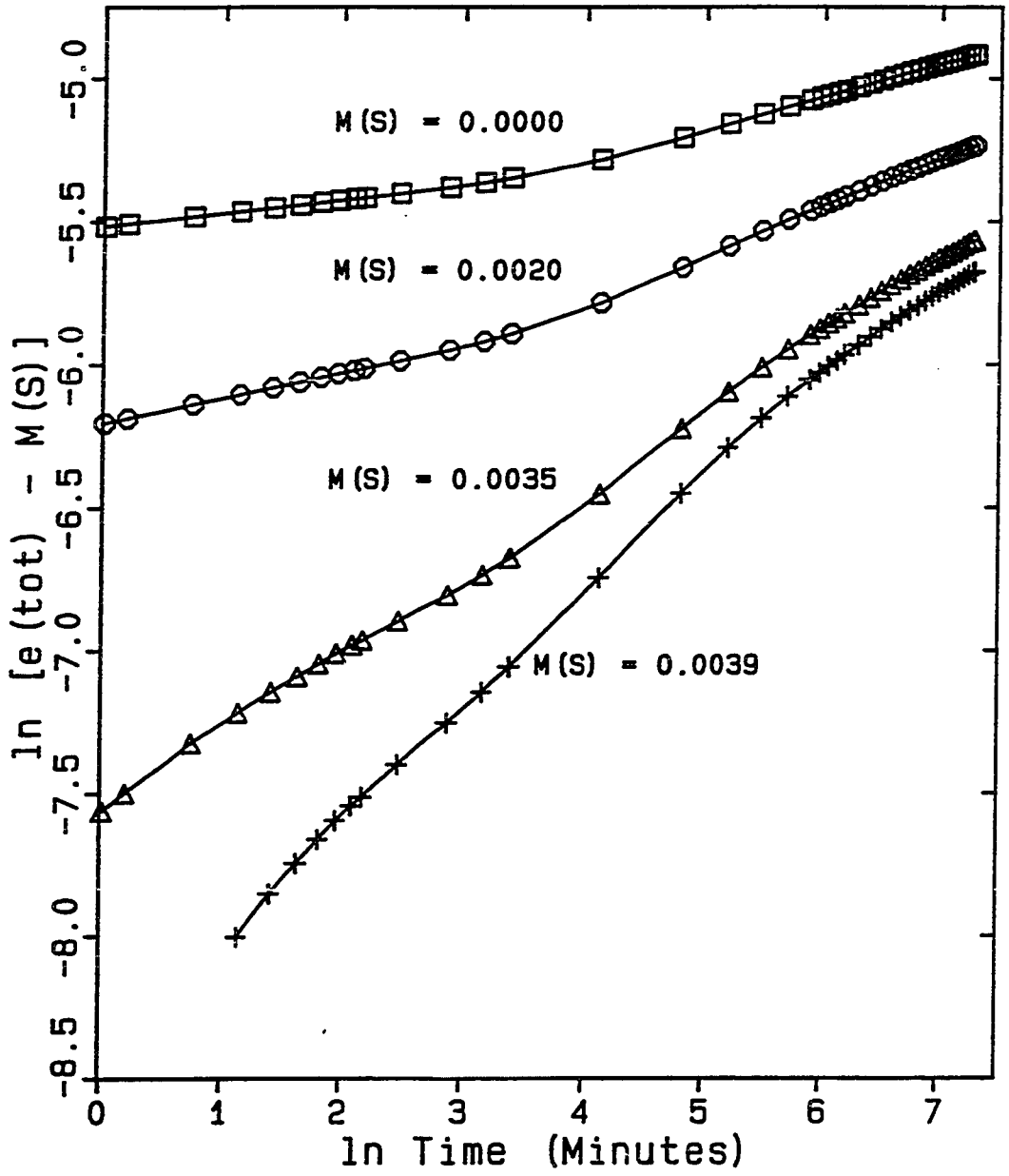

Fig 1.3.1 Manipulation of Kumar's(20) creep data. If M(S)+N.f(t) is assumed, an appropriate choice for M(S) can simplify the form of f(t).

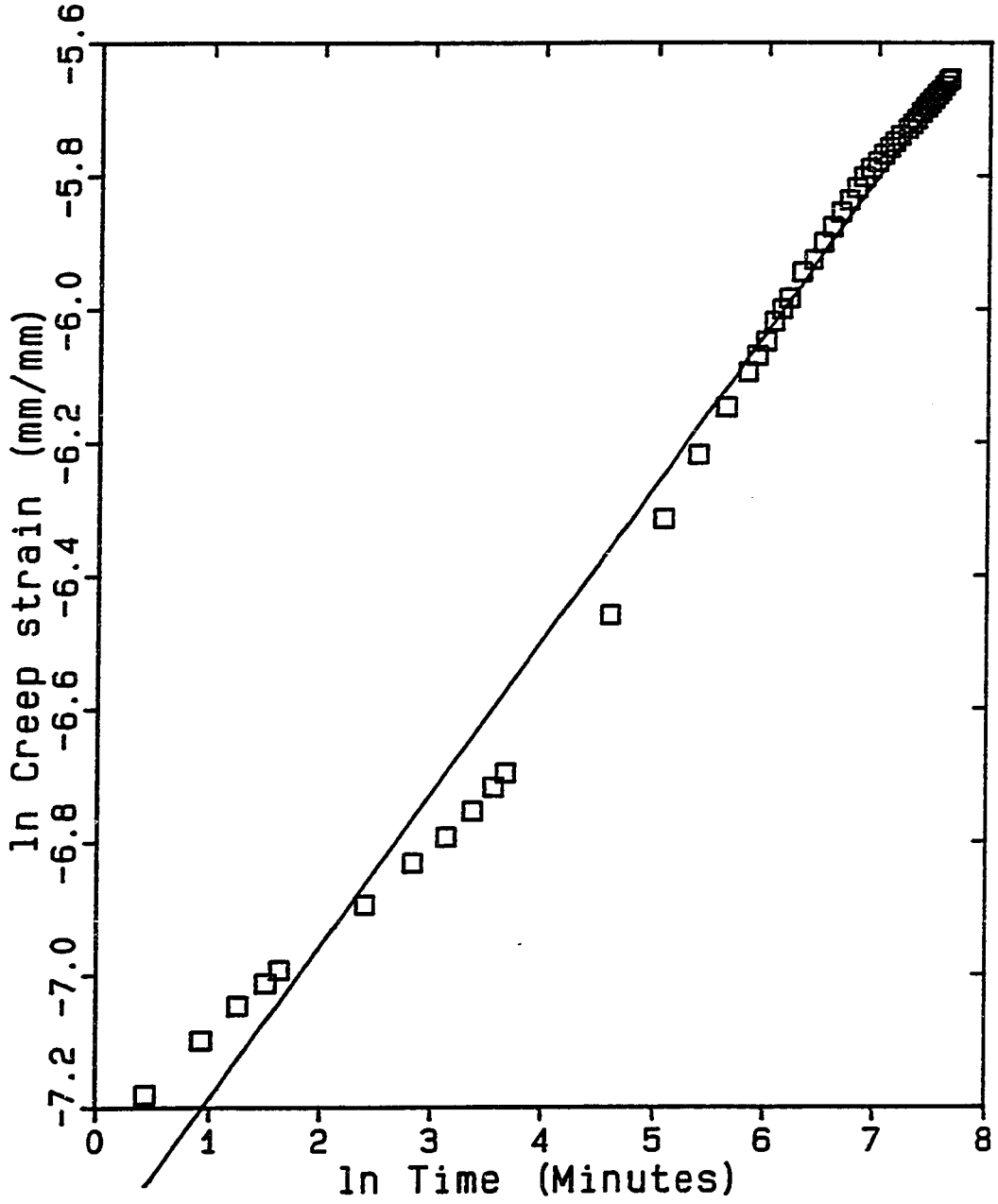

Fig 1.3.2 Isothermal creep strain vs time in an attempt to find the transient strain period (Kumar's data).

CHAPTER 2

SCOPE AND OBJECTIVES

In this research project we set out to :

1. Investigate the flexural creep of pure PMMA and MMA based polymer concrete systems under different conditions of stress, temperature and resin content.

2. Use an alternate method to that of Kumar[20] for obtaining the value of 'n', the exponent in the power law equation : $e_t = e_0 + Kt^n$. Instead of the total strain the strain rate was plotted against time in an effort to eliminate the inaccuracies owing to the sensitivity of the time independent strain e_0. The slope of the least squares fitted line would be (n-1) and the intercept K.n.

3. Study the influence of stress, temperature and resin content on the value of 'n', both in pure and filled resins.

4. Compare the creep behavior of the acrylic PC to that of the parent resin and attempt to correlate the behavior of the concrete to that of the resin.

5. Use this value of 'n' to develop an empirical expression which predicts the creep response of polymer concrete systems in terms of stress and resin content.

6. Conduct long term experiments on polymer concretes to see if the observed responses match the behavior predicted by the empirical equation.

Most of the previous work on polymer concretes has been in tension or compression. In our study we used the flexural mode of testing to generate the experimental data. It is believed that the creep process originates in the resin phase. Hence, the parameters that affect the creep behavior of the parent resin should also influence the creep response of the polymer concretes. Based on this assumption we worked on both filled and unfilled acrylic resin systems and investigated how closely the responses matched. Considerable attention has been given to the temperature dependence of creep and extensive investigations have been conducted to determine the temperature sensitivity of creep. In comparison, studies on stress and resin content, as factors which play an important role in predicting the creep response of polymer composites seem lacking. Also, the nature of the exponent 'n' in

the power law equation has not been investigated in detail. In this work we endeavored to find a method for eliminating the initial strain from the creep equation of polymeric materials in an effort to determine more accurately and easily the creep behavior of polymeric materials. This was simply accomplished by using Findley's creep equation in differential form. Instead of plotting the strain values against time we used strain rates instead. It was seen that the experimental strain responses were reasonably described by polynomial functions and a computer program was used to fit different functions to the observed data. The same program was used to generate derivatives of the interpolating functions at given time intervals. The objective of using this procedure was to provide an alternate method of finding n and K values. It shall be shown how plots of $\ln(de_{tot}/dt)$ against ln t indeed yielded straight lines whose slopes and intercepts would provide us with values for n and K, constants in the power law equation.

CHAPTER 3

EXPERIMENTAL PROCEDURE

3.1 CREEP APPARATUS

All creep experiments were carried out in flexure, using the set-up shown in Fig. 3.1. Three specimens can be loaded simultaneously using this arrangement . Dead weights are used to load the specimens. Their effect is magnified by a ten-to-one lever arrangement so that high stresses can be achieved using relatively low dead weights. The specimens are housed inside a casing used to protect the experiments from drafts and other external disturbances. Thus, significant stress - strength ratios are generated by using dead weights ranging from 500 to 3500 grams. A four-point loading mode is employed using two loading noses resting on top of the specimen The support span is 15.2 cms. Once the dead weight is applied to the lever arm the force is transmitted to the connecting rod which in turn transfers the load onto the two loading noses resting resting on the specimen. A linear variable differential transformer (LVDT) is attached to the connecting rods and its output is digitally recorded. The LVDT is first calibrated using a micrometer set up (appendix A).

Temperature fluctuations within the casing are monitored by using a copper/constantan thermocouple using ice-water as the thermocouple reference state. The average temperature under ambient conditions is 24^0C +/- 2^0C.

We covered a stress range from 5 to 17 Mpa for the unfilled polymethyl methacrylate and 6 to 11 Mpa for the polymer concretes. In the latter case lower stress values had to be used owing to quicker failure of the polymer concretes compared to the parent resin.The stress was calculated using the following relation[22] :

$$S = PL / bd^2 \qquad (3.1.1)$$

where,

P = Applied load at a given point in the load deflection curve

L = Support span, mm

b = Specimen width, mm

d = Specimen depth, mm

S = Applied stress, Mpa

The flexural creep strains correspond to the maximum strain in the outer fibers at midspan and are given by :

$$e = 4.70 (Dd/L^2) \qquad (3.1.2)$$

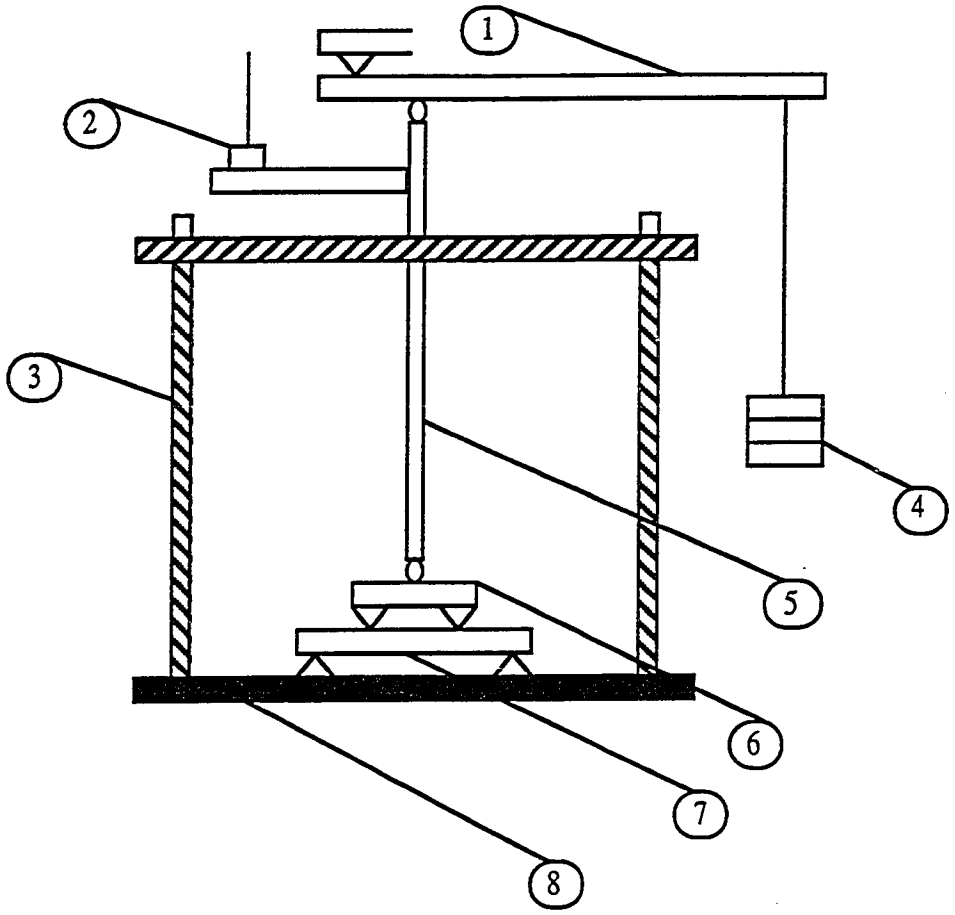

1. Lever arm
2. Linear variable differential transformer
3. Rigid frame
4. Dead weights.
5. Connecting rod
6. Loading noses
7. Specimen
8. Base plate

Figure 3.1 Sectional view of the flexural creep apparatus.

where,

e = strain, mm/mm

D = midspan deflection obtained from LVDT readings.

d = Specimen depth, mm

L = Support span, mm

It is important to note that the above relation utilises midspan deflections ($D_{L/2}$) whereas our deflections are measured at a length equal to one third of the support span ($D_{L/3}$). Some simple calculations based on the fundamentals of mechanics show that $D_{L/2} = 1.15\ D_{L/3}$. Thus midspan deflections may be easily computed and consequently creep strains measured using equation 3.1.2.

3.2 METHODS AND MATERIALS

3.2.1 Acrylic Resin System

The unfilled polymethyl methacrylate (PMMA) which was used for the first part of the experiments was provided by Rohm and Haas (available under the trade name of "plexiglass"). PMMA is a linear

thermoplastic polymer, resistant to most inorganic solvents and some organic solvents. It resists the plasticizing action of water and is therefore unaffected by atmospheric humidity. It undergoes glass transition at a temperature of 100^0C, and consequently its mechanical properties show a strong temperature dependence within the range from 0^0C to 100^0C.

Methyl Methacrylate (MMA) was the primary monomer, used for making the particle reinforced composites which were later subjected to mechanical testing. MMA was supplied by Du Pont. It is a clear, low viscosity monomer with a high volatility and a sharp, pungent odor. Approximately one part per million can be detected by smell. It polymerizes easily within temperature ranges from 0^0F to 100^0F when combined with the proper initiators, and accelerators (promoters). During our specimen preparation MMA was cured at ambient temperatures.

Acrylic resins provided by the Sartomer Company were used to provide shrinkage control. The two resins used were Sartomer 205 (Triethylene Glycol Dimethacrylate) and Sartomer 231 (Diethylene Glycol Dimethacrylate). These are clear liquids with mild odors, high boiling points and low viscosities. These resins act as crosslinking agents as they are difunctional monomers . Owing to their relatively high molecular weights the sartomers have low vapor pressures which helps reduce the unpleasant MMA

odor when they are mixed together, and reduces considerably evaporation losses at peak polymerization exotherm.

The acrylic resin used in the preparation of the polymer concrete specimens contained small amounts of PMMA powder (Elvacite 2013) provided by Du Pont. The main purpose for using this PMMA powder was to increase the viscosity of the resin in order to maintain uniform suspension of the filler particles during polymerization, as well as further decrease monomer evaporation at peak exotherm.

Free radical addition polymerization was used to prepare the specimens. Benzoyl Peroxide (BPO) was used as the initiator in the form of a paste containing 40% BPO. The promoter, DMPT, was used in conjunction with the BPO to accelerate the polymerization process by lowering the activation energy for the generation of free radicals.

3.2.2 Coupling Agents

In order that a filler not be detrimental to mechanical properties, stress must be efficiently transferred from the polymer to the filler[23]. However, unlike organics which are hydrophobic, inorganic filler particles have hydrophillic surfaces. As a result

adhesion between the resin and filler particles is poor. The tendency of the inorganics to absorb water further degrades adhesion and worsens the problem. Coupling agents are used to overcome these difficulties. The most common coupling agents are silanes with the general formula $YRSi(OR')_3$. The (OR') group reacts with the inorganic substrate and the Y group reacts (forms secondary bonds) with the polymer thereby enhancing interfacial adhesion. The silane can be added to the filler as a pre-treatment step or it can be added directly to the resin during the processing stage where it migrates to the resin/filler interface. Another advantage provided by these coupling agents is that by converting an otherwise hydrophillic surface to a hydrophobic one compatibility with the polymer is improved. This helps in producing a easier and more uniform dispersion of the filler in the polymer. Also, for a given amount of filler the viscosity may be significantly reduced, thus improving processability. For the polymer mortar in our study we used a silane coupling agent. r-Methacryloxypropyl - trimethoxy silane was provided by Polyscience. The functional groups in them react with both the sand and the resin to form hydrogen or covalent bonds. In our systems the silanes were added directly to the resin.

3.2.4 Additives

The mineral Montmorillonite, a hydrated clay mineral was

dispersed in the resin phase of the acrylic polymer concrete systems in order to control setting stresses and obtain zero cure shrinkage systems. Cure shrinkage is a typical property of most polymerization systems. The formation of macromolecular chain networks involves the conversion of secondary bonds (bond distances of 3 - 4 Å) to primary bonds with shorter bond distances (bond distance about 1.5 Å), thereby causing a decrease in volume. In highly filled polymer systems, where the solid aggregate particles occupy over 60% of the volume, the resin no longer forms a continuous phase. It is confined largely in the discrete spaces between the rigid aggregate particles, where it is forced to cure at constant volume. This constraint in cure shrinkage generates within the polymer matrix setting stresses, which are tensile in nature. When the cured composite is subjected to external loads the presence of setting stresses causes a considerable decrease in strength (ca. 25% in compression and 30-35% in tension or flexure). Consequently, special additives are used in these composites to counteract cure shrinkage and eliminate setting stresses. One such additive system developed in these laboratories[24,25] is the mineral montmorillonite. For our specimens we used specially modified montmorillonite (MMT) particles to provide the necessary shrinkage compensation . The hydration water present in the MMT was replaced by ammonia and then dispersed into the resin. The ammonia forms coordination bonds with the SiO_2 in the mineral which in turn are

broken when the temperatures rise during the exothermic reaction. The gaseous ammonia is now trapped inside the resin imbedded MMT particles and this causes them to dilate significantly. By varying the amount of ammonia-modified MMT we can thus obtain systems in which the net shrinkage is zero and setting stresses are absent. Consequently, the strengths of the PCs can be increased by about 20%-40%.

3.2.4 Aggregates

Silica sand was used as the aggregate, supplied by the Clemtex Corporation in Houston, Texas. The particle size ranged from 8 to 100 mesh. Depending on the resin content desired, the amount of filler used was varied. For our specimens we worked within a range of 78% - 85% by weight, of sand. Much of the heat generated from the polymerization exotherms is lost in the heating of the aggregate particles. As these constitute a major portion of the polymer concrete system there results a reduction in the peak exotherm temperature during cure.

3.2.5 Specimen Preparation

The composition of the acrylic polymer concrete system is shown in Table 3.2.1. Four different resin - aggregate ratios were used to give samples having resin volume fractions of 0.33, 0.36, 0.39, and 0.41. The following steps were followed in the preparation of the polymer mortar and the polymer cement systems : 1) The PMMA was dissolved in the MMA and to the resulting solution the acrylic dimers were added and mixed. 2) The initiator, promoter and coupling agents were then dissolved in the resin. 3) MMT or MMT/aggregate was then blended into the resin. 4) The polymer mortar mixture was poured into rectangular molds along with the siliceous aggregates. The mixture was now left to cure at ambient temperatures. After curing, the specimens were allowed to cool down before demolding. The polymer concrete bricks now obtained had dimensions of 6" x 4" x 2". For testing purposes these were cut up into smaller specimen sizes having average dimensions 6" x 1" x 1/2" using a circular saw. Diamond blades provided by Felker were used for cutting the samples. In addition, the surfaces of the samples were further finished on the belt sander to achieve (reasonably) uniform thickness and parallel surfaces. Our specimens were now ready for the creep experiments. The elapsed time between the cure and the testing had no effect on the creep responses of the material.

TABLE 3.2.1 Composition of acrylic polymer concrete systems.

Component	Weight %
Acrylic Resin System	
Methyl methacrylate (MMA)	42.7
Triethylene glycol dimethacrylate (Sartomer 205)	20.0
Diethylene glycol dimethacrylate (Sartomer 231)	12.0
Poly methyl methacrylate (PMMA)	15.0
Fumed silica (Cab-O-Sil)	2.0
Benzoyl Peroxide (40 % paste)	1.0
N, N' dimethyl p-toluidine (DMPT)	0.3
3-methacryloxypropyltrimethoxy silane	1.0
Ammonia modified Montmorillonite (MMT)	6.0
Mineral aggregates	
#1 Sand (8-20 mesh size)	40.0
#3 Sand (16-40 mesh size)	30.0
#6 Sand (60-100 mesh size)	30.0

Note : A combination of the acrylic resin system and mineral aggregates was used to make PC samples having differents amount of resin by weight. For example PCs with v=0.39 contain 20 % acrylic resin and 80 % mineral aggregates.

3.3 LOADING MODE

Beams can be subjected to four different modes of deformation : tensile, compressive, flexural and torsional. In our study we used the flexural mode of testing which is both easier and more economical than compression tests. Using the lever arm arrangement for the flexural tests, large stress - strength ratios may be generated using relatively low weights, whereas in compression, much higher loads would be required to produce similar stress - strength ratios. In pure bending of a beam, the longitudanal fibers on the convex side (i.e. below the neutral axis) suffer an extension, while those on the concave side (i.e. above the neutral axis) undergo compression. On this basis flexural behavior may be used to provide information on both the tensile and compressive properties of the material.

Flexural tests may be performed using a distributed load, three-point or four-point load. For a simply supported beam, three-point loading imposes the load on a single point or line in the center of the beam. It is on this line that we have the maximum bending moment and the maximum axial fiber stress. On the other hand, in four-point loading, the shear force is zero and the bending moment constant over the central portion of the beam between the two loads. The maximum fiber stress acts uniformly over the distance between the two loading noses, which in our case is one-third of the total support span. Thus, any irregularities

in measuring flexural responses owing to the presence of point defects on a line in three-point loading, are removed in the four-point mode, as the maximum bending moment in this case occurs over an area and not a line. Figure 3.3.1 shows the shear and bending moment diagrams for a beam loaded in four-point[26,27].

In figure 3.3.1 (a) the beam shown is loaded by two equal forces P each at a distance of L/3 away from the supports, where L is the total support span. Figure 3.3.1 (b) isolates a section of the beam at a distance of x from the left support. This section is applicable for any value of x just to the left of the applied force P. As can be seen from figure 3.3.1 (c), the shear remains constant irrespective of the distance from the support and its value is +P.

On the other hand, the bending moment varies linearly from the support, and reaches a maximum of +P.L/3. In figure 3.3.1 (d) we have shown an arbitrary section applicable anywhere between the two applied loads. In this section no shearing force is necessary to maintain equilibrium of a beam segment. In this zone a constant bending moment of +P.L/3 must be resisted by the beam. Under such conditions of flexure the bending is called 'pure' bending. There is no axial force at any section in the beam, hence the absence of axial-force diagrams. The complete shear and bending-moment diagrams are shown in figures 3.3.1 (c) and (e).It should be noted that the LVDT readings correspond to deflections

at a distance of one-third of the support span. We are, however, interested in midspan deflections for the purpose of our strain calculations. The two values can be interrelated fairly easily from

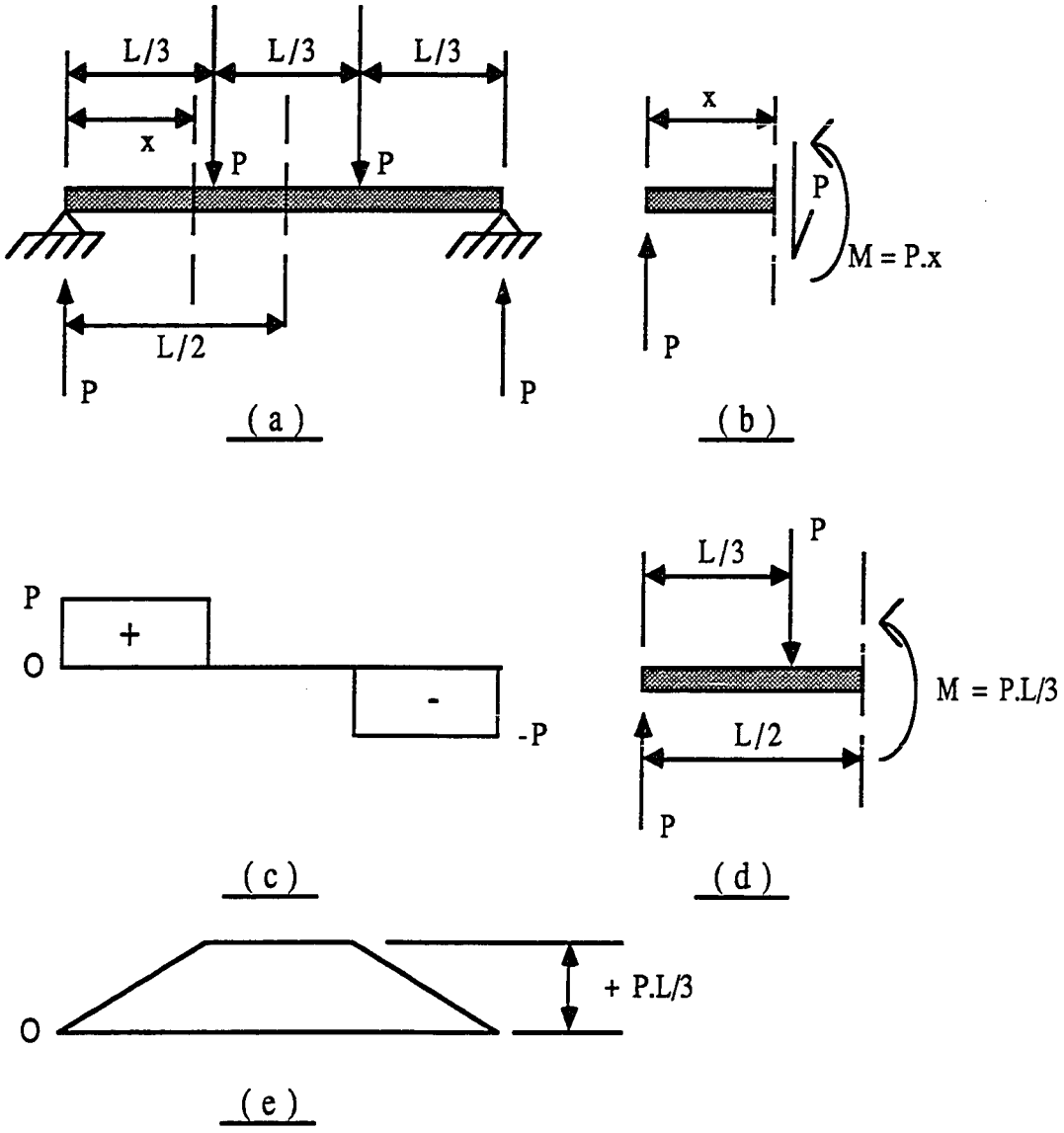

Figures 3.3.1 (a) - (e). Shear and bending - moment diagrams for a beam loaded in four - point.

basic mechanical equations[20]. For the beam loaded as shown in

figure 3.3.2 the deflections at midspan and at one-third the length were calculated using the following equations developed for elastically deforming materials,

$$D_{L/3} = 0.030864 \; . \; (\; PL^3/EI \;) \qquad (3.3.1)$$

$$D_{L/2} = 0.035494 \; . \; (\; PL^3/EI \;) \qquad (3.3.2)$$

where, E = elastic modulus, I = first moment of area,
P = applied load & L = support span.

From the above two equations the deflections at midspan can be estimated from the deflections at the point of measurement (one-third of the support span), so that, $D_{L/2} = 1.15 \; D_{L/3}$. In materials where E is time - dependent we assume that D follows the same dependence.

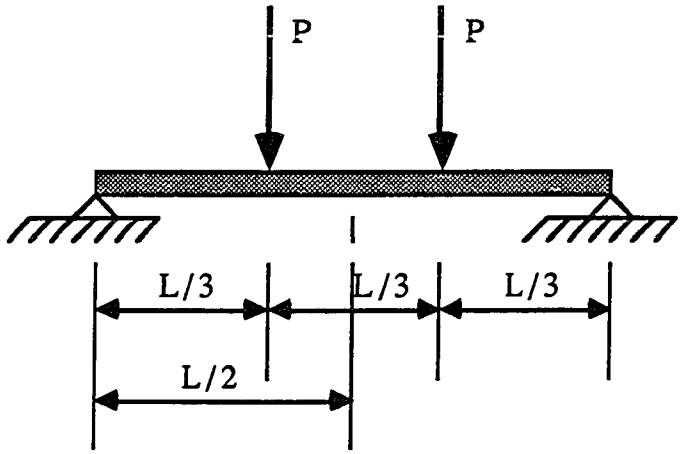

$$D_{L/2} = 1.15 \; . \; D_{L/3}$$

Figure 3.3.2 The relation between deflections at one-third the support span and those at midspan.

CHAPTER 4

RESULTS AND DISCUSSION

4.1 FLEXURAL CREEP BEHAVIOR OF UNFILLED PMMA

The total time - dependent strain in a creep experiment can be separated into three components : the elastic component (e_{el}), transient component (e_{tr}) and the creep component (e_{cr}). The transient strains include short term changes caused by rapid equilibration of stress concentrations owing to small misalignments of the polmer specimen. For flexural experiments the total time dependent strain is given by d/2R, where d is the beam thickness and R the radius of curvature of the bent beam.

Fig. 4.1.1 shows the nature of the strain - time curves obtained in flexural creep experiments with pure PMMA at a constant temperature of 45^0C, with different imposed stresses. It is evident from the creep curves that stress has a strong influence on the isochronal creep strains, an increase in stress levels causing higher values of creep strain. Accordingly to Findley[6], the total strain can be expressed as seperate functions of time-independent

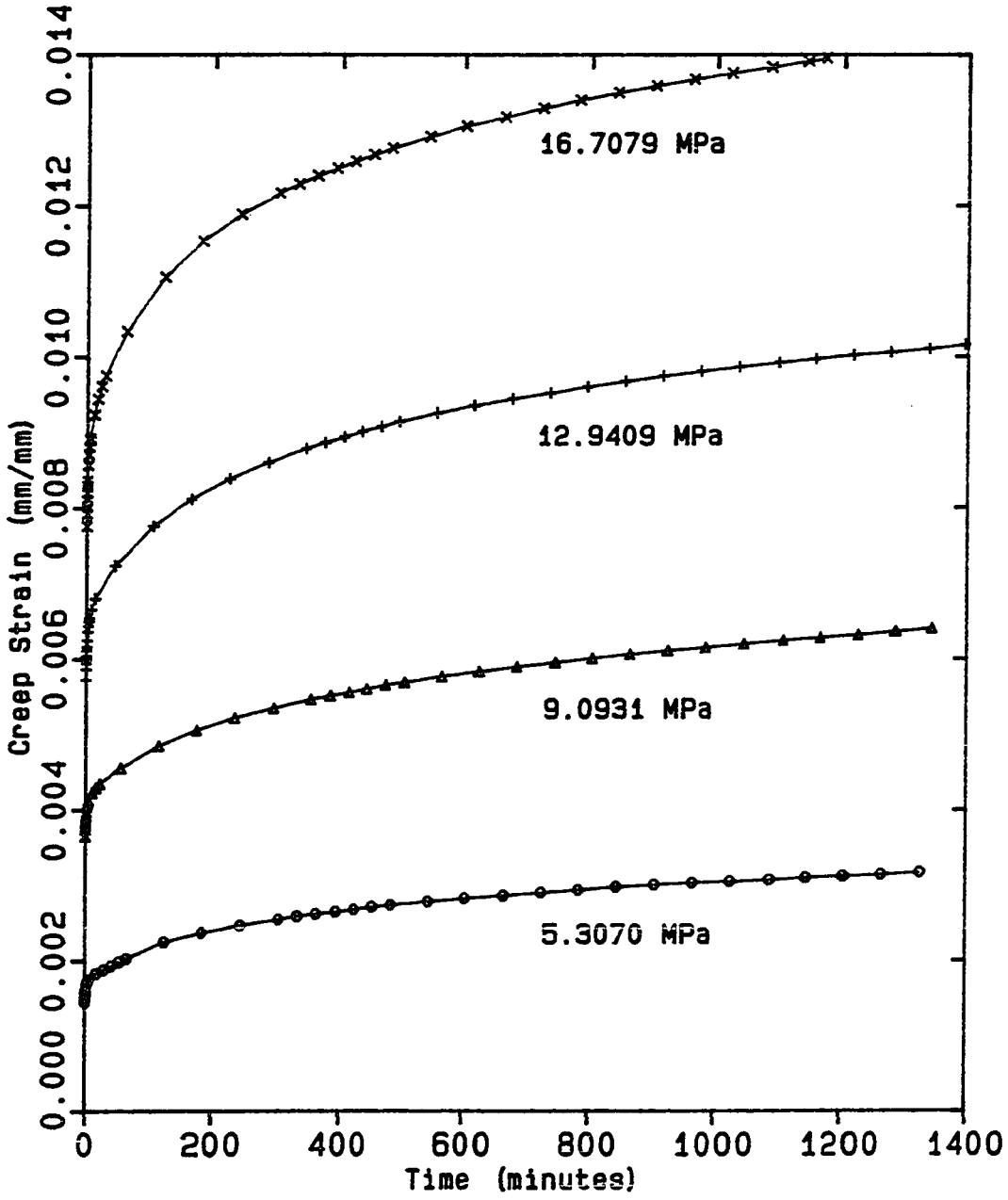

Fig 4.1.1 Flexural strain versus time for PMMA at 45C and changing stress levels.

and time - dependent strains such that :

$$e_{tot} = e_0 + Kt^n \qquad (4.1.1)$$

where e_0 is the time - independent strain, and n and K are constants.

It should be noted that e_0 may or may not be the same as the elastic strain. It is merely a value of strain used to fit the data. Plots of total strain minus the time independent strain ($e_{tot} - e_0$) versus time on a logarithmic scale should therefore yield linear plots provided a proper value of the initial strain is used. Fig. 4.1.2 shows the effect of different e_0 values on the creep resonse curves for PMMA. There is a significant shifting of the creep curves and for the initial part of the experimental data one does not get straight lines at all. In this work we endeavored to find a method for eliminating the initial strain from the creep equation of polymeric materials in an effort to determine more accurately and easily the creep behavior of polymeric materials. This was simply accomplished by using Findley's creep equation in differential form. Instead of plotting the strain values against time we used strain rates instead.

Differentiating equation (1.3.5) we get :

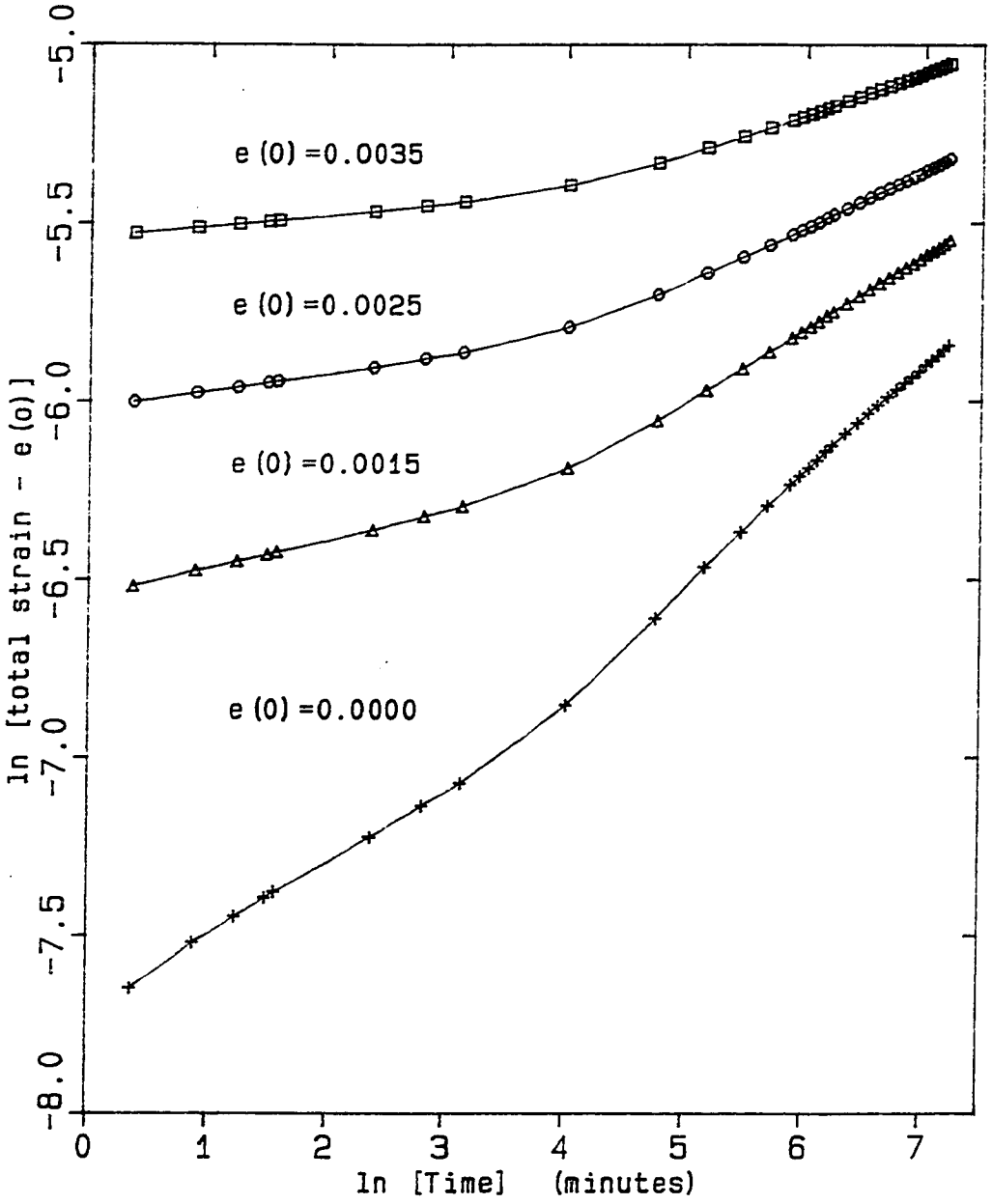

Fig 4.1.2 The effect of the initial strain e(0) on the nature of creep curves.

$$de_{tot} / dt = n \cdot K \cdot t^{(n-1)} \qquad (2.1)$$

assuming that the time independent strain e_0 is a constant under the given conditions. Taking logarithms on both sides of the above equation we then have :

$$\ln (de_{tot} / dt) = \ln (n \cdot K) + (n-1) \ln t \qquad (2.2)$$

Since the exact form of the time-dependent creep equation is not known we used curve fitting techniques to describe the data. A computer program was used to generate polynomial functions to interpolate between the experimental data points. It was seen that polynomials fit the data quite well. The values of the derivatives of the interpolating functions at different times were computed by the same program. Plots of $\ln(de_{tot}/dt)$ against ln t were now made as shown in Fig 4.1.3 and Fig.4.1.4, at two different temperatures and stress levels. Thus, an easier alternative was used to evaluate the n and k values, constants in the power law equation. As expected from theory we got good straight line correlations. The values of 'n' remained constant at a patricular temperature level but seemed to show some variation with changing temperatures. Variations in stress did not seem to have a noticeable effect on 'n'. Within a temperature range from 22 to 45^0C 'n' ranged from 0.18 to 0.27 which corresponds well with

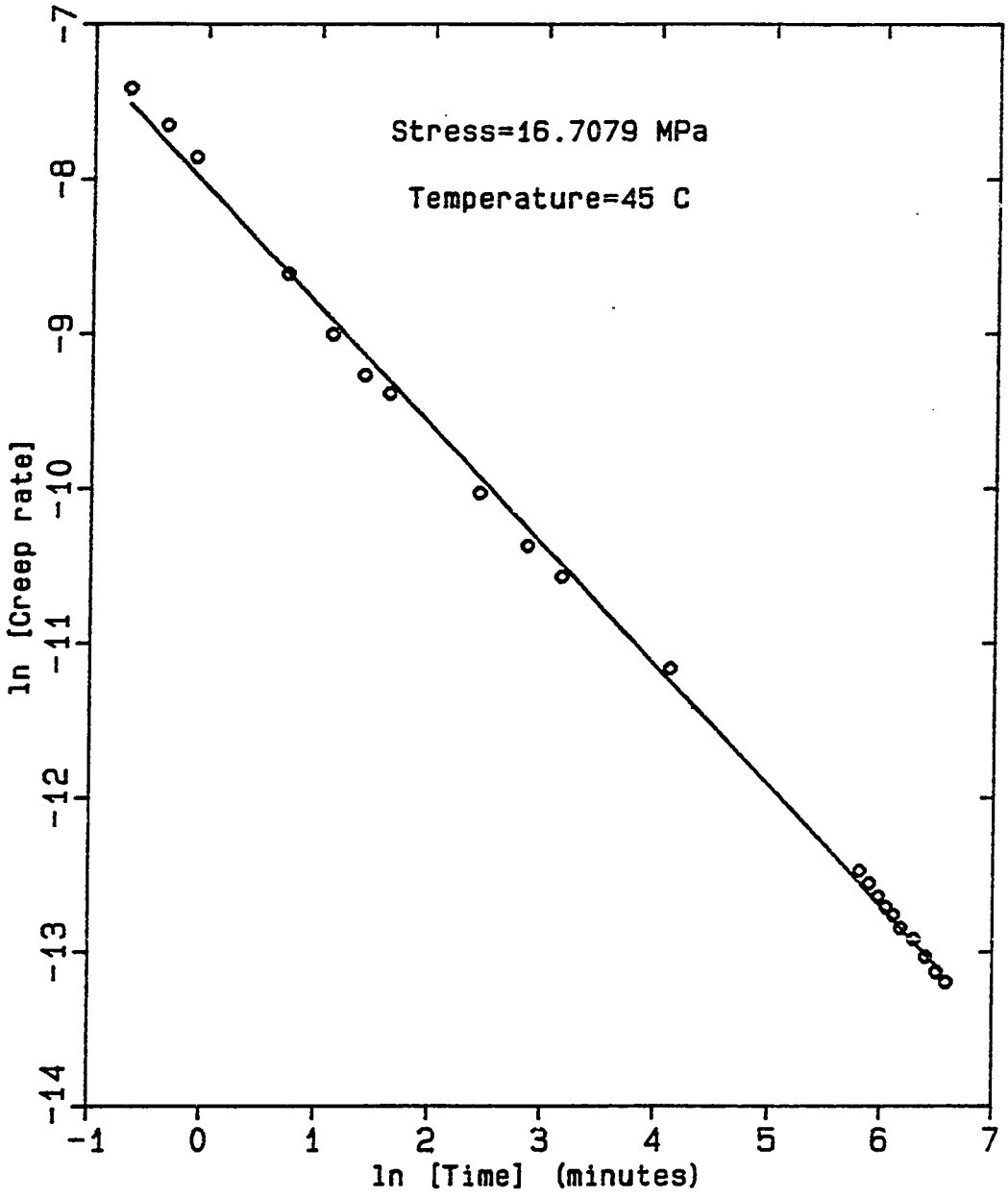

Fig 4.1.3 Creep rate versus time for PMMA at 45 C and 16.7079 MPa stress using the. differential form of Findley's equation.

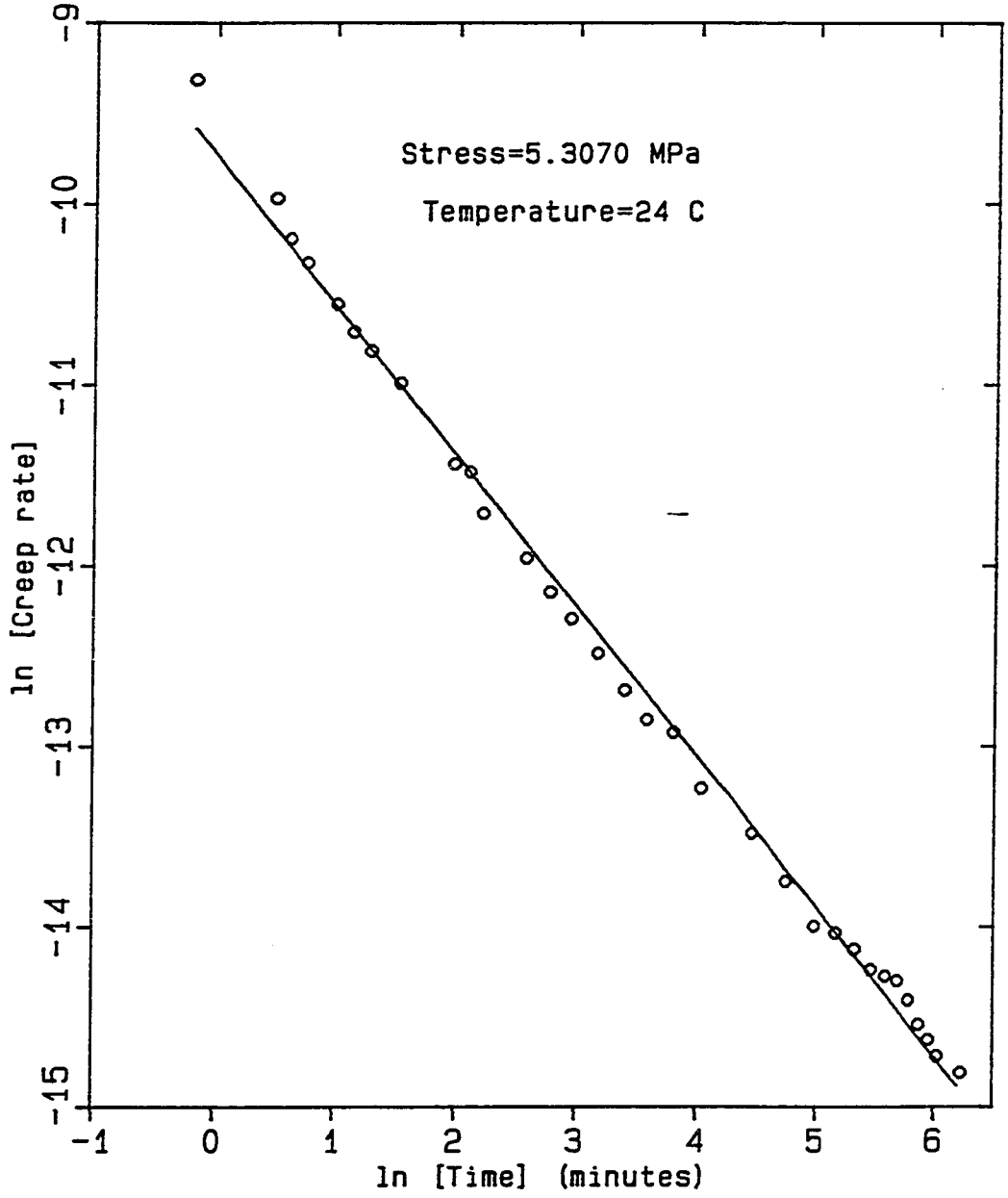

Fig 4.1.4 Creep rate versus time for PMMA at ambient temperature and 5.3070 MPa stress using the differential form of Findley's equation.

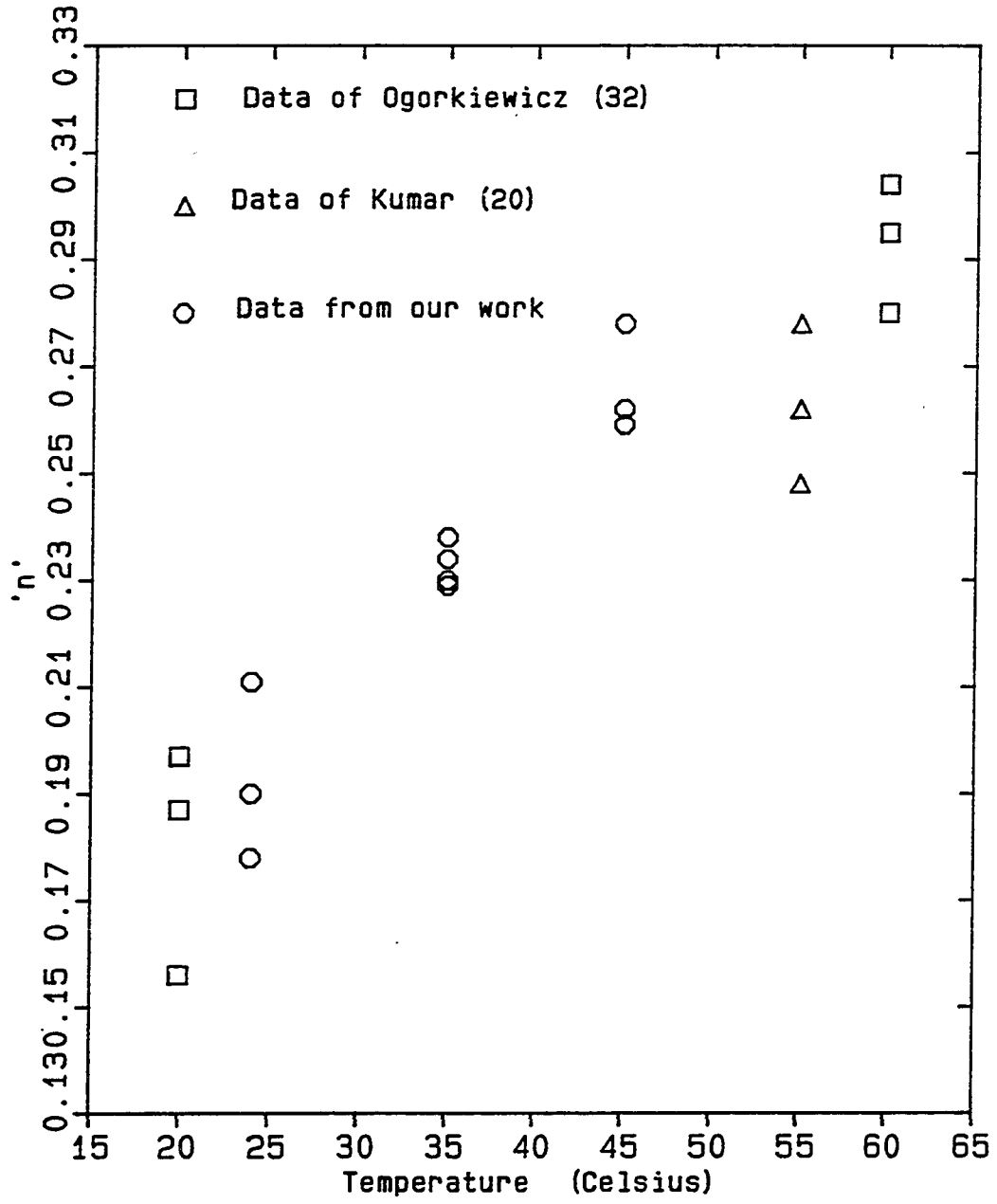

Fig 4.1.5 The effect of temperature on the value of 'n'.

the value of 0.24 observed by Kumar[20] in his work using "plexiglass". Fig. 4.1.5 shows how temperature affects 'n' values, though not much confidence can be put into this behavior, due to considerable scatter of the n values. The plot includes previous experimental data on PMMA from other investigators.

4.2 EFFECT OF STRESS

Creep data for the PMMA samples were collected at various stress levels at constant temperature. Fig.4.1.1 shows the creep curves for PMMA at 45^0C at progressively increasing stresses : 5.31, 9.09, 12.95 and 16.71 MPa. The creep rates for these curves were now computed using the differential form of the power law equation and Fig.4.2.1 shows plots of creep rates versus time on logarithmic coordinates . The solid lines in Fig.4.2.1 represent the best least square linear fit to the data at different stresses. The curves are all linear and parallel to each other with a constant slope (n - 1). An increase in stress causes an increase in the overall creep rate of the specimens. The 'n' values are fairly constant and occur within a range from 0.25 - 0.27. Fig. 4.2.2 shows similar plots at a different reference temperature (35^0C). The 'n' value in this case ranges between 0.22 - 0.24.

In order to reduce the expense associated with the generation of

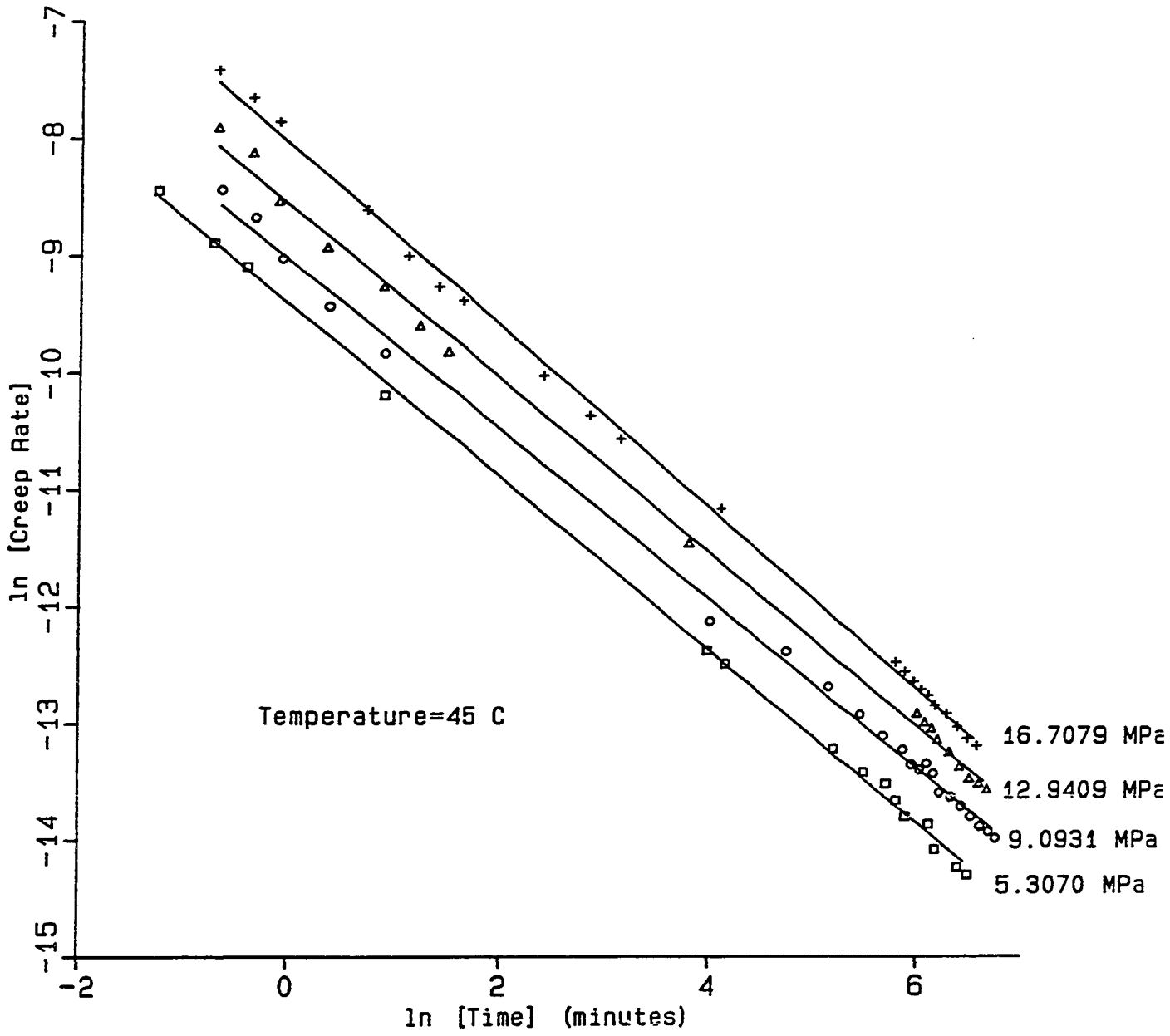

Fig 4.2.1 Creep rates versus time for PMMA at stress levels of 5.3070 MPa, 9.0931 MPa, 12.9409 MPa and 16.7079 MPa.

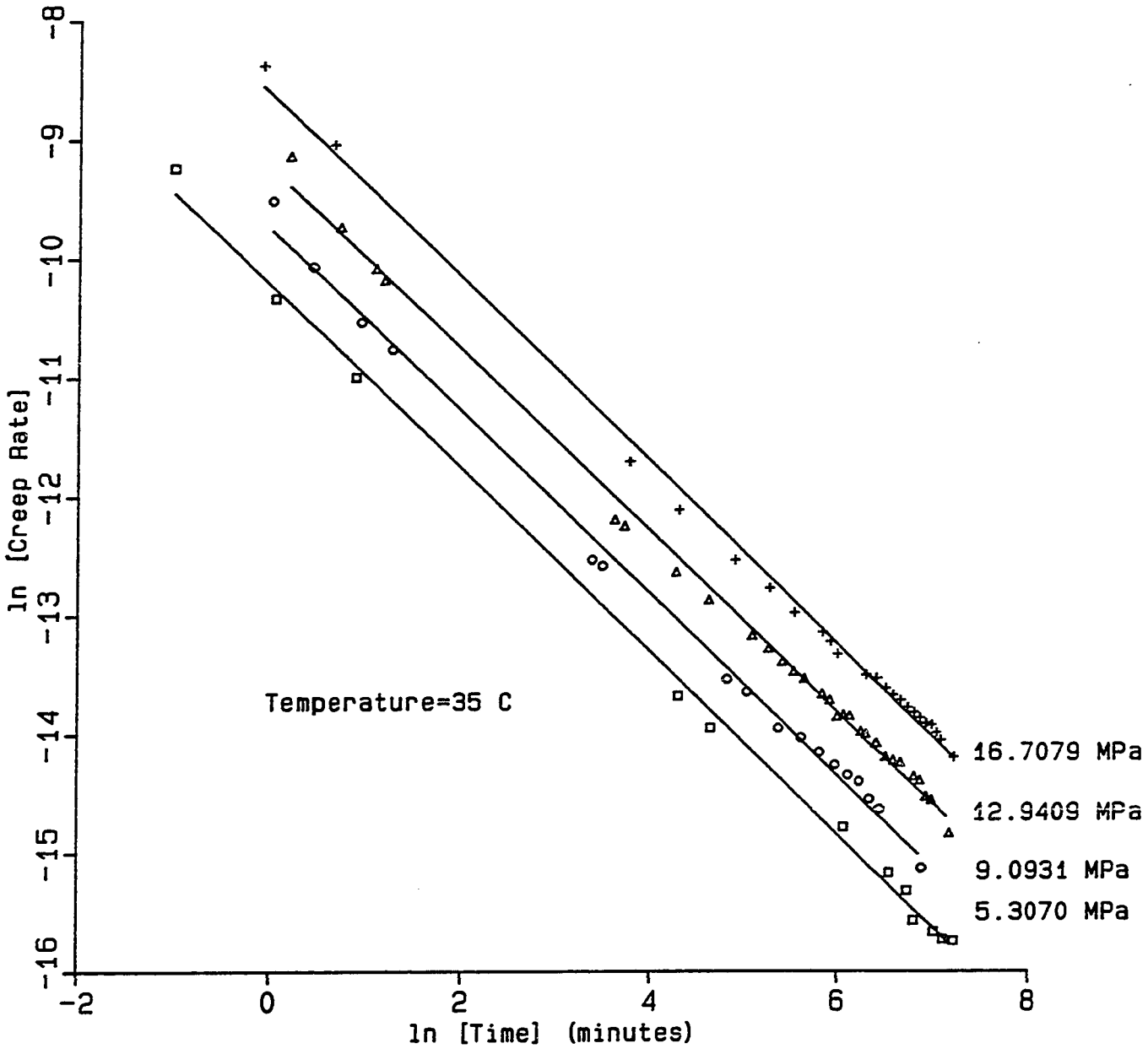

Fig 4.2.2 Creep rates versus time for PMMA at stress levels of 5.3070 MPa, 9.0931 MPa, 12.9409 MPa and 16.7079 MPa at 35 C

sufficient creep information for design purposes, methods for interpolating and extrapolating the experimental data are required. From a practical standpoint it would be of great importance if one could hasten these tests, for example, by increasing the stresses or the temperatures to which the specimens are subjected. However, a fundamental prerequisite[28] to any such kind of acceleration, is that the mechanisms active in the accelerated situation and the actual situations are the same.

For linear viscoelastic polymeric materials a considerable amount of work has been done on extending creep, stress relaxation and other data through the method of time - temperature superposition. The main concept behind this method is to perform short term creep experiments at progressively increasing temperatures and then superpose the creep curves by means of 'shift factors' onto a lower reference temperature, thereby creating a "master curve" predicting behavior for times much longer than the duration of the actual experiment.

Probably the most well known form of such temperature shift-factors was provided by Williams, Landel and Ferry[29]. For polymeric materials above glass transition the shift -factor (a_T) for most amorphous polymers was given by :

$$\text{Log}_{10}\, a_T = (17.44 (T - T_g)) / 51.6 + T - T_g \qquad (4.2.1)$$

where Tg, the glass transition temperature , is used as the reference temperature.

Owing to the severely restricted chain mobility in glassy polymers, they are not expected to follow the W-L-F equation. However, alternate methods of creep data superposition are possible. For many polymers below their glass transition temperature, a_T follows the exponential form of an activated rate process[30] .

We dealt with an analogous process called stress - time superposition, where a master curve was obtained by shifting creep curves at progressively increasing stresses by using different stress shift-factors. For the superposition to be applicable we had to work outside temperature ranges where major thermodynamic changes take place (e.g. glass transition).

Having obtained values for 'n' and K from the gradients and intercepts of the creep curves in Figs. 4.2.1 and 4.2.2 we now use these values to provide a value for the initial time - independent strain e_0. Plots can now be made of total strain minus the instantaneous strain, against time on logarithmic axes. Ignoring data for the first six hours, during which time the plots are nonlinear (owing to the presence of transient strains), we see that the creep curves are linear and parallel (Fig. 4.2.3 & Fig. 4.2.4).

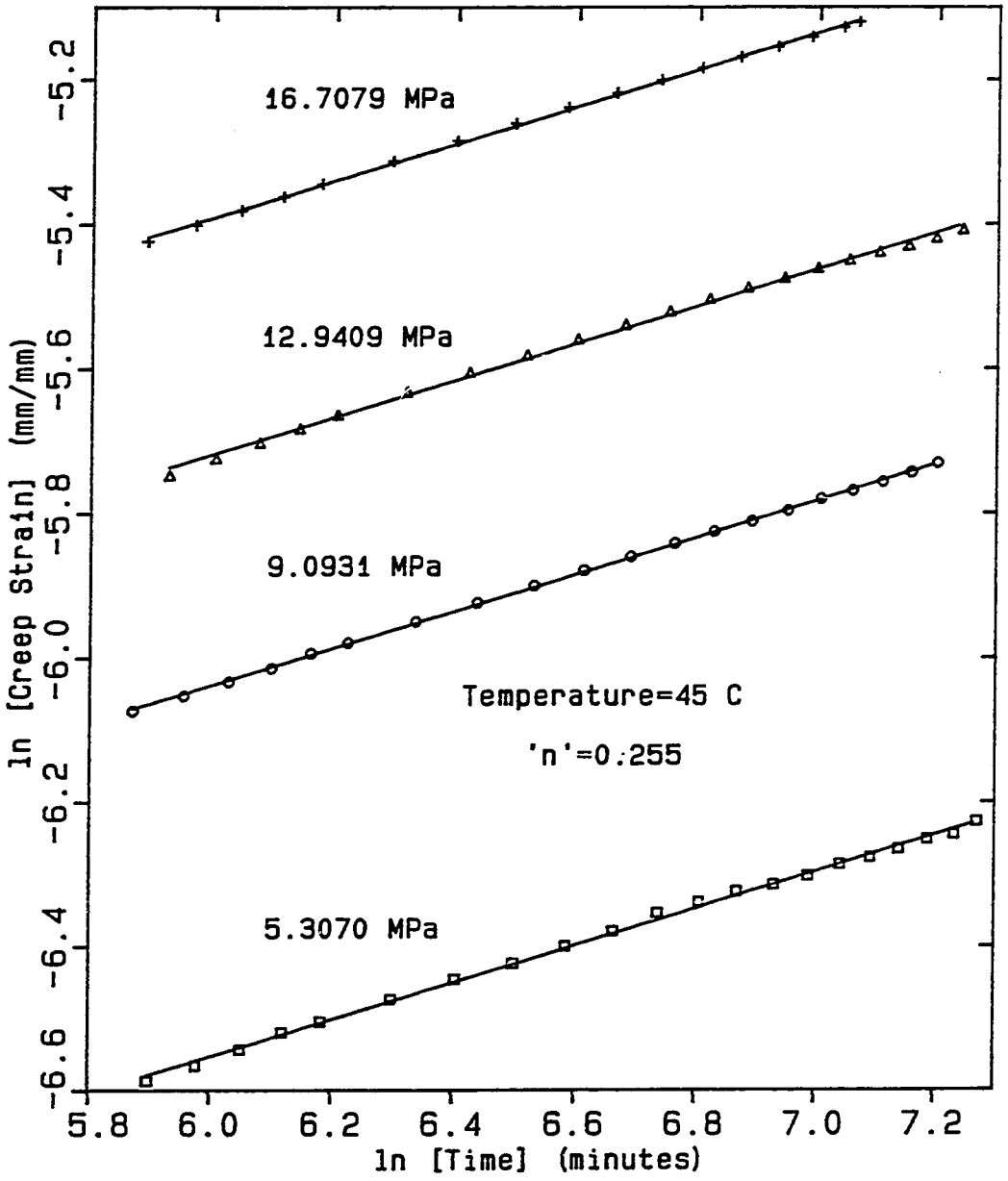

Fig 4.2.3 Creep strain versus time for PMMA at stress levels of 5.3070 MPa, 9.0931 MPa, 12.9409 MPa and 16.7079 MPa at 45 C.

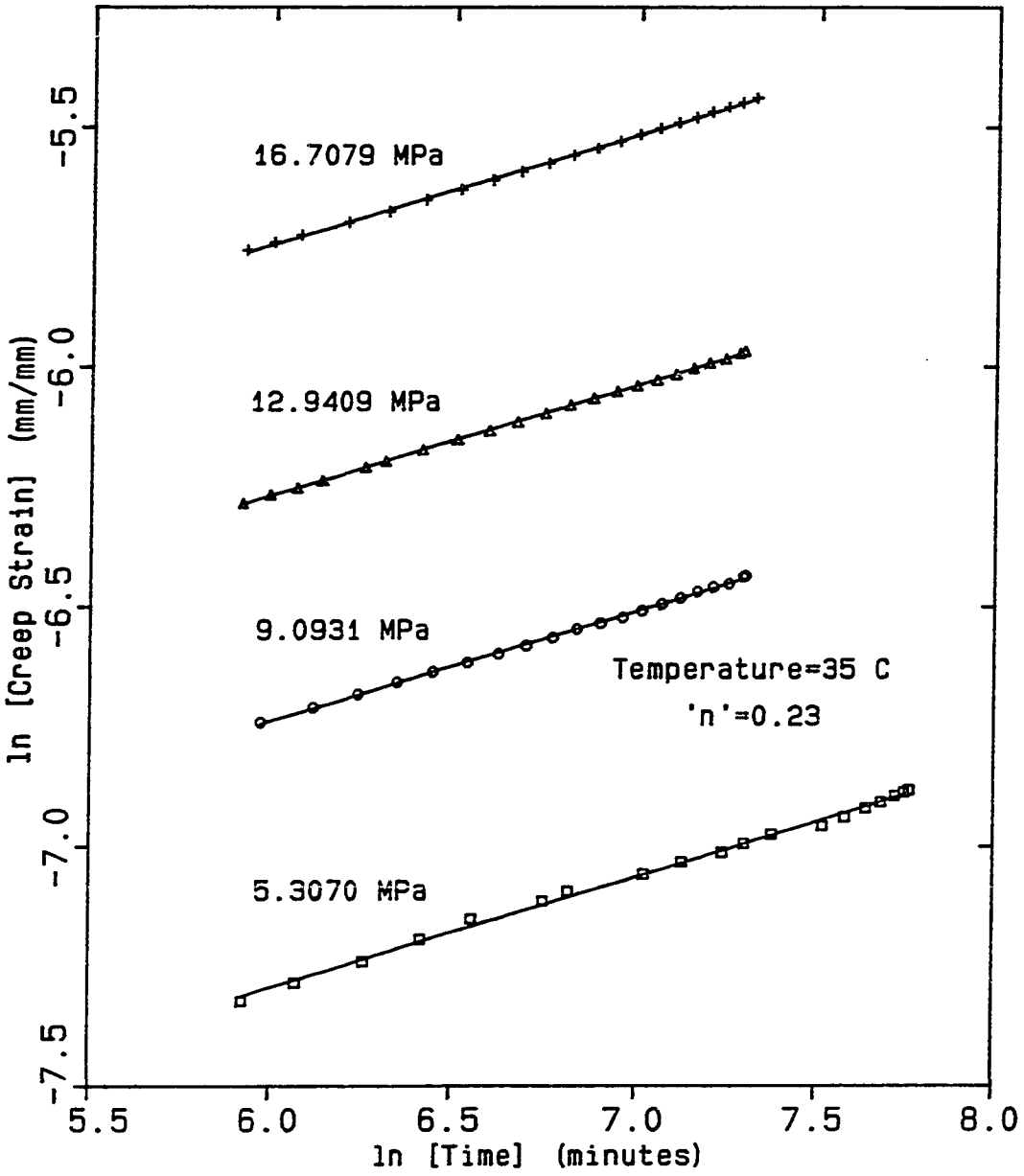

Fig 4.2.4 Creep strain versus time for PMMA at stress levels of 5.3070 MPa, 9.0931 MPa, 12.9409 MPa and 16.7079 MPa at 35 C.

Also, isochronal creep strains increase with increasing stresses indicating a non-linear viscoelastic response at the chosen stress levels. The horizontal shifting of creep curves at different stresses along the log-time axis until they superimpose, can be mathematically represented by:

$$e (S_r, t) = e (S, t/a_S) \qquad (4.2.2)$$

where S_r is the chosen reference stress in MPa and a_S is the stress shift-factor. The creep curves being linear and parallel to one another, two different types of superposition may be used, namely, horizontal or vertical. Horizontal superposition has been used extensively in past studies and has been briefly discussed before. It results in an equivalent shift along the log-time axis. Since the curves are parallel with a constant time exponent we can also use a vertical shifting procedure which is easier in application. In this case the shift factor is expressed as :

$$a_S = e / e_{ref} = K_S \; t^n / K_{S(ref)} \; t^n \qquad (4.2.3)$$

Therefore, the shift factor for vertical superposition simply reduces to :

$$a_S = K_S / K_{S(ref)} \qquad (4.2.4)$$

Franceschini and Momo[28] have proposed a relation between the stress - time superposition and the Zhurkov equation[31] for polymer life. According to them the stress shift-factor a_S is given by:

$$a_S = e^{K (S - S (ref)) / RT} \qquad (4.2.5)$$

where R is the universal gas constant , K is a material constant and S(ref) is the reference stress.

Both horizontal and vertical superposition have been used by Cessna[30] in studies involving filled and unfilled Polypropylene. He used vertical superposition to eliminate time - independent strain and horizontal superposition to produce a "master curve" for true creep at a reference stess level. His vertical superposition is equivalent to our removing initial strain (e_0) from the total strain data.

The stress shift-factors as obtained from the vertical shifting of the creep curves are plotted against against applied stress on semi-logarithmic coordinates in Fig.4.2.5. A linear dependence of ln a_S on stress is noticed thus indicating that the Arrhenius relationship is followed quite well.

$$a_S = e^{(K_S S)} \qquad (4.2.7)$$

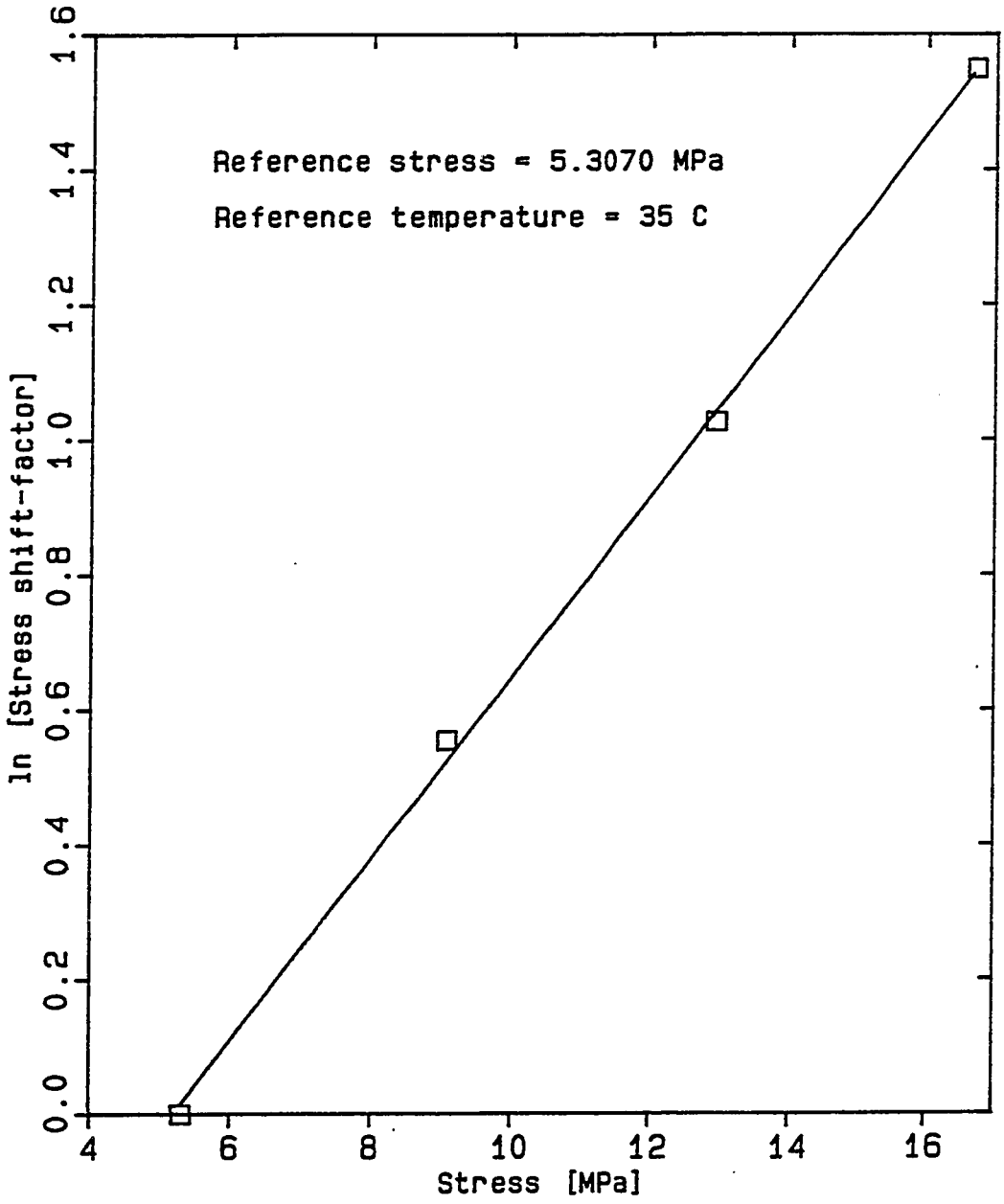

Fig 4.2.5 Stress shift-factors versus applied stress for PMMA at 35 C.,

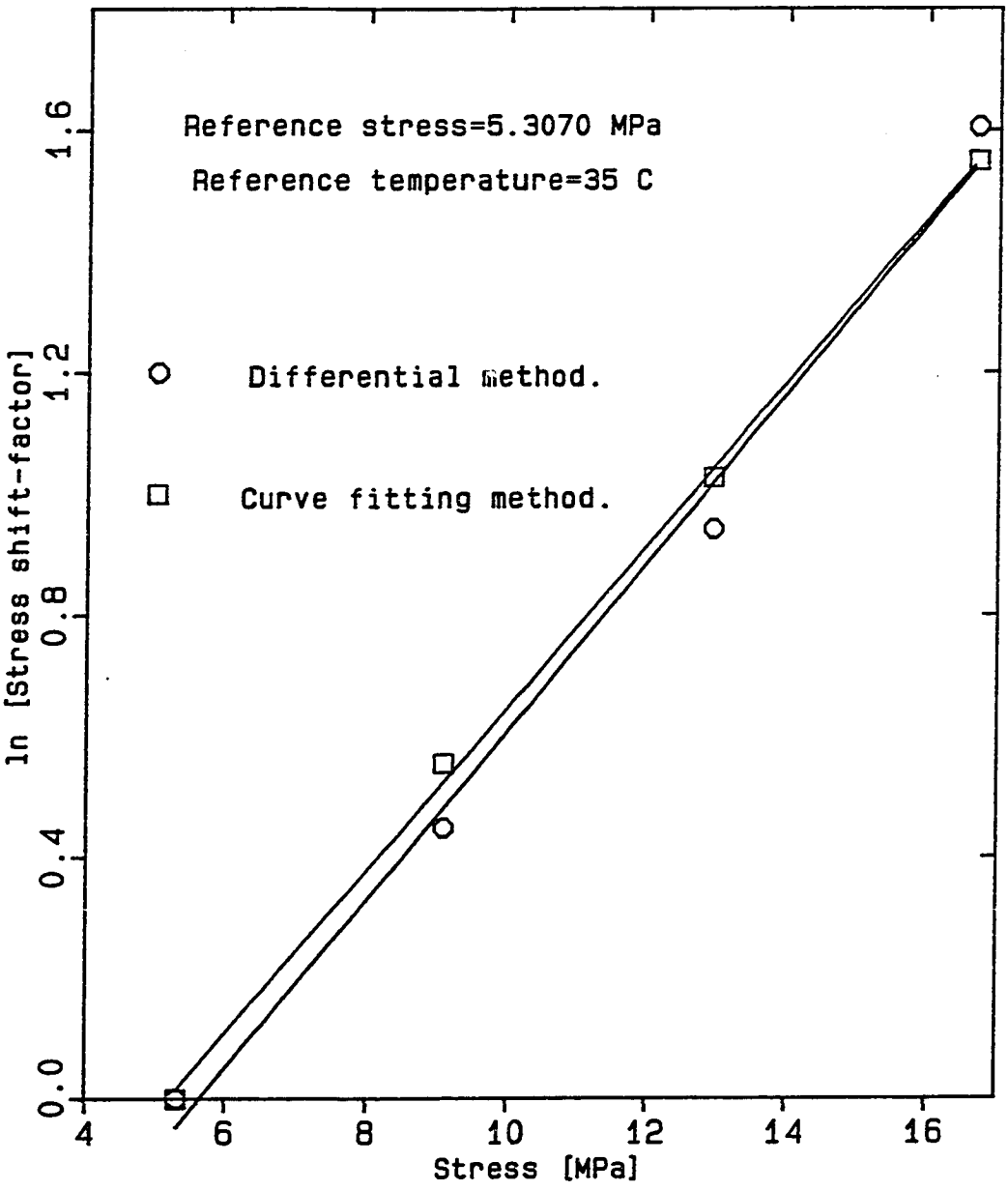

Fig 4.2.6 Stress shift-factors (using different methods) versus applied stress for PMMA at 35 C.,

where K_S is expressed in terms of material constants and temperature.

Fig. 4.2.6 compares the shift-factors obtained from the two different methods. The values are fairly close to one another and the plots have very similar gradients. Thus, we have successfully developed a method by which we can define shift-factors without entering into complexities associated with the uncertain nature of the initial and transient strains.

4.3 FLEXURAL CREEP BEHAVIOR OF POLYMER CONCRETE

After having established a new method for determining the power law coefficient and generating vertical shift-factors based on the differential form of Findley's equation with PMMA samples we now extend this principle to polymer concrete systems using methyl methacrylate as the parent resin. Our object was to study the effect of varying both the stress and the resin volume fraction, on the isochronal creep strains of the PC systems. Fig. 4.3.1 shows typical time-dependent strain curves of the PC at increasing levels of stress and resin loadings. The creep strains increase with an increase in stress levels as seen before with pure PMMA. The increase in creep strains with increasing resin loadings was not surprising since it is believed that creep originates in the resin

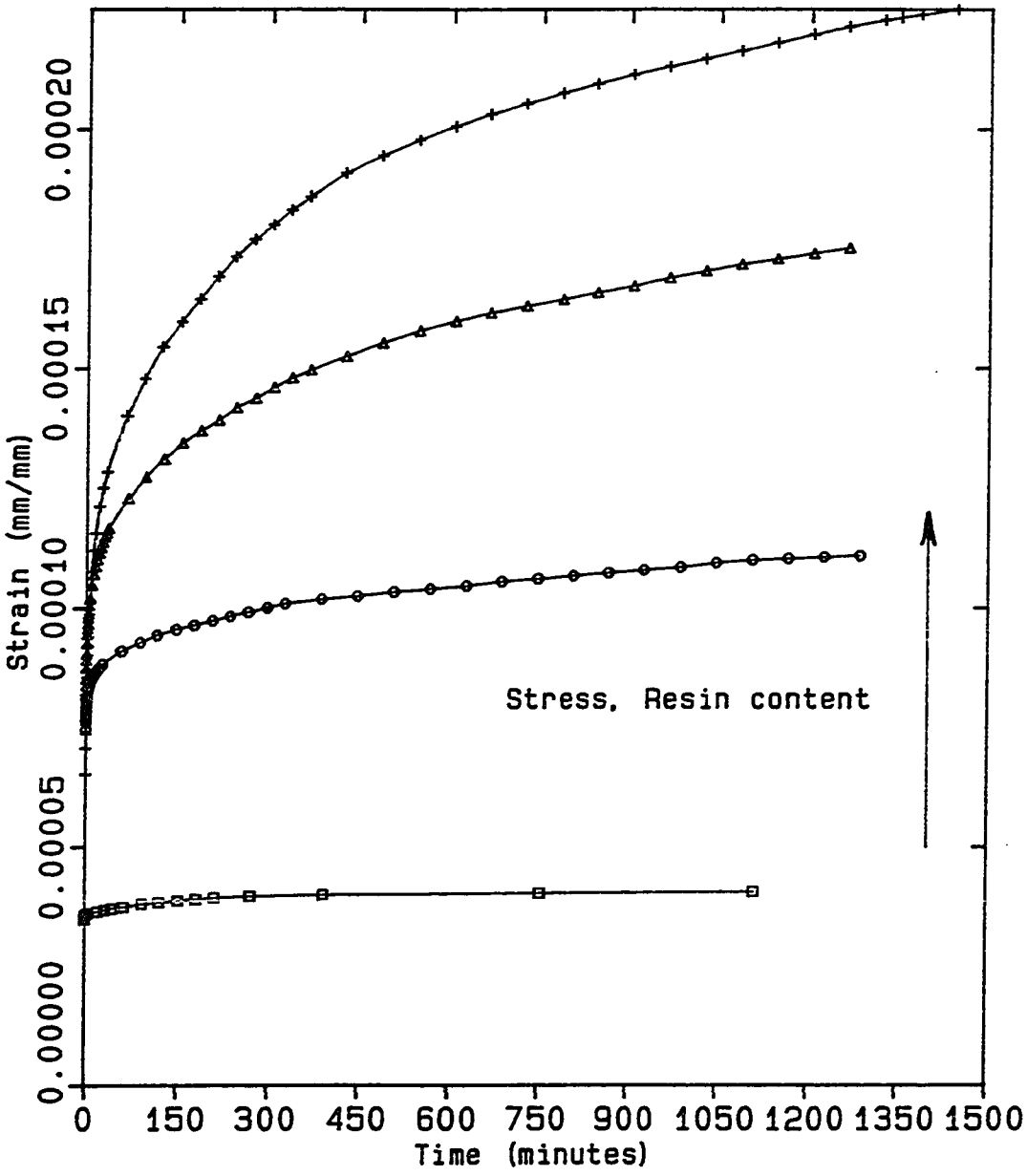

Fig 4.3.1 Strain Versus time curves for PC at increasing levels of stress and resin content.

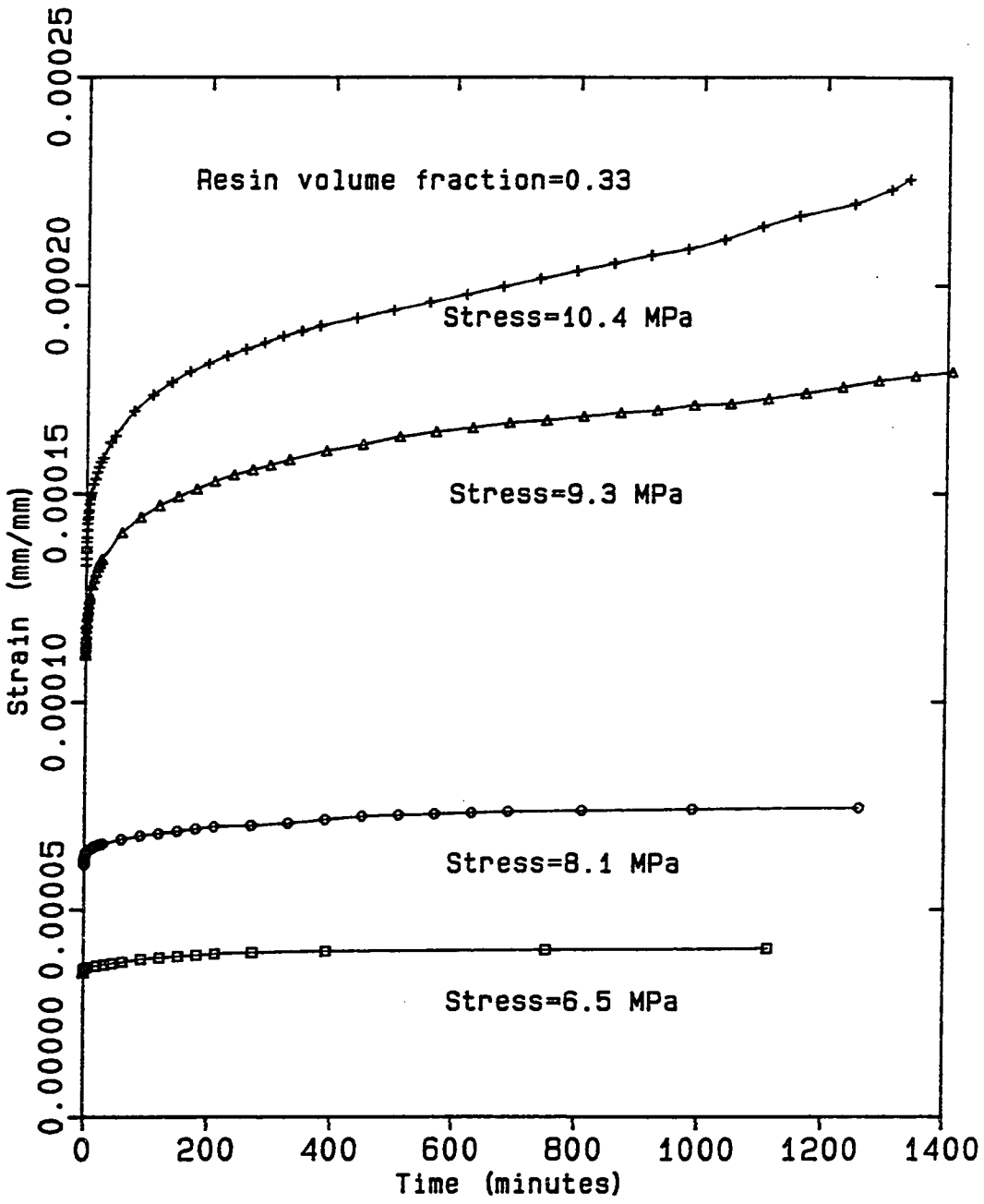

Fig 4.3.2 Strain Versus time curves for PC at increasing stresses and constant resin content.

phase itself. We used five stress-strength ratios, from 0.22 to 0.38. In most cases the specimens fractured soon after the start of the experiment at the highest ratio so our data was restricted to the first four ratios (0.22, 0.26, 0.29 and 0.33). As the stresses became higher the creep responses became unstable and at sufficiently high times led to rupture of the specimens. Fig. 4.3.2 shows the creep curves for PC at progressively increasing stresses. The value of the power exponent 'n' under such unstable creep conditions no more remains constant but increases significantly.

4.4 EFFECT OF STRESS

Keeping the temperature and the resin contents constant the PC beams were subjected to progressively increasing stresses ranging from 6 MPa to 9 MPa. Fig. 4.4.1 and Fig. 4.4.2 show plots of creep rates versus time for the PC systems at two different reference states. The solid lines indicate the best least square linear fit to the data. As, with the pure PMMA we notice an increasing trend in the creep rates with increasing stresses. The curves are fairly parallel to one another with the exponent 'n' varying between 0.16 and 0.19. The slight variation was probably due to experimental variations in specimen preparation and cutting. Since the differences in the values showed no regular pattern we adopted a constant average value for 'n' in our analysis.

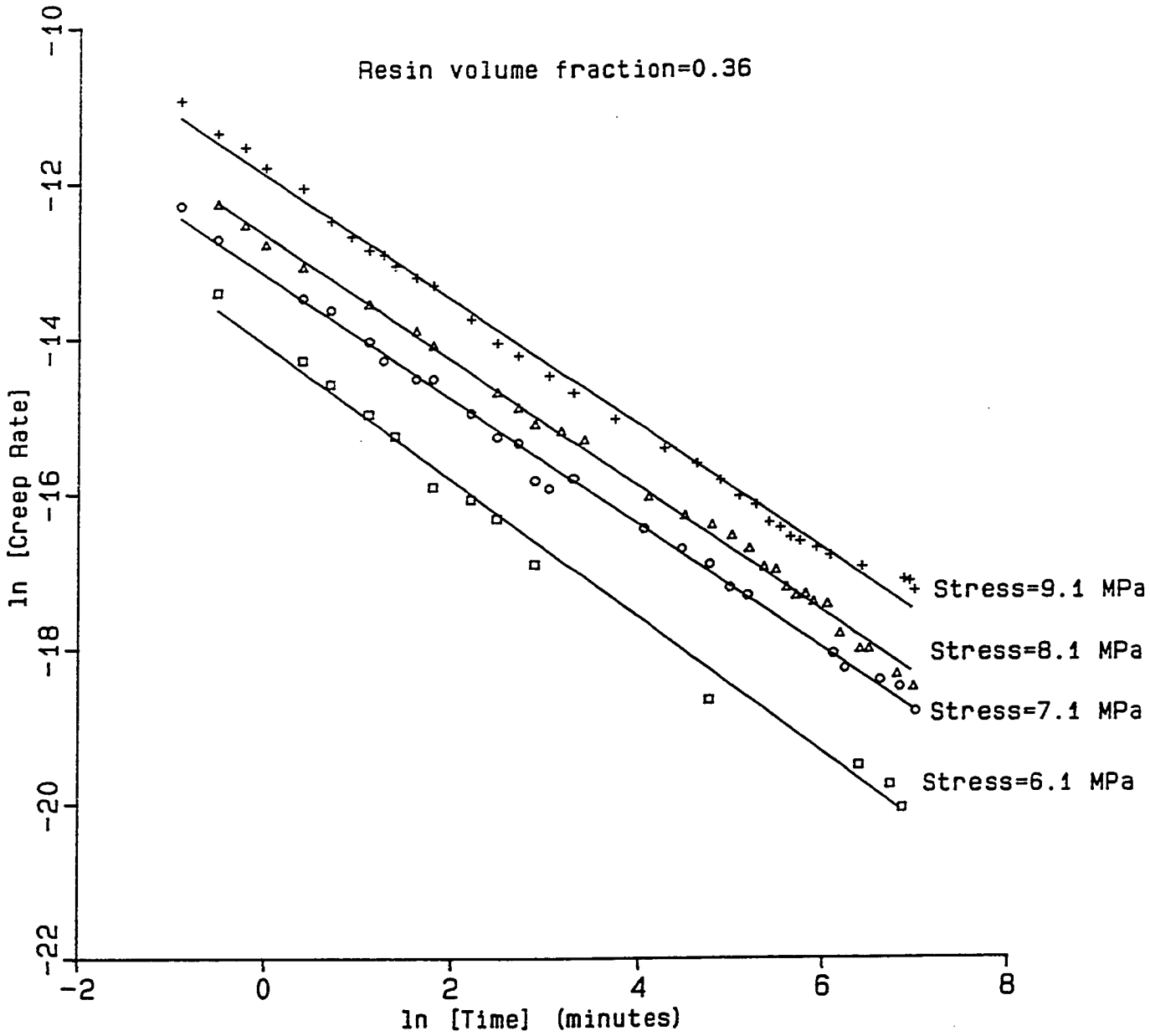

Fig 4.4.1 Creep rates versus time for PC at increasing stresses and constant resin content (0.36).

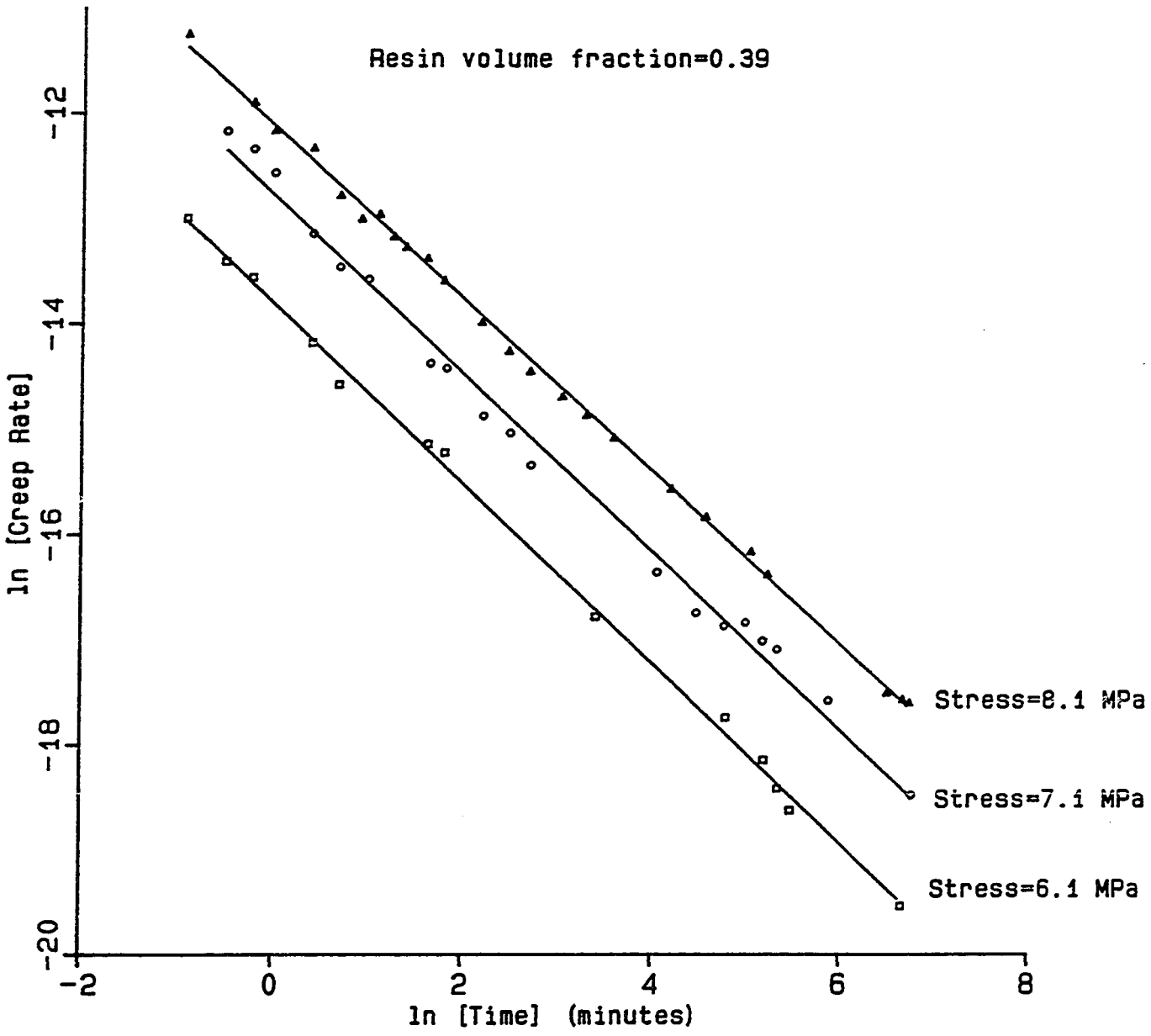

Fig 4.4.2 Creep rates versus time for PC at increasing stresses and constant resin content (0.39).

Figs. 4.4.3 and 4.4.4 are plots of creep strains versus time on logarithmic coordinates. As with the data from the PMMA samples a non-linear curve fitting program was used, where the 'n' values obtained from figs 4.4.1 and 4.4.2 were used to find the values of the time - independent strains. Now plots of creep strain versus time could be made. Unlike the PMMA samples, however, where the first six hours of data had to be neglected to get good straight correlations, in our PC systems data from the first minute itself yielded good linear fits. A possible reason for such behavior could be the successful elimination of setting stresses and transient strains by using montmorillonite to get zero cure-shrinkage systems. Another reason may be high percentage of inert material (58% - 67 %) in the PCs, which is reflected in a reduction of the non-linearity associated with the pure resin.

The stress shift-factors (a_S) obtained from the creep curves are plotted against stress on semi-logarithmic cootdinates in Fig. 4.4.5. These shift-factors also show an exponential dependence on stress and good linear fits are obtained.

$$a_S = \exp (K_S . S) \qquad (4.4.1)$$

Fig. 4.3.8 shows the difference in the values of the shift-factors using two different methods and as with the pure resin the values show good agreement with one another, proving once again the accuracy of the differential method.

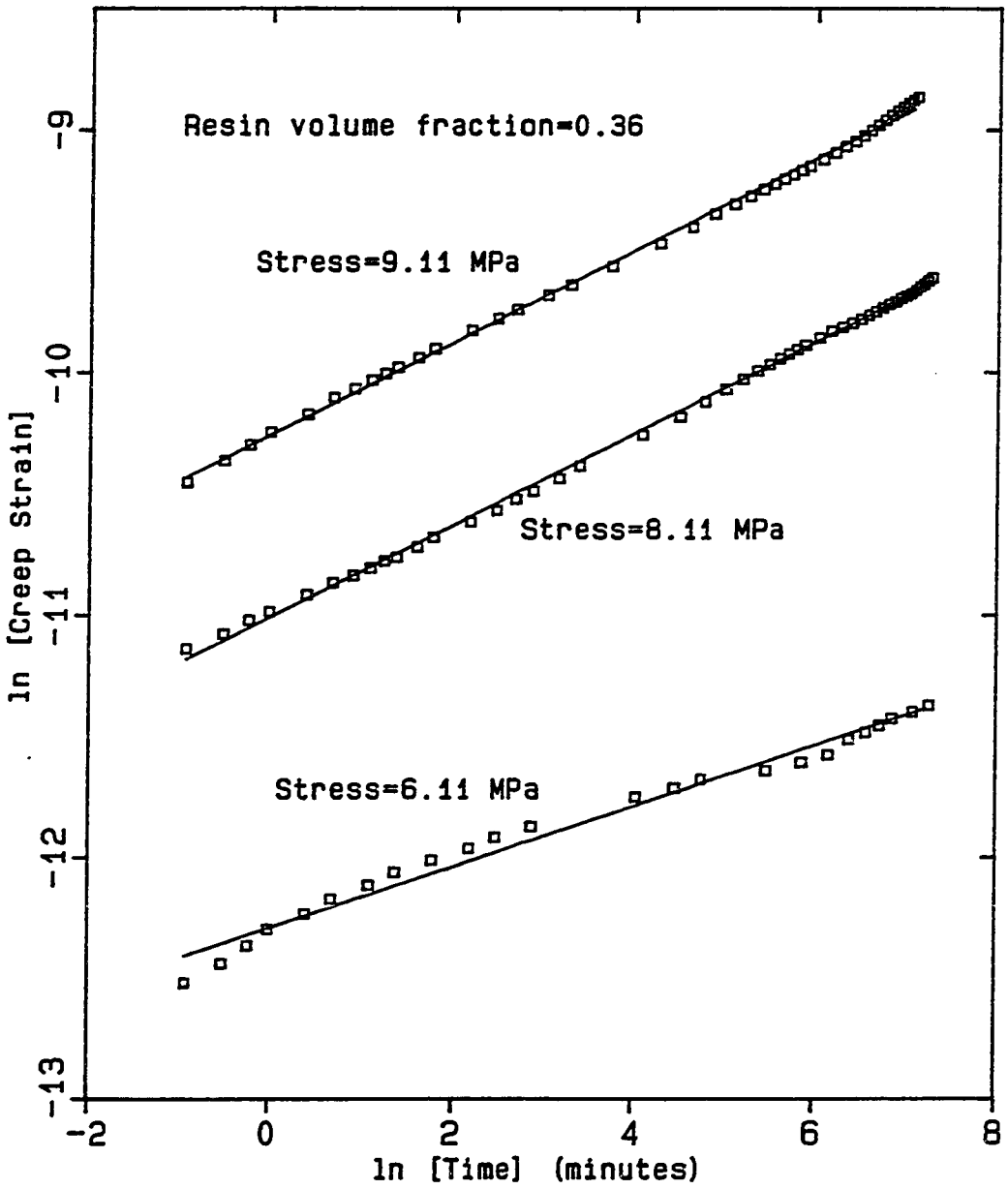

Fig 4.4.3 Creep strain versus time for PC at stress levels of 6.11 MPa, 8.11 MPa and 9.11 MPa, and 0.36 resin volume fraction

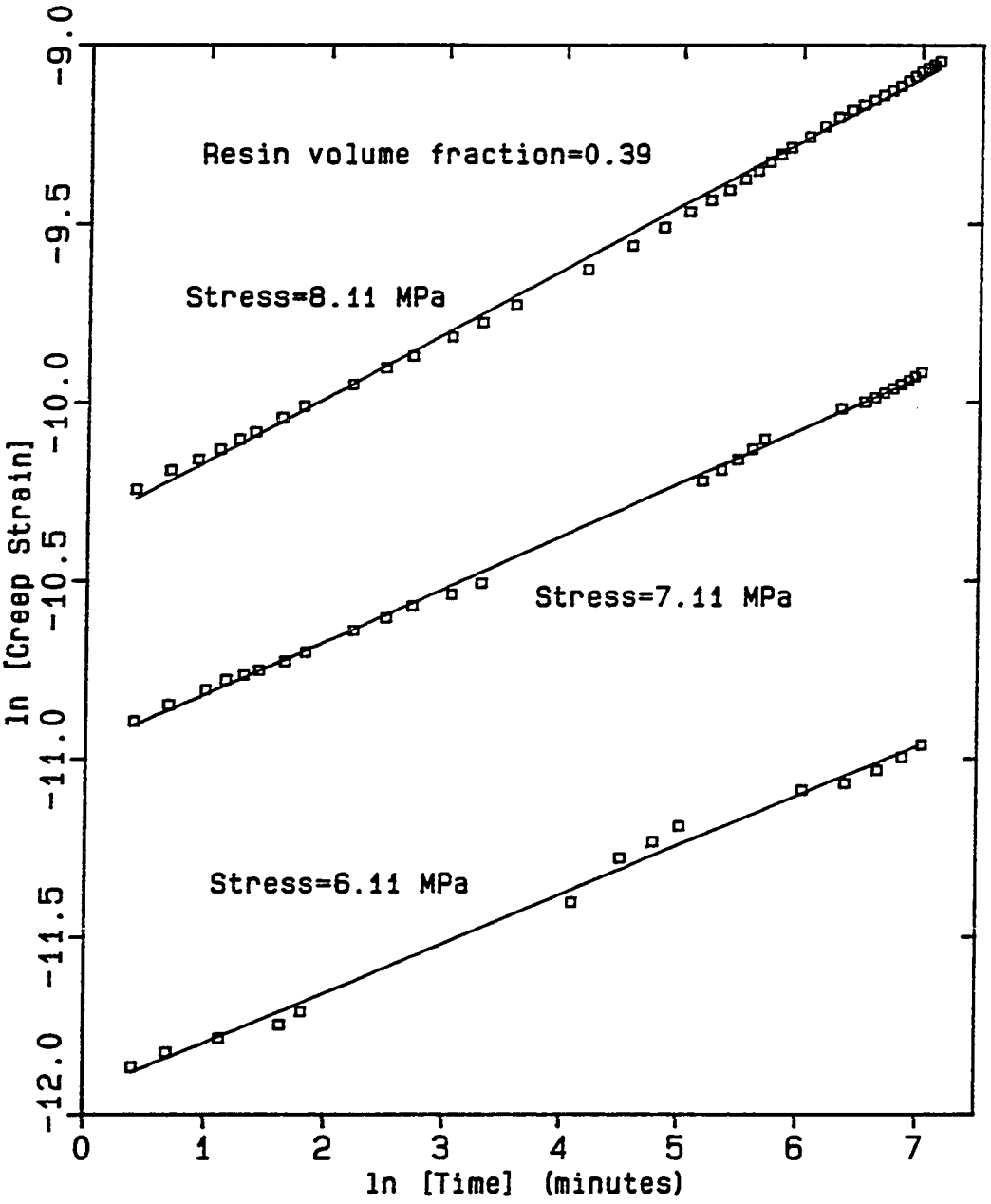

Fig 4.4.4 Creep strain versus time for PC at stress levels of 6.11 MPa, 7.11 MPa and 8.11 MPa, and 0.39 resin volume fraction

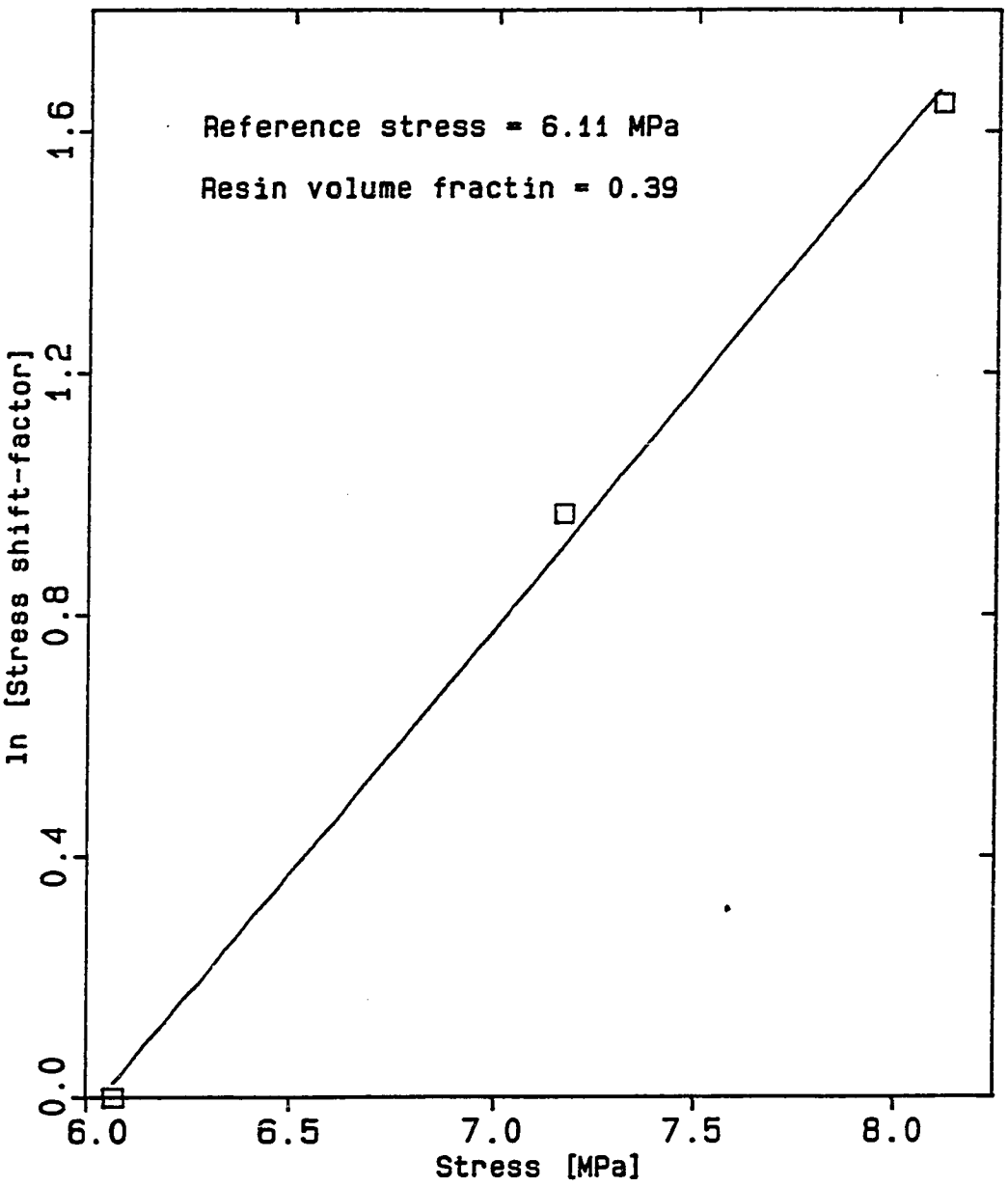

Fig 4.4.5 Stress shift-factors versus applied stress for PC (V=0.39).

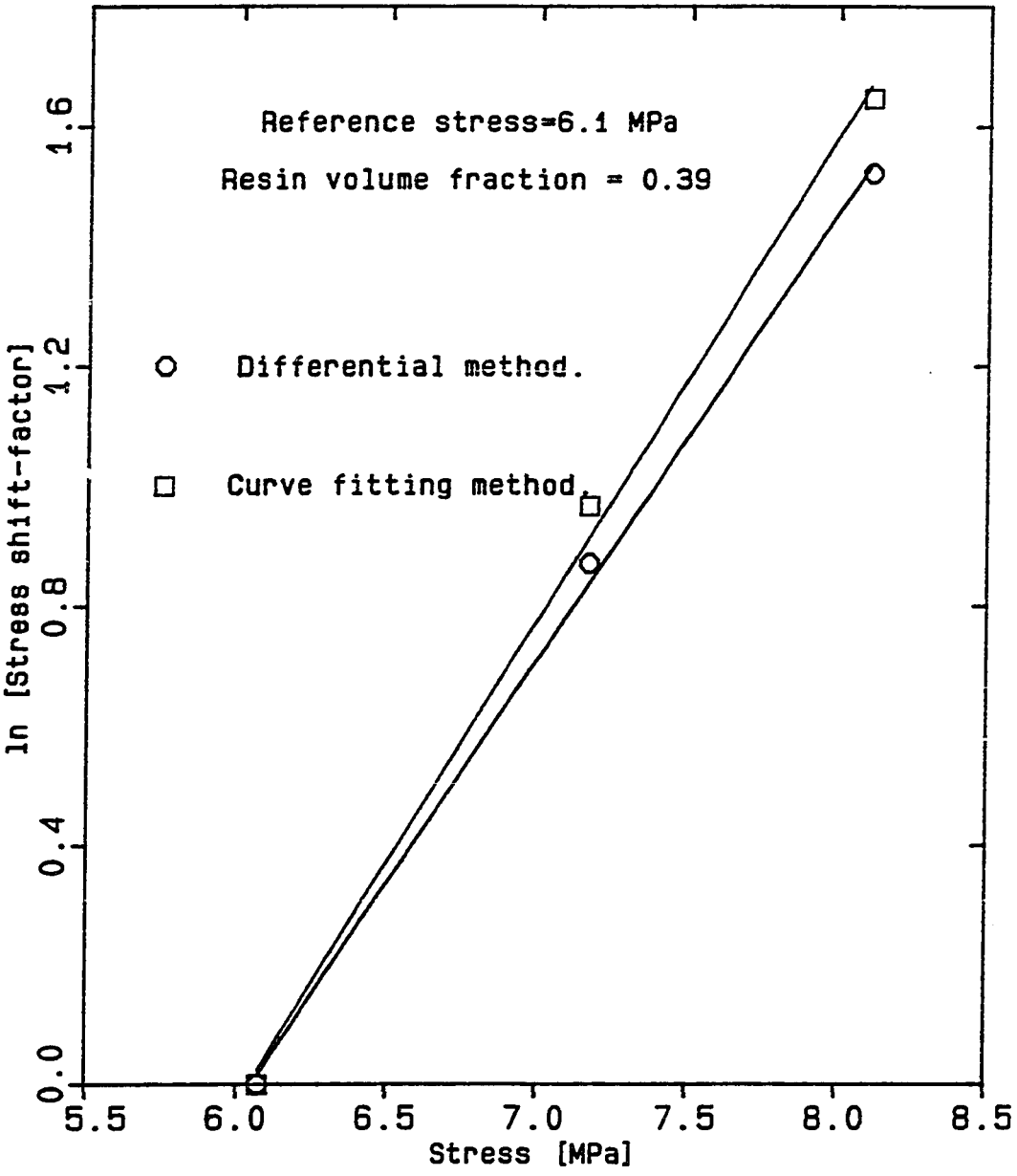

Fig 4.4.6 Stress shift-factors (using different methods) versus applied stress for PC (v=0.39)

4.5 THE EFFECT OF RESIN CONTENT

The volume fraction of the resin (v) also influences the creep behavior of the acrylic PC systems. At constant temperature and stress the isochronal creep strains increase with increasing resin contents as can be seen from Fig. 4.5.1 We worked within a range of v=0.33 to v=0.41. At lower resin contents there was not enough resin to support the polymer/aggregate mix with the result that undesirable air bubbles formed within the specimen leading to their premature failure. At higher resin contents, on the other hand, the excess resin appeared to "float" above the bed of aggregates thus resulting in a non-homogenous PC specimen. For our experimental puposes, therefore, we had to restrict ourselves to a narrow range of resin volume fractions.

Fig 4.5.2 shows the linearized curves for the creep rates verus time at a constant stress level using the differential method. In Fig 4.5.3 and 4.5.4 the creep strains have been plotted against time at different reference stress levels. Once again the curves are linear and parallel to one another, thereby, enabling us to use our superposition methods.

The vertical resin loading shift-factors, are given by a relation similar to the one used for the stress shift-factors. In this case :

$$a_V = K_V / K_{V\,(ref)} \qquad (4.5.1)$$

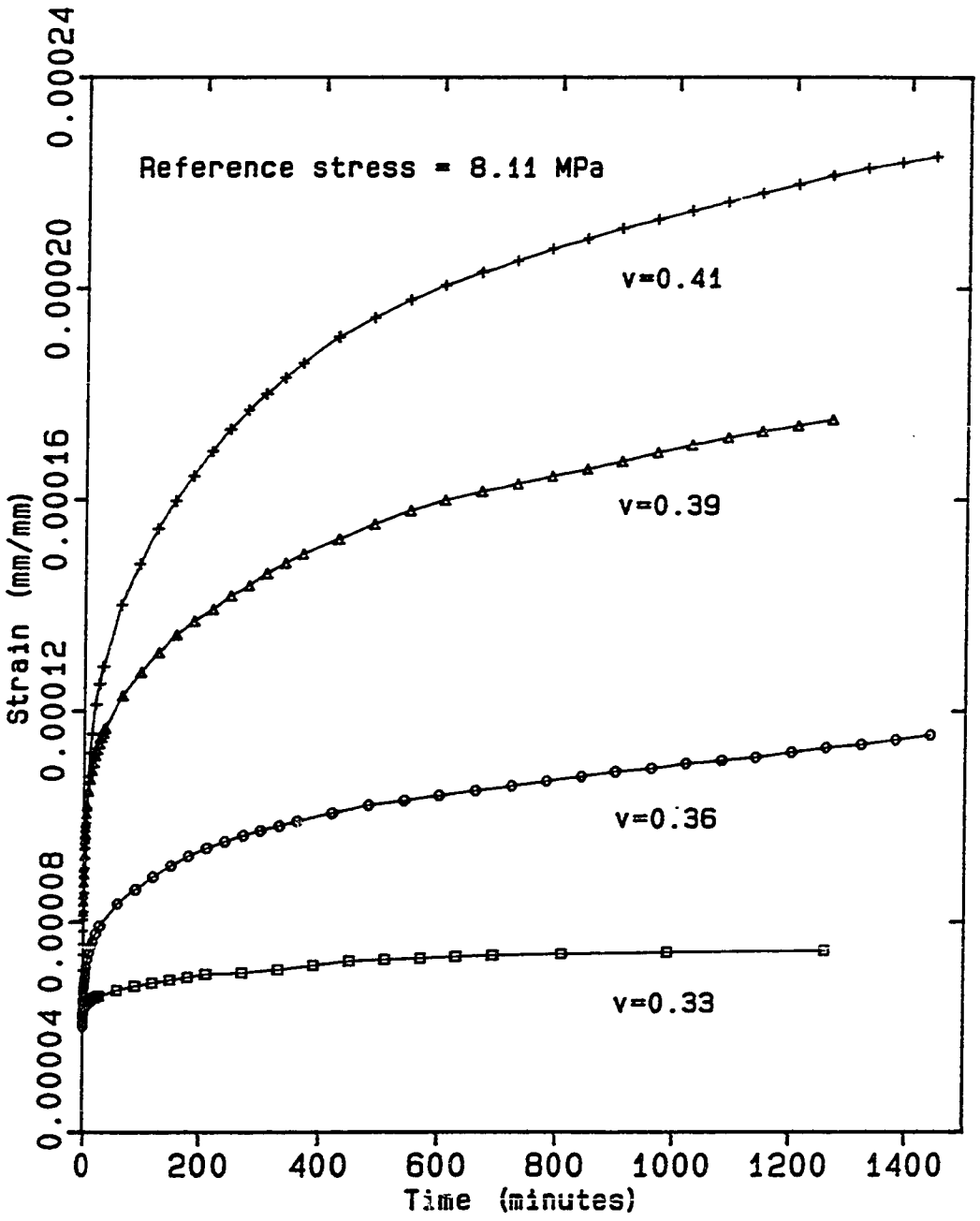

Fig 4.5.1 Strain Versus time curves for PC at constant stress and increasing levels of resin volume fraction.

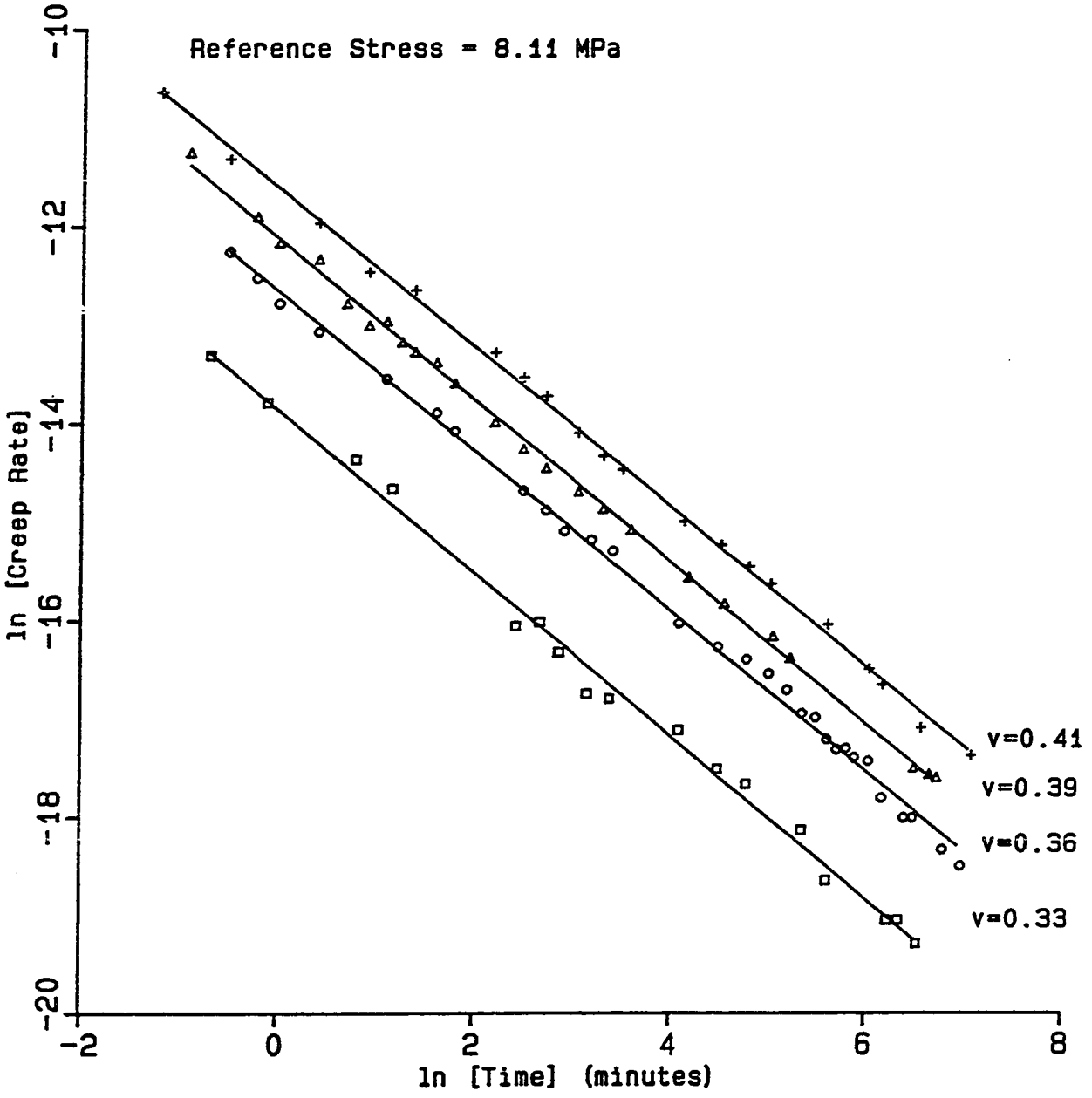

Fig 4.5.2 Creep rates versus time for PC at constant stress and increasing resin contents.

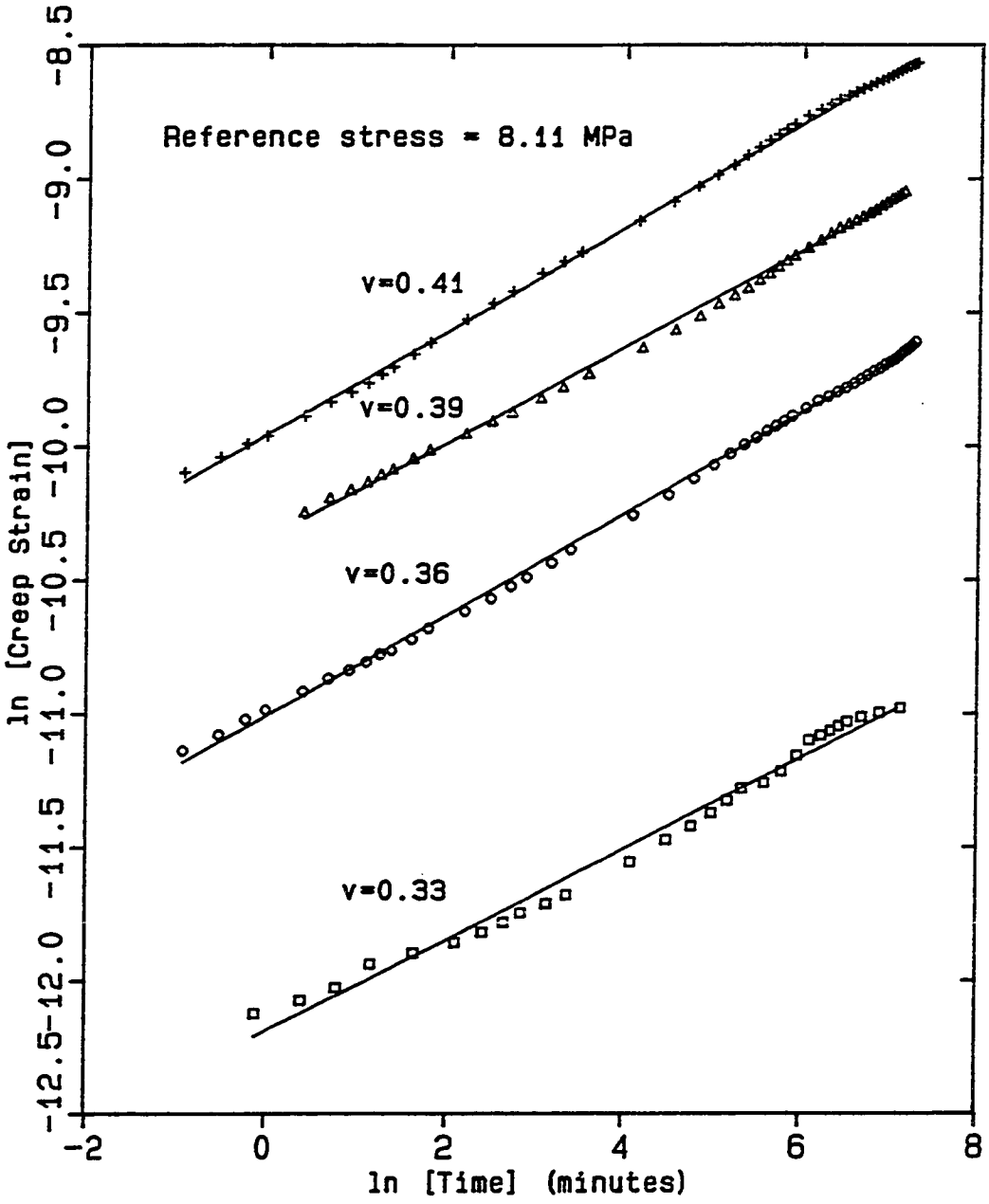

Fig 4.5.3 Creep strain versus time curves for PC at resin levels of 0.33, 0.36, 0.39 and 0.41 and a reference stress of 8.11 MPa.

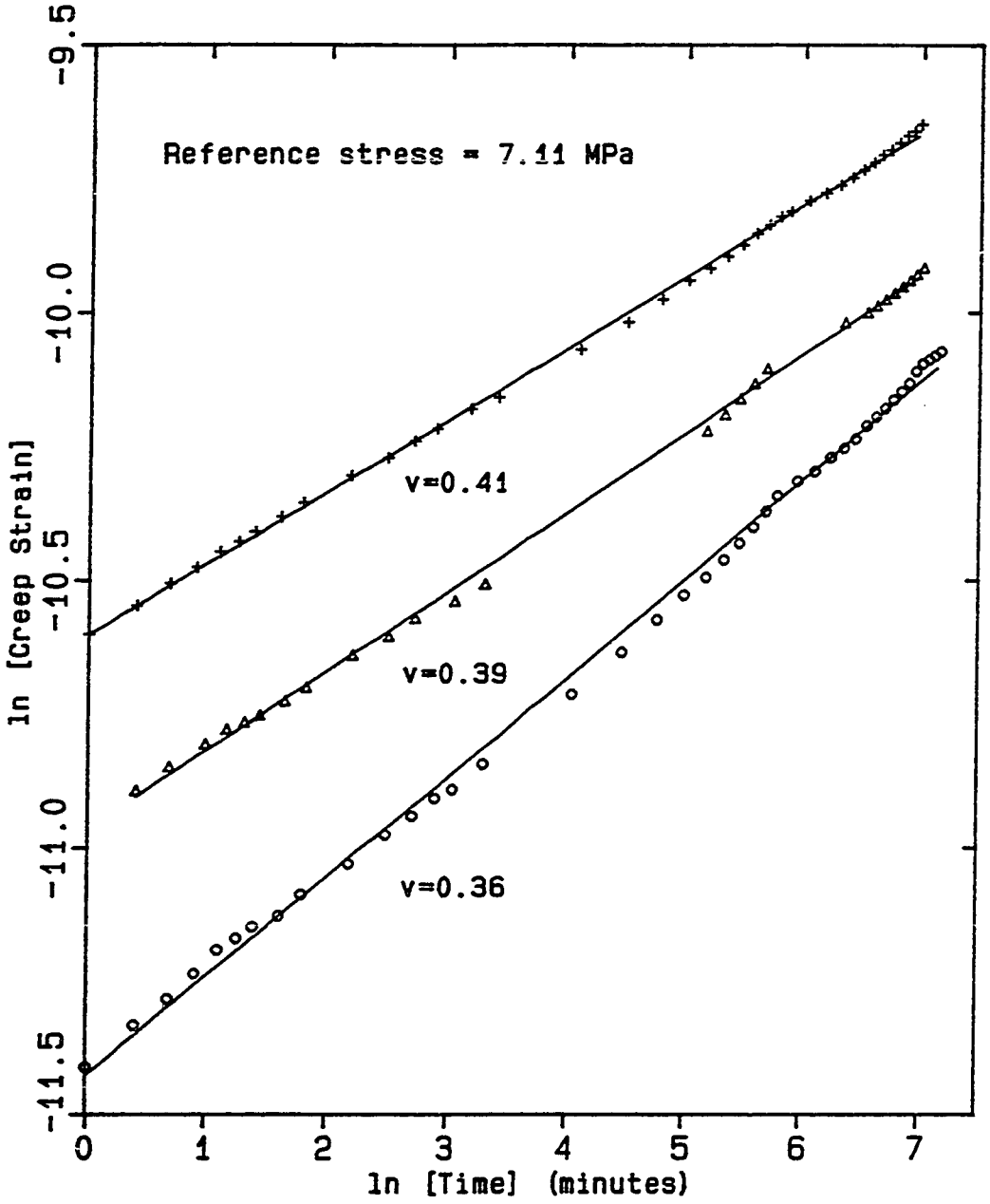

Fig 4.5.4 Creep strain versus time curves for PC at resin levels of 0.36, 0.39 and 0.41 and a reference stress of 7.11 MPa.

Having obtained the shift-factors from the intercepts, plots of a_v versus v were made on semi-logarithmic axes (fig 4.5.5) to see whether the Arrhenius relationship was obeyed. Good linear fits suggested that the resin loading shift-factors were given by:

$$a_v = EXP\ (\ K_v\ .\ v\ ) \qquad (4.5.2)$$

where K_v is expressed in terms of temperature and other material constants. Fig 4.5.6 is a comparison of the Arrhenius plots obtained from the two different methods.

4.6 TIME - STRESS - RESIN CONTENT (DOUBLE) SUPERPOSITION

Once we have obtained the different shift-factors, namely, the stress and resin content shift-factors, we now attempt to obtain an empirical expression which describes the creep strains for the PCs as a product of separable functions of time (t), stress (S) and resin volume fraction (v). From Figs. 4.4.3, 4.4.4, 4.5.3 and 4.5.4 we see that the creep response curves at different conditions of the dependent variables for the PC systems are linear with near identical slopes. The slight variation in the slopes arising from small deviations in the value of 'n' is attributed to experimental

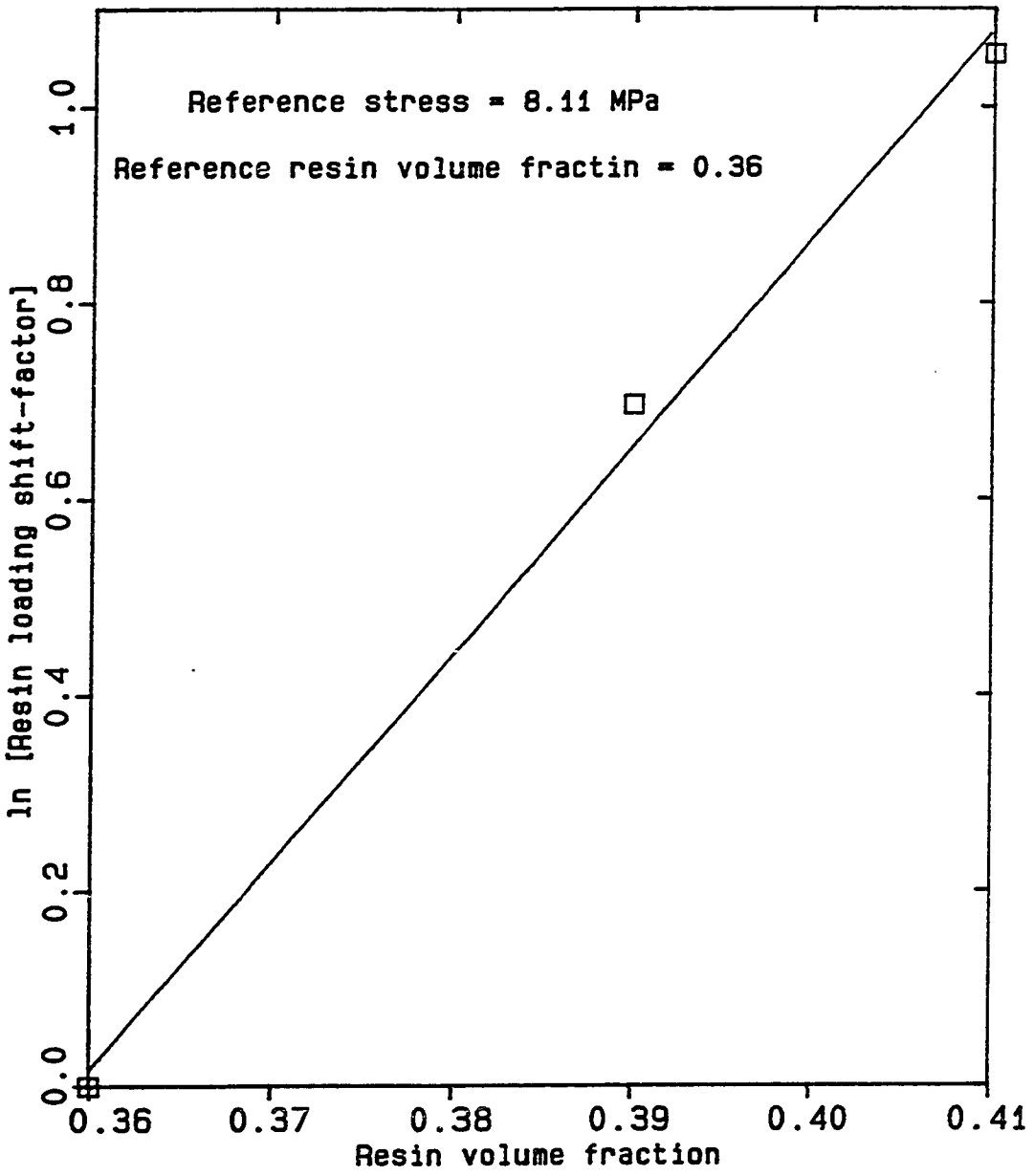

Fig 4.5.5 Resin loading shift-factors versus resin volume fraction for PC (V=0.39).

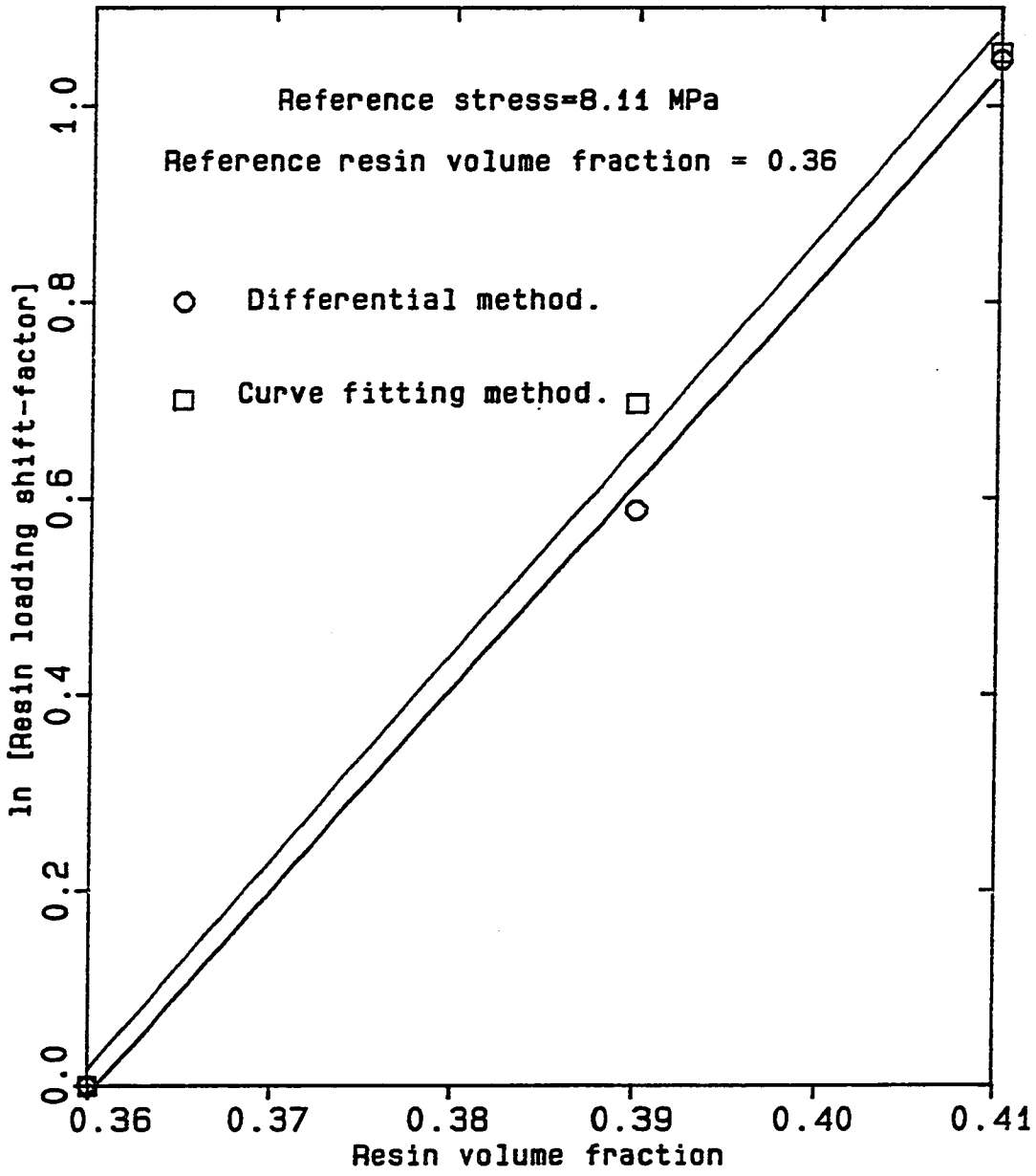

Fig 4.5.6 resin loading shift-factors (using different methods) versus resin volume fraction for PC (v=0.39)

error associated with specimen preparation and cutting. For all practical purposes the curves are parallel to one another. (It is of interest to note that in the pure resin, in this case "plexiglass", at constant temperatures, the variation in 'n' values was a lot smaller. Here, all the tested specimens had identical preparation history and dimensions).

The linear and parallel curves make it possible to achieve a complete superposition of all the creep strain data obtained at different stresses and resin loadings onto a single "master" curve at a chosen reference state. In principle, this kind of superposition is similar to one used by Dharmarajan[19] in which he deals with time, temperature, stress and resin content, thus using what he calls a "triple superposition" scheme. Our method, on the other hand uses double superposition. Unlike Dharmarajan who used horizontal shifting of the parallel curves, we have used vertical superposition for advantages mentioned earlier. It can also be related easily to horizontal superposition (appendix B). The vertical shift-factor may be related to a shift in the time axis as follows:

$$t_{S \text{ or } v} = (K_{S \text{ or } v} / K_{ref})^{1/n} \cdot t_{ref} \qquad (4.6.1)$$

The superposition scheme can be applied only under the condition that changes in stress and resin loadings should bring about

identical changes in the relaxation times of the PC systems. Also, the stress-strength ratios should be such that all measurements should be made within the range of stable creep. In other words, reduction of the creep curves using this method would only be possible in cases where creep leading to rupture did not occur.

In the previous sections we have shown how the different shift-factors based on resin content and stress can be expressed in the Arrhenius forms. Also the creep behavior as a whole is well represented by the power law equation, with 'n' being the time exponent. This suggests the possibility of writing the creep equation as a product of these functions such that :

$$e(t, S, v) = e_0 \cdot a_S \cdot a_v \cdot t^n \qquad (4.6.2)$$

where the preexponential e_0 is the creep strain of the PC measured at a reference level of each of the three parameters. We chose our reference state as : t = 1 minute, T = 24^0C, S = 6.11 MPa, v = 0.36. Substituting the expressions for a_S and a_v in eqn. 4.6.2 we now get,

$$e(t, S, v) = e_0 \cdot EXP(K_S \cdot [S - S_{ref}]) \cdot EXP(K_v \cdot [v - v_{ref}]) \cdot t^n \qquad (4.6.3)$$

The original form of the above equation was developed by

Dharmarajan and Armeniades[32] and later modified by Kumar[20]. Our form is more similar to the one used by Kumar. In both the previous forms, however, there is a certain uncertainty about the value of the power exponent 'n' owing to the irregularities associated with the time - independent strains. They both used trial and error to get to the value of 'n'. We have, by using creep rates instead of creep strains (using the power law equation in differential form) found a more definite and easier way to find 'n' as well as the shift-factors.

To check for the validity of the empirical creep equation, long term tests were made (ca. 7 days), and the data compared with the response predicted by our creep equation. The results are in good agreement as can be seen from Fig 4.6.1. Though n ranged between 0.16 and 0.19 for the PCs, the higher value of 0.19 was assumed for the creep equation as this was in closer agreement with the n values of the parent resin. Also, insufficient data on PCs necessitated this assumption. When the power exponent in the empirical expression for the PCs is replaced by the value of n obtained from the pure resin samples, the long term prediction for creep is even more accurate, as can be seen from Fig 4.6.1. This further confirms the assumption that creep originates in the polymer matrix itself. For design purposes it is therefore advisable to use the power exponent calculated from the data on pure resins. Table 4.6 lists all the parameters used in eqn 4.6.3.

Table 4.6 Parameters in the empirical creep equation for acrylic based polymer concrete systems.

Parameter	Value
K_S	0.74
K_v	22.18
e_0	9.7685 E-05
T_{ref}	297 ^{0}K
S_{ref}	6.11 MPa
t_{ref}	1.0 minute
v_{ref}	0.36
'n', power exponent	0.19

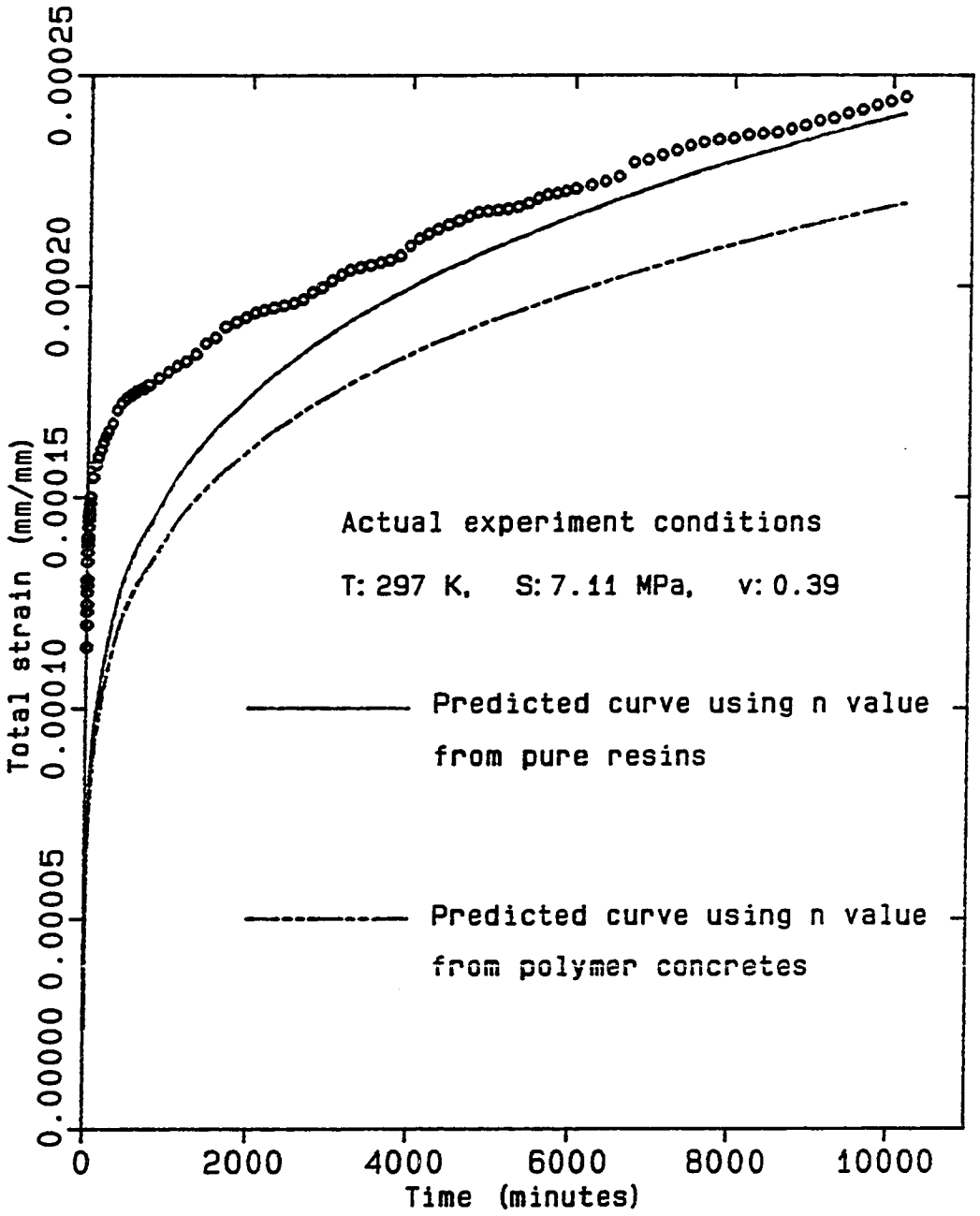

Fig 4.6.1 Verification of the validity of the creep equation with actual long term experiment.

4.7 APPLICATION OF OUR METHODS TO CREEP DATA FROM PREVIOUS INVESTIGATIONS

In this study we have found an alternate way to find the value of the power exponent 'n', by using the power law equation in its differential form and using the slopes of the creep rate versus time curves to provide us with values of 'n'. Findley[6], as outlined in the introduction used a method of succesive approximations to find the value of the initial time - independent strain e_0. Plots could then be made for the total strain minus e_0 versus time. The value of the power 'n' was then obtained from the trigonometric slope of the straight line drawn through the data. He chose three values of time t_1, t_2 and t_3 such that t_3 = Sq.rt ($t_1.t_2$). From his equations e_0 is now given by:

$$e_0 = e_1.e_2 - e_3^2 \,/\, e_1 + e_2 - 2.e_3 \qquad (4.7.1)$$

where e_1, e_2 and e_3 are the strains corresponding to the three times. We applied this procedure to our data to see how well the 'n' values from the different methods compared with one another. Fig. 4.7.1 shows plots of (e_{tot} - e_0) versus time. The different values of e_0 and 'n' are noted next to each curve. We get good straight line fits, and the 'n' values compare well with ones

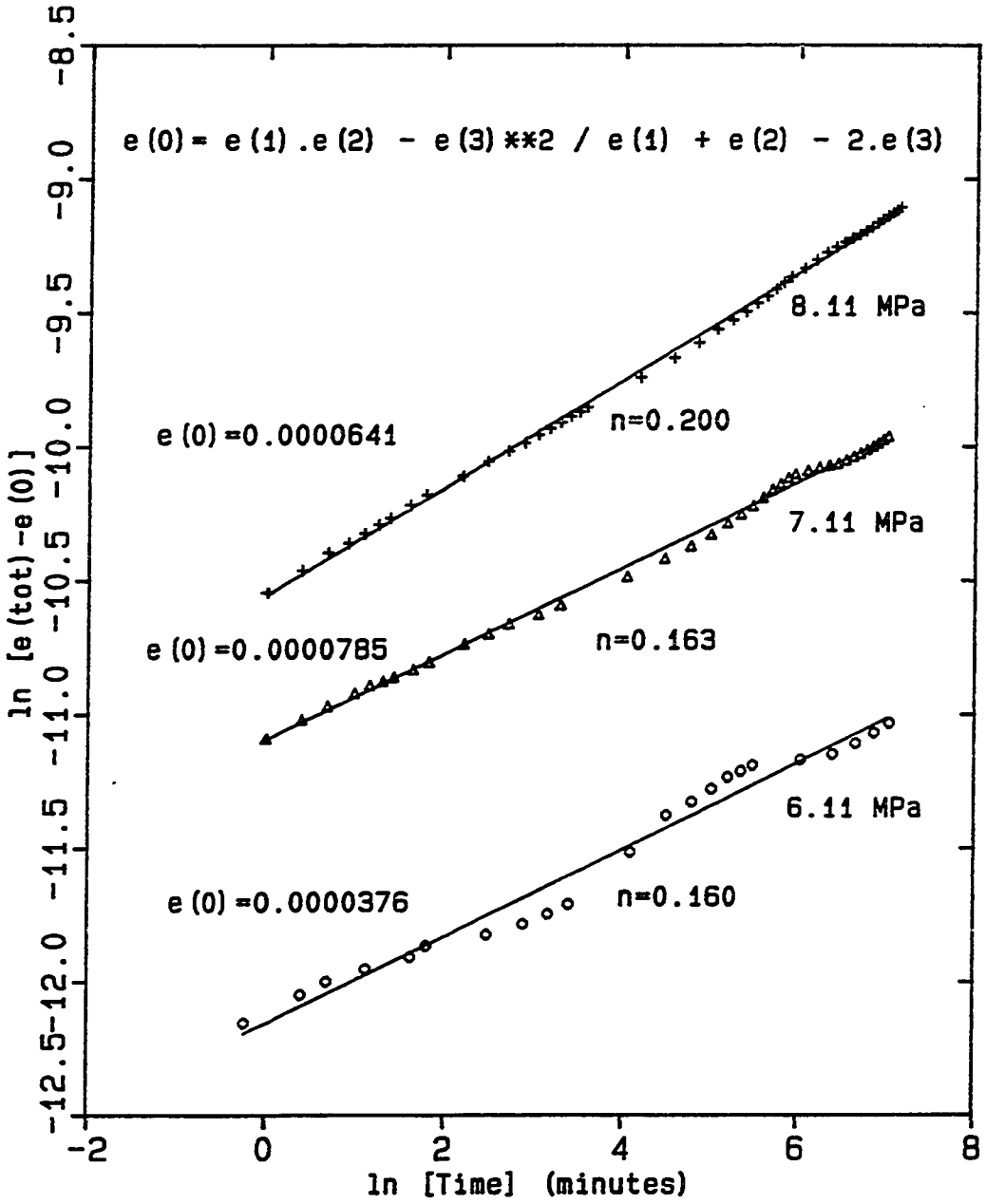

Fig 4.7.1 Use of Findley's method of successive approximations to find e(0) and consequently plot e(tot)-e(0) versus time to determine the value of 'n'.

obtained from our method. The proximity of these numbers with those obtained from our methods is an indication of the accuracy and feasibility of our method. Another observation we made was that though Findley's method worked well with most data sets, in some cases where the creep data was slightly irregular it was extremely difficult to get a proper value of e_0 owing to deviations from the power law equation caused by fluctuations of the experimental strain values . In such cases we either did not get good linear fits or the 'n' values were very erratic. In our method, however, since we first smoothed out the curves by curve fitting with appropriate functions, any possible outliers from the experimental data were automatically taken care of. As a result it was possible to get reasonably accurate values even from relatively scattered data sets.

We now extended our method of linearization to tensile creep data generated by Ogorkiewicz[33] at 20^0C and 60^0C on acrylic cast sheets at progressively increasing stresses. Fig 4.7.2 shows how straight line fits are obtained for the creep rate versus time curves. At 60^0C 'n' was 0.3 and at 20^0C 'n' was 0.18. The n values obtained from his data are in reasonable agreement with those obtained from our work on PMMA, if one takes into account the temperature dependence (see Fig.4.1.5). We went one step

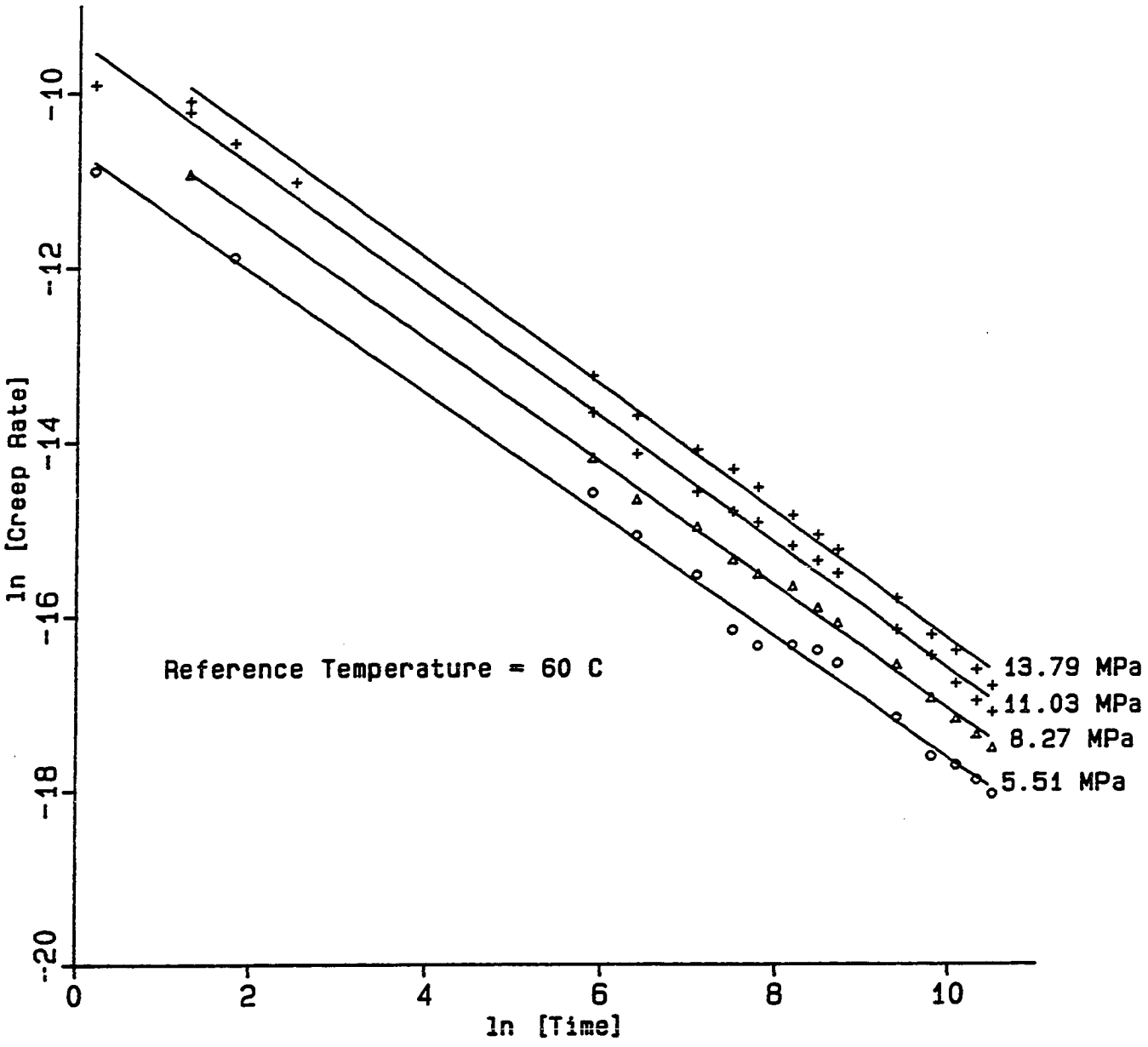

Fig 4.7.2 Creep rates versus time generated from Ogorkiewicz's (33) data on acrylic cast sheets (perspex at a temperature of 60 C and increasing stresses.

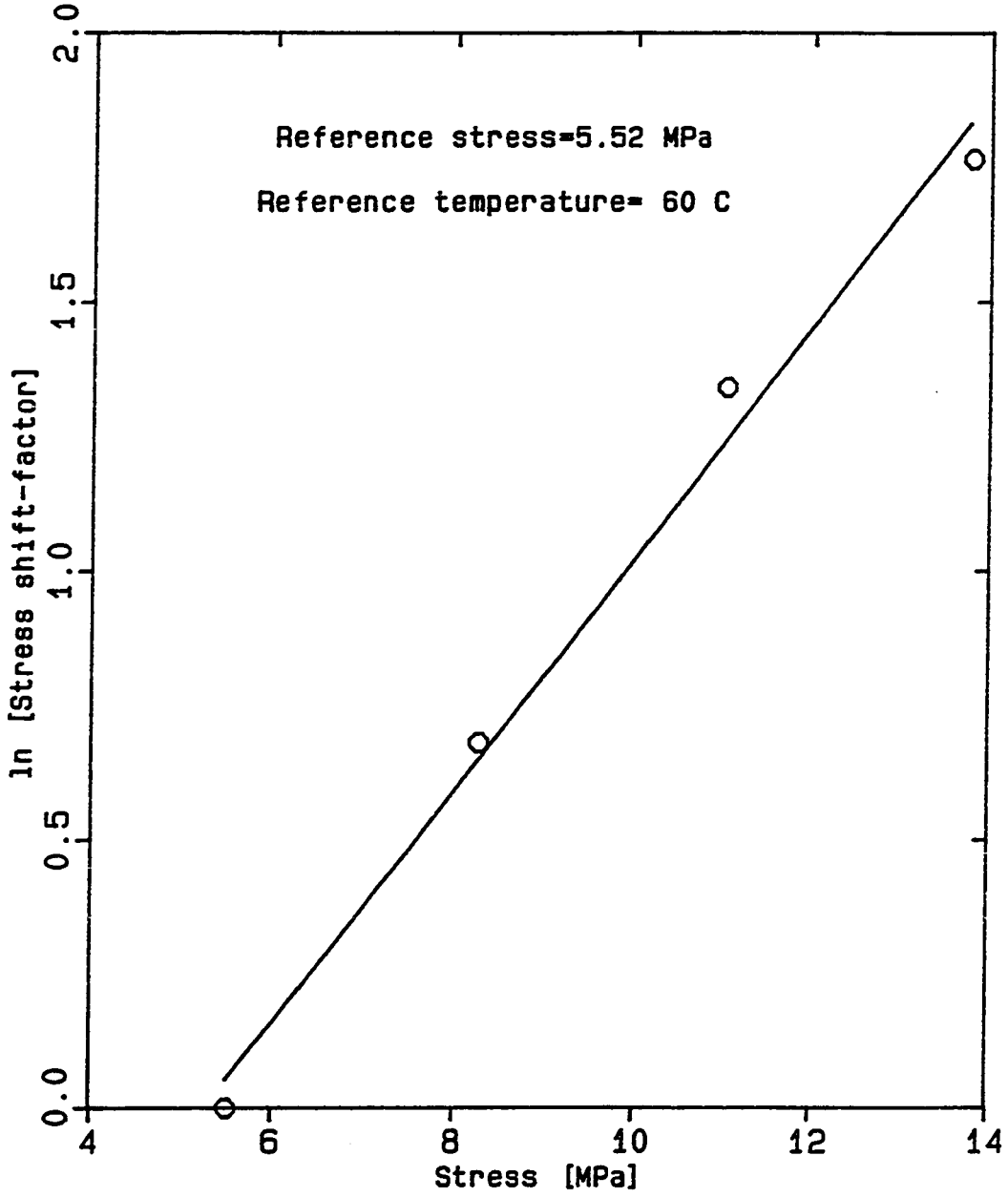

Fig 4.7.3 Stress shift-factors versus applied stress for acrylic cast sheets at 60 C using Ogorkiewicz's data.

further and calculated the stress shift-factors from the intercepts of the lines in Fig 4.7.2. Here too the shift-factors followed an Arrhenius dependence as can be seen from the plots of a_S versus stress in semi-logarithmic coordinates in Fig 4.7.3.

Though a considerable amount of creep data is available on pure acrylics, work on acrylic polymer concretes has been somewhat limited. Hsu[18] studied the flexural creep behavior of acrylic based PCs. He used MMA based PCs with formulations somewhat similar to ours. His data was generated over a considerable period of time (ca. 1 year). Despite the fact that our linearization principle was applied over much shorter times it worked excellently on Hsu's data. Fig 4.7.4 shows the linearized plots at the three different stress-to-strength ratios. At stress-to-stength ratios of 0.3 and 0.4 we get a constant time exponent of 0.165 which is very close to our 'n' values for the PCs (0.17). At a higher stress-to-strength ratio of 0.5 the specimens used by him fractured. We thus had a very high value of 'n' (0.31) at such high stresses owing to catasrophic creep which is exactly what we had observed from our work on the PCs at high stresses.

Ayyar and Deshpande[34] performed compressive creep experiments on epoxy and polyester mortars at varying stresses and constant ambient temperatures. We again used our method to treat their data on epoxies. From the plots in Fig 4.7.5 we obtained

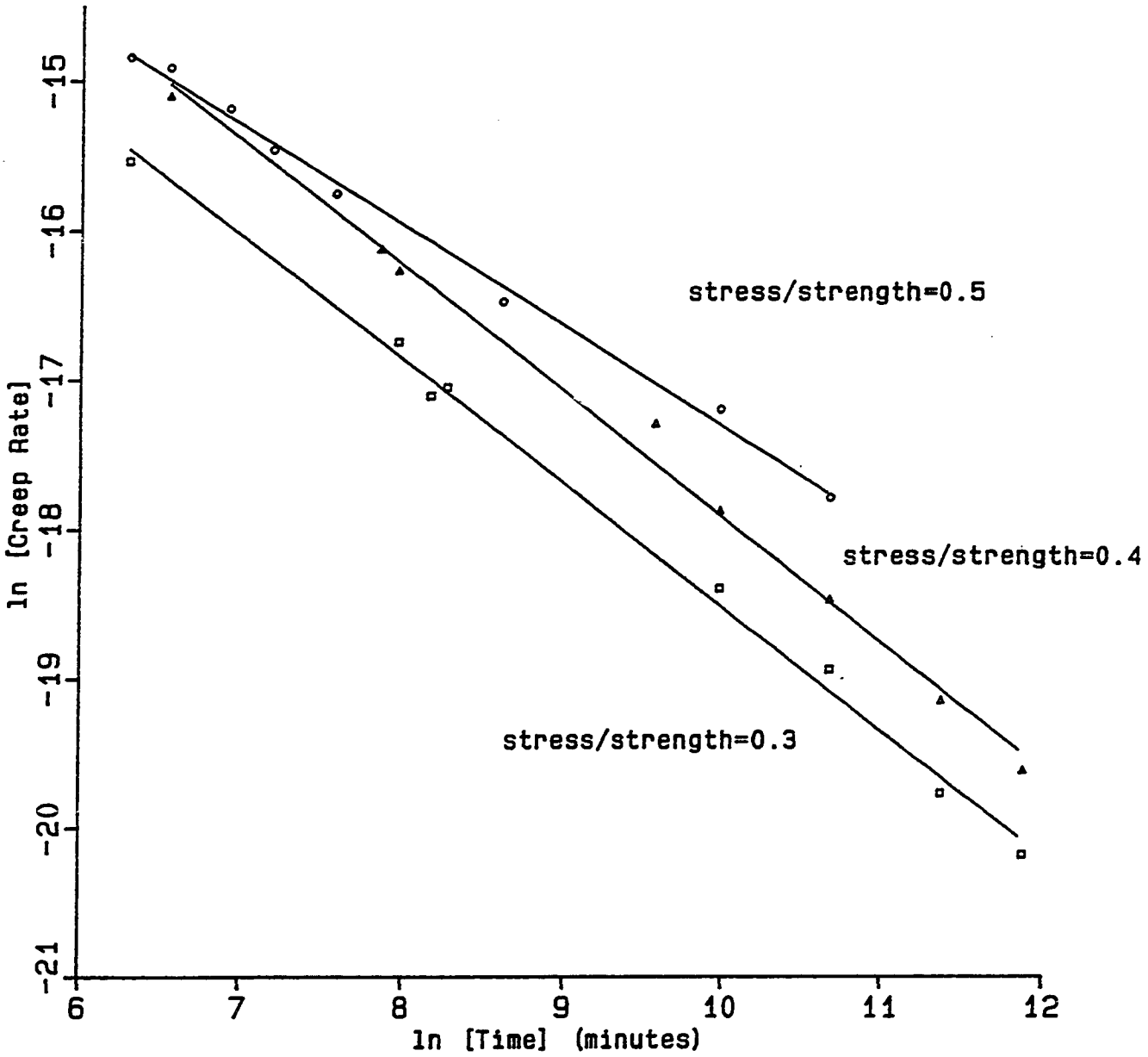

Fig 4.7.4 Creep rates versus time for Hsu's (18) data on acrylic polymer concrete at stress-strength ratios of 0.3, 0.4 and 0.5, at ambient temperatures.

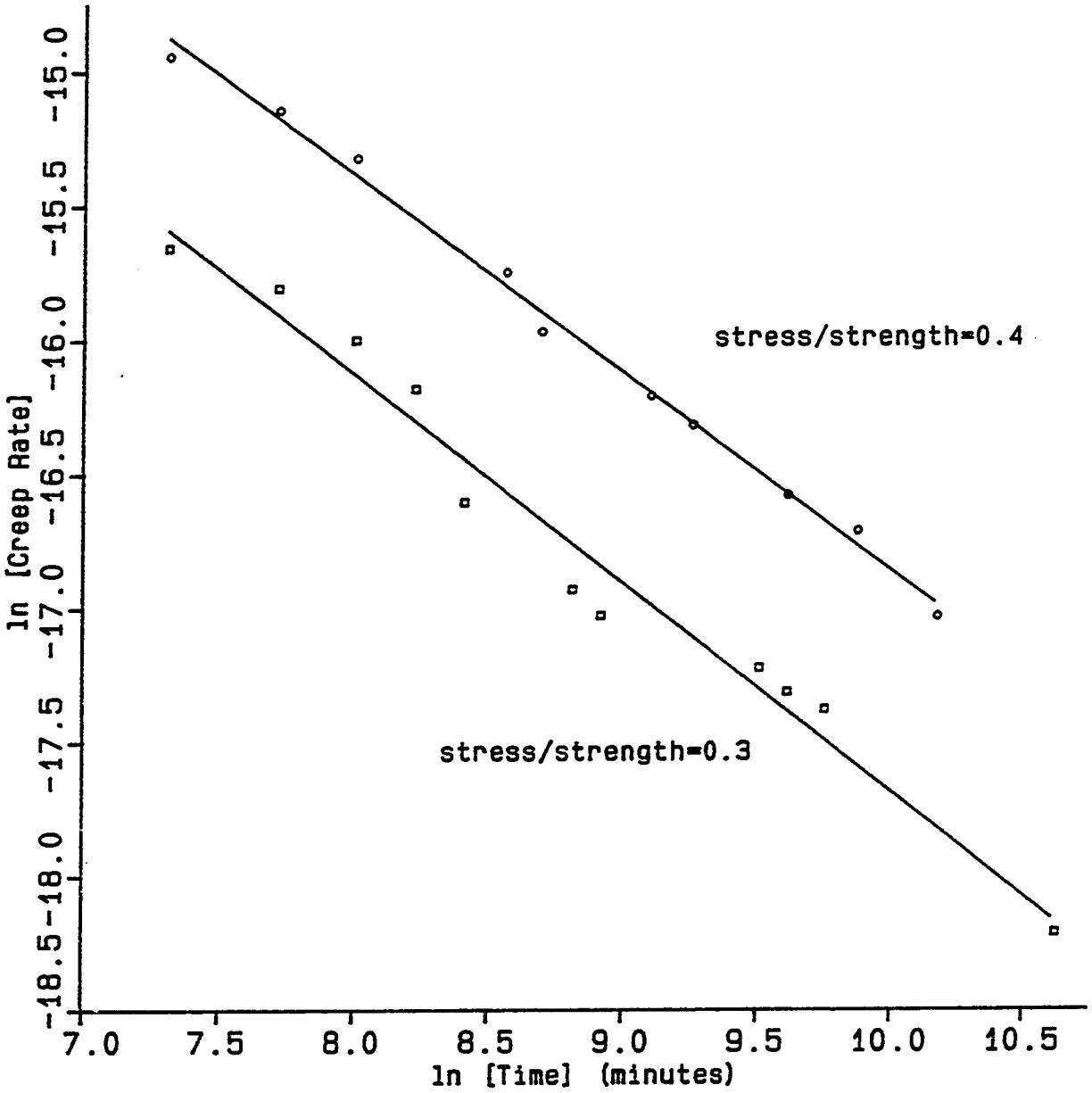

Fig 4.7.5 Creep rates versus time from Ayyar and Deshpande's (34) compressive creep data on epoxy polymer mortar at stress to strength ratios of 0.3 and 0.4, at ambient temperature.

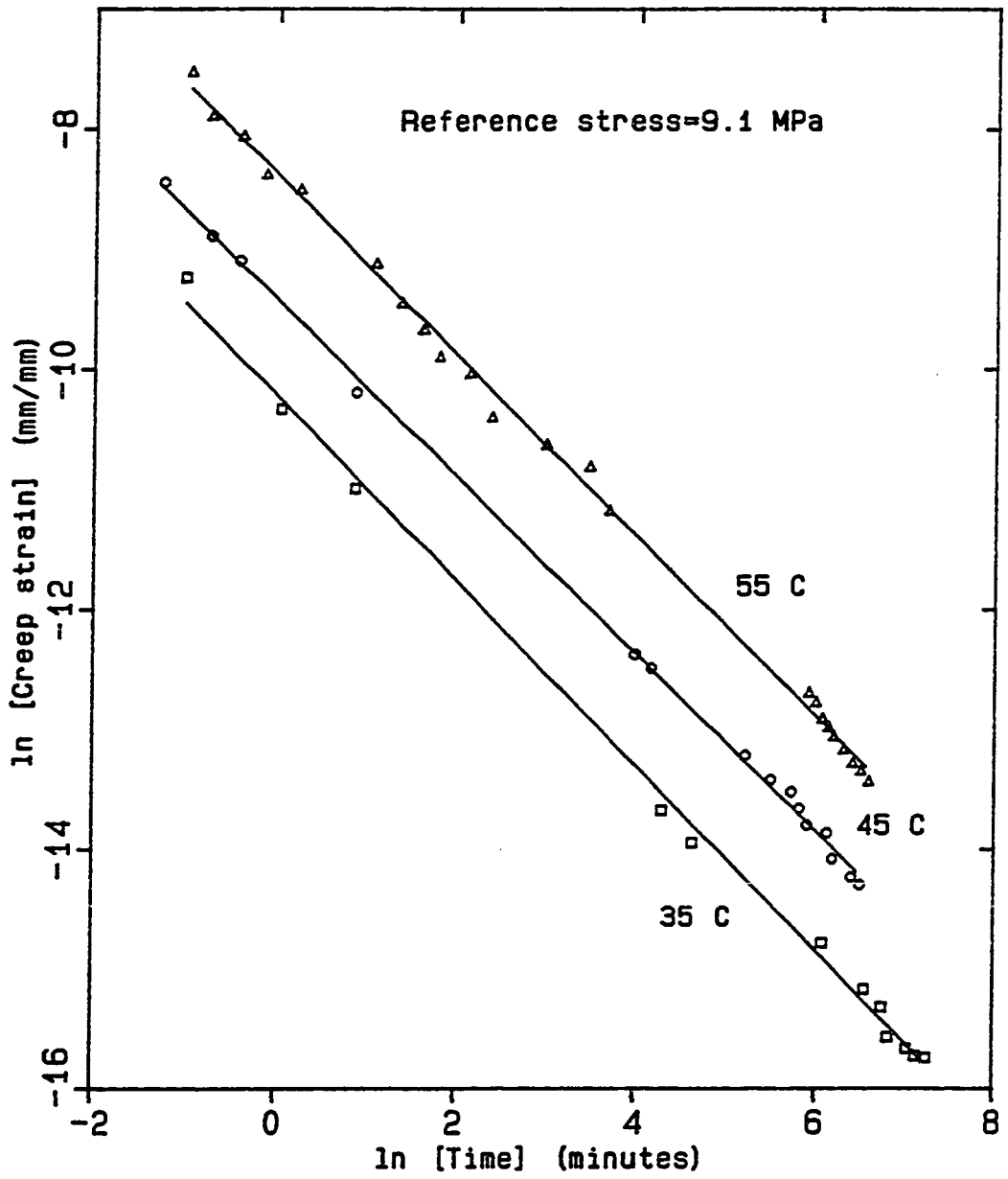

Fig 4.7.6 Treatment of Kumar's(20) data on PMMA at different temperatures and constant stress using our linearization methods.

'n' values of 0.24 which were lesser than 0.30 predicted by them. The data, however, responded well to our linearization technique.

The results obtained from treating data of previous investigators indicate the success of our linearization techniques in predicting accurate values for the power exponent 'n'. It also shows how a constitutive equation in terms of time and stress can successfully describe creep behavior. It is a well known fact that creep is significantly affected by temperature changes and Fig. 4.7.6 applies our methods to Kumar's[20] data on PMMA at different temperatures. The plots are all linear and parallel with strains increasing with temperature increases. The temperature shift-factors obtained can also be related by an Arrhenius relationship :

$$a_T = \text{EXP} (-\Delta H / R (1/T - 1/T_{ref}) \qquad (4.7.2)$$

Good linear plots confirmed the Arrhenius dependence (Fig.4.7.7). This implies that temperature shift-factors can also be incorporated into our creep equation so that creep can now be defined in terms of time, temperature and stress.

In addition to temperature and stress we have shown how the volume fraction of the resin present in the polymer concretes also affects creep behavior , and how resin loading shift-factors can be

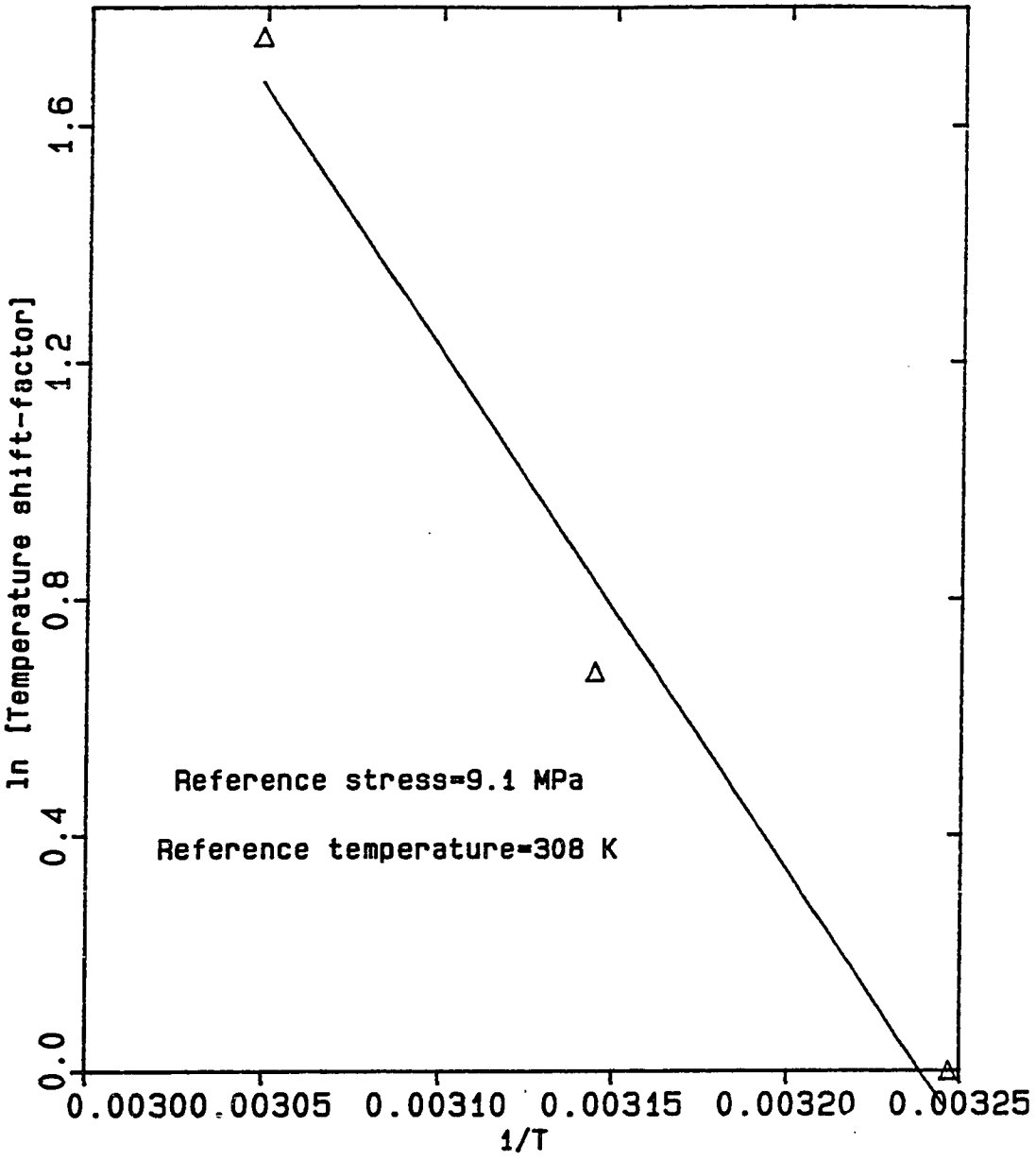

Fig 4.7.7 Arrhenius plot of temperature shift-factors versus 1/T from Kumar's data at a reference temperature of 35 degrees centigrade and reference stress of 9.1 MPa.

included in the creep equation. Though it would be of interest to treat previous data based on varying resin contents, such data is not easily available.

Dharmarajan[19] did some work on resin shift-factors on polyester and epoxy PCs. He used horizontal shift-factors and Fig. 4.7.8 shows a linear dependence similar to ones observed in our study. He used the pure resin (v=1) as the reference resin volume fraction. Dharmarajan also worked on low shrinkage systems using montmorillonite to control setting stresses and incorporated glass fiber reinforcement for additional strength enhancement. By analogies with his work we can possibly include two more shift factors, one based on MMT, a_M, and the other on fiber reinforcement a_F, such that the overall creep equation may now be expressed in the form

$$e_{tot}(\, t,\, T,\, S,\, v,\, M,\, F\,) = e_0 \cdot a_T \cdot a_S \cdot a_v \cdot a_M \cdot a_F \cdot t^n \qquad (4.7.3)$$

where all the shift-factors have been previously defined and e_0 is the pre-exponential.

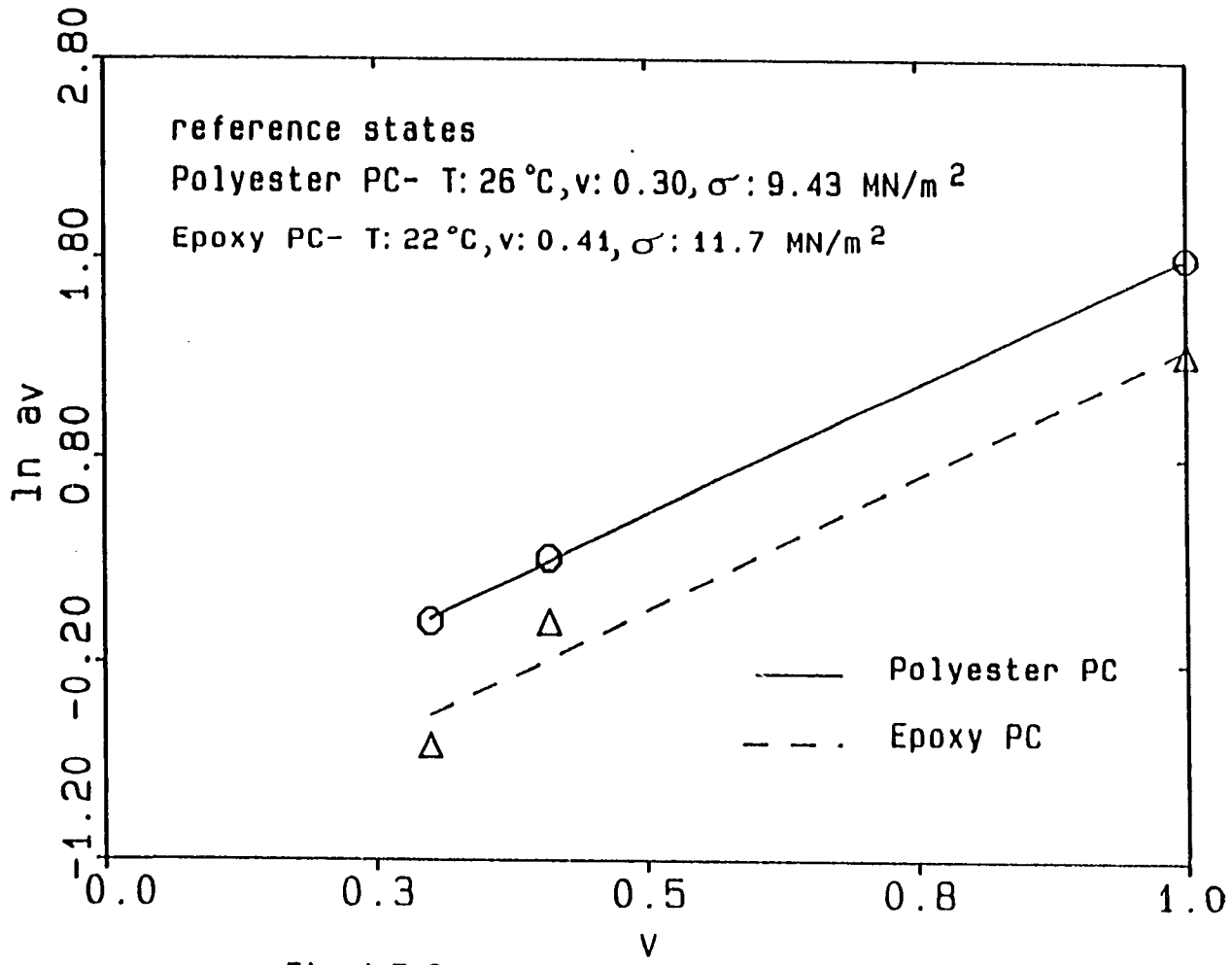

Fig 4.7.8. Logarithmic plots of resin loading-shift-factors (a_v) versus resin content.

CHAPTER 5

CONCLUSIONS

1. Creep in both pure and filled acrylic resin systems is strongly dependent on temperature and stress, and in the case of the PCs on the resin content as well. For stress - to - strength ratios less than 0.4 the PC systems exhibit stable creep behavior which can be successfully expressed in terms of separable functions of time, stress and resin volume fractions.

2. Within the stable stress - to - strength range for the PCs it is possible to sucessfully superpose data at varying stresses and resin contents onto a single "master curve", thus enabling us to predict long term creep behavior from short term observations (ca. 18 to 24 hrs). This superposition scheme, with the help of the various shift-factors can be used to provide an empirical expression which describes long term creep behavior in the acrylic PC systems.

3. Creep in both the pure and filled acrylic resin systems is highly stress dependent, and increases with increasing stresses. The stress shift-factors obeyed the Arrhenius dependence well. Creep

in the PCs also increases with increasing resin contents and here too the resin loading dependence, described in terms of resin loading shift-factors followed the Arrhenius relationship.

4. In all cases the creep data followed a power law dependence on time.

5. The value of the power exponent 'n' can be determined using the power law equation of Findley in its differential form. The exponent is determined from the slopes of the creep rate versus time curves. The creep rates increase with increasing stresses and resin loadings. The good linear fits obtained using this method provides an easy way to find 'n' and k values, both constants in the power law equation.

6. The power exponent shows negligible variation with changing stresses and remains mostly constant. A change in the resin loadings also left n unaffected. However, a slight increasing trend in 'n' values is observed with increasing temperatures for the pure PMMA samples.

7. The addition of the mineral montmorillonite to the PC systems during sample preparation helps reduce setting stresses by eliminating cure shrinkage, which in turn minimizes the transient

strains. The high percentage of inert material in the PCs also leads to an overall reduction in the duration of the transient strains. Thus,in the case of the PCs we could use data from the first minute whereas for the PMMA samples we eliminated the first six hours of data to get reasonable results. Annealing the PMMA samples beforehand, however, helps in reducing the transient strains.

CHAPTER 6

RECOMMENDATIONS FOR FUTURE WORK

One of the principle objects of this study was to provide a simple and efficient tool to determine some of the coefficients in the power law creep equation by eliminating complexities associated with the irregular behavior of the initial and transient strains. This leaves us with room for further investigations on the nature of these coefficients, specially 'n', the power exponent. A wide range of experiments at different values of stress, temperature, etc. should provide substantial information on the effects of such parameters on the power exponent. This in turn would help in modifying the existing constitutive equation to give more accurate predictions of long term creep strains.

In our study we noticed some dependence of 'n' on temperature which could not be substantiated owing to the lack of sufficient data. However, the fact that the 'n' values increase with T, offers us with interesting possibilities of modifying the creep equation. One such possibility could be to see if 'n' can be related to some form of "reduced" temperature (in the case of polymers, say, T/T_g where Tg is the glass transition temperature), similar to that used in the theory of corresponding states. A correction for 'n' based

on this scheme would reduce the creep equation to:

$$e_{cr} = k \cdot t^{\,n\,(T/Tg)}$$

It would be a significant achievement if one could come up with such a theory but it would also mean plenty of experimenting with different materials and comparisons of 'n' values at reduced temperatures.

The methods developed in this study should be extended to various other commercially available PC systems, containing different polymerizing systems such as epoxies, esters, etc. It would be of interest to see if our methods of data reduction could be applied to all such systems as well. One could also compare the activation volume and the activation energy values of different PC systems with those of their parent resins and thereby relate the deformation characteristics of the composites to their parent resins.

Another drawback of this study was our inability to compare the responses predicted by the empirical expression with actual long term experiments exceeding times of more than one year. It is recommended that creep experiments be conducted for such long

durations at sufficiently low stress - to - strength ratios so as to avoid catastrophic creep. A more conclusive check on the accuracy of the empirical equation could then be made.

Lastly, I would like to recommend certain changes be made to the existing apparatus. The supporting frame should be made as rigid as possible such that the relative deformations of its members are negligible. Another problem we encountered was with experiments with changing temperatures. The environmental chamber itself was fragile and slight increases in the pressure of the circulating fluid caused leakages which had to be sealed from time to time. Also with water cooled chambers there exists temperature gradients between the surface of the bath and the specimen. An air cooled chamber using circulating air at the desired temperature could reduce this problem. A heat exchanger may be used to provide the correct temperature and a dehumidifier in series could help remove moisture. Such conditioned air at the proper temperature and relative humidity should help in creating more stable experimental conditions.

CHAPTER 7

REFERENCES

1. Nielsen, L.E., *Mechanical Properties of Polymers and Composites,* Volume 1, Marcel Dekker, Inc., New York, 1974, pp.68-72.

2. Baer, E., *Engineering Design for Plastics,* Reinhold Pulishing Corporation, New York, 1964, pp.307-308.

3. Weber, W., "Ueber de Elasticitat der Seidenfaden", *Pogg. Ann. Physik* (3) 12, 1835.

4. Norton, F.H., *Creep of Steel at High Temperatures,* McGraw-Hill Book Co., Inc., New york, 1929, pp.58.

5. Jenkins, A.D. (Ed.), *Polymer Science,* Volume 1, Chapter 11 : "The Mechanical properties of plastics", by Kambour, R.P. and Robertson, R.E.

6. Findley, W.N., "Creep Characteristics of Plastics", *Synposium on Plastics, Philadelphia Districts Meeting, ASTM,* Feb.22-23, 1944.

7. Findley, W.N., "Derivation of a Stress-Strain Equation from Creep Data for Plastics", *Proceedings of the First National Congress of Applied Mechanics,* 1952, pp.595-602.

8. Marin, J., Pao, Y.H., and Cuff, G., "Creep Properties of Lucite and Plexiglass for Tension, Compression and Bending", *Transactions of the ASME,* 1951, p.73.

9. Mcloughlin, J.R., "The Analysis of Creep and Stress Relaxation Data for Plastics and Reinforced Plastics", *29th Annual technical Conference, Reinforced plastics/Composites Institute, Society of the Plastics Industry, Inc.,* 1974.

10. McVetty, P.G., *Transactions of the ASME,* 1933, 99, p.55.

11. Howdyshell, P.A., "Creep Characteristics of Polyester Concretes", *Technical Report, U.S. Army Construction Engineering Research Laboratory,* Champaign, Illinois, 1975.

12. Prin, D. and Cubaud, J.C., "Polyester Polymer Concrete Applications in Civil Engineering", *Materiaux et Constructions,* Volume 8, 1975, pp.291-304.

13. Knab, L.I., *Flexural Behavior of Conventionally Reinforced Polyester Concrete Beams,* Ph.D dissertation, University of Cincinatti, 1972.

14. Ohama, Y., "Creep of Resin Concrete and Polymer-Impregnated Concrete", *Japan Congress on Materials Research, 17th,* 1974, pp. 140-143.

15. Okada, K., *1st International Congress on Polymers in Concrete (Proceedings),* Volume 1, Nihon University, Fukushima, Japan, 1982, pp.504-523.

16. Broniewski, T., Jamrozy, Z. and Kapko, T., *1st International Congress on Polymer Concretes (Proceedings),* England, May 1975, pp.179-184.

17. Helal, S., *Experimental Study of Mechanical Properties and Structural Applications of Polymer Concrete,* Ph.D Dissertation, Rice University, 1978.

18. Hsu, H.T., *Flexural Behavior of Polymer Concrete Beams,* Ph.D Dissertation, University of Texas (Austin), 1984.

19. Dharmarajan, N., *Flexural Creep Behavior of Polymer Concrete Systems,* Ph.D Dissertation, Rice University, 1987.

20. Kumar, S., *A Constitutive Equation for Creep in Glassy Polymers and Composites,* M.S. Thesis, Rice University, 1988.

21. Turner, S., "Creep in Glassy Polymers", *The Physics of Glassy Polymers,* R.N. Heyward (Ed.), 1973, pp.233-275.

22. "Standard Test Methods for Flexural Properties of Unreinforced and Reinforced Plastics and Electrical Insulating Materials", *ASTM Standards, Metric,* D790 M, 1984.

23. Rosen, S.L., *Fundamental Principles of Polymeric Materials,* John Wiley and Sons, New York, 1982, pp.305-307.

24. Liu, C.F. and Armeniades, C.D., "Interaction of Dilating Additives with Polymerizing Resins For Cure Shrinkage Control at Ambient Temperatures", *47th Annual Technical Conference, (Proceedings) Society of Plastics Engineers,* New York, May 1989, pp.834-837.

25. Armeniades, C.D., Stormer, J.C. and Haque, E., "Cure Shrinkage Control with Strength Enhancement in Polymer Concrete by Combining Polymerization with Mineral Dehydration", *5th International Congress on Polymers in Concrete (Proceedings),* Brighton, England, September 1987, pp. 187-191.

26. Byars, E.F. and Snyder, R.D., *Engineering Mechanics of Deformable Bodies,* International Textbook Company, Pennsylvania, 1963, p.211.

27. Den Hartog, J.P., *Strength of Materials,* McGraw-Hill Book Company, Inc., New York, 1949, p.35.

28. Franceschini, A. and Momo, A., "Time - Stress Superposition in some Creep Experiments", *Polymer,* Volume 21, 1980, pp.725-727.

29. Williams, M.L., Landel, R.F. and Ferry, J.D., *Journal of American Chemical Society,* 77, 1955.

30. Cessna, L.C., "Stress - Time Superposition of Creep Data for Polypropylene and Coupled Glass Reinforced Polypropylene", *Polymer Engineering and Science,* Volume 11, May 1971, p.211.

31. Zhurkov, S.N. and Narzullaev, B.N., *Zhur. Tech. Fiz,* 23, 1953.

32. Dharmarajan, N., Kumar,S. and Armeniades, C.D., "Constitutive Equation for Creep in Polymer Concrete and their Resin Binders", *Journal of Applied Polymer Science,* Volume 35, 1988, pp.353-364.

33. Ogorkiewicz, R.M. (Ed.), *Engineering Properties of Thermoplastics,* Wiley, New York, 1970.

34. Ayyar, R.S and Deshpande, S.N, "Creep of Polymer Concrete at Elevated Temperature", *Fifth International Congress on Polymers in Concrete (Proceedings),* Brighton,England,1987, pp.103-108.

APPENDIX A

CALIBRATION OF THE LVDT

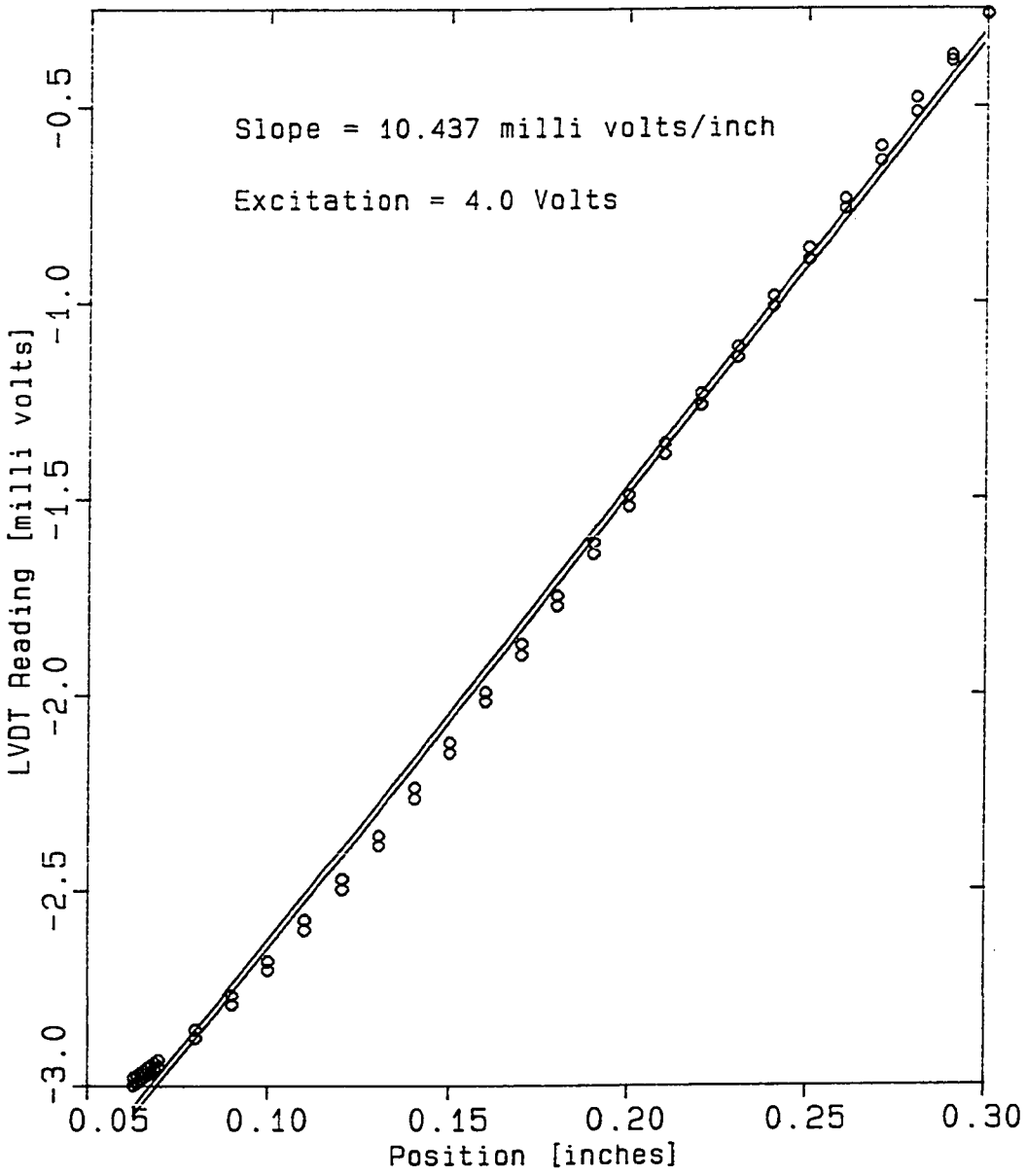

Fig A.1 Calibration curve for the linear variable differential transformer (LVDT).

Calibration Readings:

Excitation = 4.0 Volts

Position (inches)	LVDT reading (mV)
0.063	-2.998
0.064	-2.992
0.065	-2.985
0.066	-2.978
0.067	-2.971
0.068	-2.965
0.069	-2.958
0.070	-2.951
0.080	-2.876
0.090	-2.791
0.100	-2.703
0.110	-2.601
0.120	-2.497
0.130	-2.385
0.140	-2.265
0.150	-2.148
0.160	-2.016
0.170	-1.898
0.180	-1.773
0.190	-1.640
0.200	-1.520
0.210	-1.386
0.220	-1.262
0.230	-1.141
0.240	-1.010
0.250	-0.891
0.260	-0.761
0.270	-0.639
0.280	-0.515
0.290	-0.384
0.300	-0.264

Calibration Readings:

Excitation = 4.0 Volts

Position (inches)	LVDT reading (mV)
0.063	-2.979
0.064	-2.974
0.065	-2.967
0.066	-2.961
0.067	-2.953
0.068	-2.946
0.069	-2.940
0.070	-2.933
0.080	-2.856
0.090	-2.767
0.100	-2.681
0.110	-2.576
0.120	-2.471
0.130	-2.361
0.140	-2.237
0.150	-2.122
0.160	-1.993
0.170	-1.870
0.180	-1.748
0.190	-1.612
0.200	-1.491
0.210	-1.359
0.220	-1.233
0.230	-1.114
0.240	-0.984
0.250	-0.863
0.260	-0.736
0.270	-0.603
0.280	-0.479
0.290	-0.371
0.300	-0.264

APPENDIX B

HORIZONTAL AND VERTICAL SUPERPOSITION

In our study we used a vertical superposition scheme to evaluate the different shift-factors. A more commonly used procedure is one which involves horizontal shifting. The shift-factors calculated from the two different methods can, however, be fairly easily interrelated.

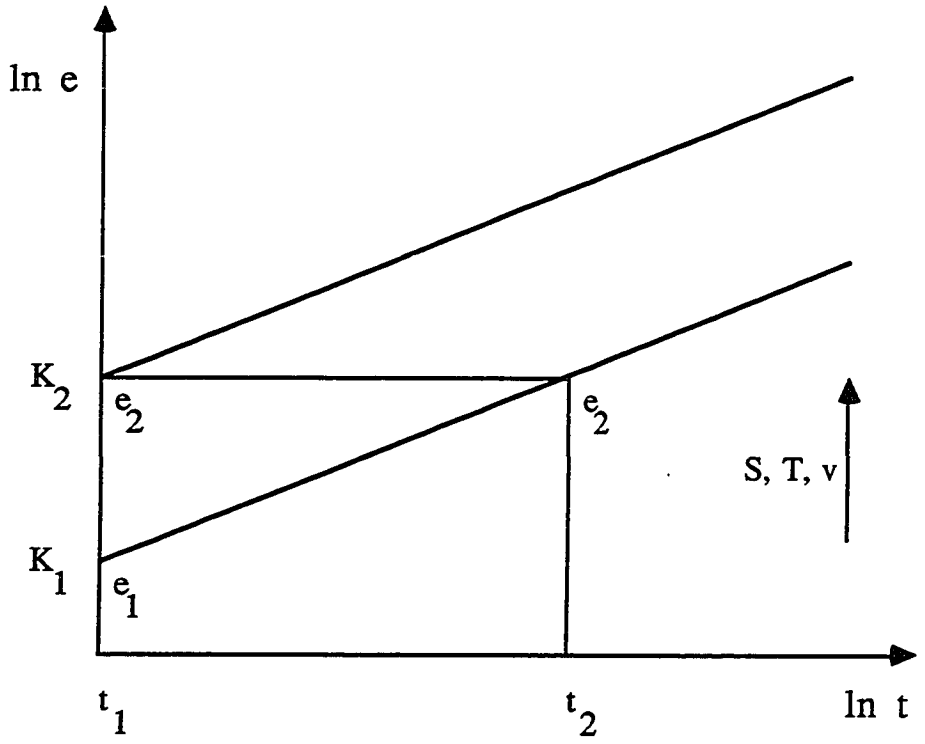

Fig B.1 Comparison of horizontal and vertical superposition.

From the above figure we have,

$$e_1 = K_1 \, t_1^{\,n} \qquad (B.1)$$

$$e_2 = K_1 \, t_2^{\,n} = K_2 \, t_1^{\,n} \qquad (B.2)$$

The shift factors may be defined as follows,

$$a_{H(S,\ T \text{ or } v)} = (t_2 / t_1) \qquad (B.3)$$

& $$a_{V(S,\ T \text{ or } v)} = (e_2 / e_1) \qquad (B.4)$$

From B.1, B.2, B.3 and B.4 we therefore get,

$$a_{H(S,\ T \text{ or } v)} = (K_2 / K_1)^{1/n} \qquad (B.5)$$

& $$a_{V(S,\ T \text{ or } v)} = (t_2 / t_1)^{n} \qquad (B.6)$$

or, $$a_{V(S,\ T \text{ or } v)} = (a_{H(S,\ T \text{ or } v)})^{n} \qquad (B.7)$$

Thus, the two shift-factors can be easily interrelated provided the value of n is known.